SYSTEMATIC ANALYSIS AND INTEGRATED OPTIMIZATION OF TRAFFIC SIGNAL CONTROL SYSTEMS IN A CONNECTED VEHICLE ENVIRONMENT

By

Byungho Beak

A Dissertation Submitted to the Faculty of the

DEPARTMENT OF SYSTEMS AND INDUSTRIAL ENGINEERING

In Partial Fulfillment of the Requirements

For the Degree of

DOCTOR OF PHILOSOPHY

In the Graduate College

THE UNIVERSITY OF ARIZONA

2017

THE UNIVERSITY OF ARIZONA

GRADUATE COLLEGE

As members of the Dissertation Committee, we certify that we have read the dissertation prepared by Byungho Beak, titled Systematic Analysis and Integrated Optimization of Traffic Signal Control Systems in a Connected Vehicle Environment and recommend that it be accepted as fulfilling the dissertation requirement for the Degree of Doctor of Philosophy.

_____ Date: 8/18/2017
K. Larry Head

_____ Date: 8/18/2017
Young-Jun Son

_____ Date: 8/18/2017
Ricardo Valerdi

_____ Date: 8/18/2017
Yao-Jan Wu

Final approval and acceptance of this dissertation is contingent upon the candidate's submission of the final copies of the dissertation to the Graduate College.

I hereby certify that I have read this dissertation prepared under my direction and recommend that it be accepted as fulfilling the dissertation requirement.

_____ Date: 8/18/2017
Dissertation Director: K. Larry Head

STATEMENT BY AUTHOR

This dissertation has been submitted in partial fulfillment of the requirements for an advanced degree at the University of Arizona and is deposited in the University Library to be made available to borrowers under rules of the Library.

SIGNED: Byungho Beak

ACKNOWLEDGEMENTS

It is a great pleasure to acknowledge my deepest thanks and gratitude to Professor Larry Head, who guided me through the past four years. He always encouraged me to look at problems differently and constantly to find new approaches and methodologies. It is a great honor to work under his supervision.

I would also like to thank Prof. Young-Jun Son, Prof. Ricardo Valerdi, and Prof. Yao-Jan Wu who served as my committee members. Their mentoring and guidance have been greatly valuable to this dissertation.

My appreciation also extends to my laboratory colleagues: Yiheng Feng, Mehdi Zamanipour, Shayan Khoshmagham, Sara Khosravi, Sriharsha Mucheli, and Zuoyu Miao. I will never forget the time we spent together in the lab and the test field.

Finally, I am grateful to my family: my father Seungkyu Baek, my mother Kyunghee Kim, my wife Hyunna Bae, my son Eungyo Baek, and my daughter Eunbyul Baek, who have always supported and believed in me. I want to give my deepest love especially to my wife. Without her support and help, I could not have finished my research.

DEDICATION

To my wife, Hyunna Bae,

who always supports, loves me, and have always been there for me.

TABLE OF CONTENTS

LIST OF FIGURES

LIST OF TABLES

Abstract

Traffic signal control systems have been tremendously improved since the first colored traffic signal light was installed in London in December 1868. There are many different types of traffic signal control systems that can be categorized into three major control types: fixed-time, actuated, and adaptive. Choosing a proper traffic signal system is very important since there exists no perfect signal control strategy that fits every traffic network. One example is traffic signal coordination, which is the most widely used traffic signal control system. It is believed that performance measures, such as travel times, vehicle delay, and number of stops, can be enhanced by synchronizing traffic signals over a corridor. However, it is not always true that the coordination will have the same benefits for all the traffic in the network. Most of the research on coordination has focused only on strengthening the major movement along the coordinated routes without considering system-wide impacts on other traffic.

Therefore, before implementing a signal control system to a specific traffic network, a thorough investigation should be conducted to see how the control strategy may impact the entire network in terms of the objectives of each type of traffic control system. This dissertation first considers two different kinds of systematic performance analyses for traffic signal control systems. Then, it presents two types of signal control strategies that account for current issues in coordination and priority control systems, respectively.

First, quantitative analysis of smooth progression for traffic flow is investigated using connected vehicle technology. Many studies have been conducted to measure the quality of progression, but none has directly considered smooth progression as the significant factor of coordination, despite the fact that the definition of coordination states that the goal is to have

smooth traffic flow. None of the existing studies concentrated on measuring a continuous smooth driving pattern for each vehicle in terms of speed. In order to quantify the smoothness, this dissertation conducts an analysis of the speed variation of vehicles traveling along a corridor. A new measure is introduced and evaluated for different kinds of traffic control systems. The measure can be used to evaluate how smoothly vehicles flow along a corridor based on the frequency content of vehicle speed. To better understand the impact of vehicle mode, a multi-modal analysis is conducted using the new measure.

Second, a multi-modal system-wide evaluation of traffic signal systems is conducted. This analysis is performed for traffic signal coordination, which is compared with fully actuated control in terms of a systematic assessment. Many optimization models for coordination focus mainly on the objective of the coordinated route and do not account for the impacts on side street movements or other system-wide impacts. In addition, multi-modality is not considered in most optimized coordination plans. Thus, a systematic investigation of traffic signal coordination is conducted to analyze the benefits and impacts on the entire system. The vehicle time spent in the system is measured as the basis of the analysis. The first analysis evaluates the effect of coordination on each route based on a single vehicle mode (regular passenger vehicles). The second analysis reveals that how multi-modality affects the performance of the entire system.

Third, in order to address traffic demand fluctuation and traffic pattern changes during coordination periods, this dissertation presents an adaptive optimization algorithm that integrates coordination with adaptive signal control using data from connected vehicles. Through the algorithm, the coordination plan can be updated to accommodate the traffic demand variation and remain optimal over the coordination period. The optimization framework consists of two levels: intersection and corridor. The intersection level handles phase allocation in real time based on

connected vehicle trajectory data, while the corridor level deals with the offsets optimization. The corridor level optimization focuses on the performance of the vehicle movement along the coordinated phase, while at the intersection level, all movements are considered to create the optimal signal plan. The two levels of optimizations apply different objective functions and modeling methodologies. The objective function at the intersection level is to minimize individual vehicle delay for both coordinated and non-coordinated phases using dynamic programming (DP). At the corridor level, a mixed integer linear programming (MILP) is formulated to minimize platoon delay for the coordinated phase.

Lastly, a peer priority control strategy, which is a methodology that enhances the multi modal intelligent traffic signal system (MMITSS) priority control model, is presented based on peer-to-peer (P2P) and dedicated short range communication (DSRC) in a connected vehicle environment. The peer priority control strategy makes it possible for a signal controller to have a flexible long-term plan for prioritized vehicles. They can benefit from the long-term plan within a secured flexible region and it can prevent the near-term priority actions from having a negative impact on other traffic by providing more flexibility for phase actuation. The strategy can be applied to all different modes of vehicles such as transit, freight, and emergency vehicles. Consideration for far side bus stops is included for transit vehicles.

The research that is presented in this dissertation is constructed based on Standard DSRC messages from connected vehicles such as Basic Safety Messages (BSMs), Signal Phasing and Timing Messages (SPaTs), Signal Request Messages (SRMs), and MAP Messages, defined by Society of Automotive Engineers (SAE) (SAE International 2016).

Chapter 1 Introduction

1.1 Background

Although there has been tremendous improvement in traffic signal systems since they were invented, signal delay at intersections still constitutes a significant portion of the travel time for vehicles, especially in urban areas. According to studies from US Department of Transportation (Mineta 2006; US Department of Transportation 2007), ineffective traffic signal plans account for an estimated 10 percent of all traffic delay, which is approximately 300 million vehicle hours. The cost of traffic congestion is $87.2 billion per year in wasted fuel and lost productivity, which could translate to $750 per traveler. The studies also reveal that almost 75 percent of the 330,000 traffic signals in the United States could be enhanced more efficiently by adjusting the signal timing plans, coordinating with adjacent signals, or updating relevant equipment. Retiming traffic signals, which optimizes the operation of signalized intersections and includes the implementation of new signal timing plans or enhanced control strategies, has been considered as a relatively low-cost approach to reducing traffic congestion (Denney 2012; Sunkari 2004). However, optimizing signals is labor intensive for most of the conventional traffic signal control systems. In addition, retiming signals still incurs costs ranging from $2,500 to $3,100 per signal, and the signals should be updated at least every three to five years, which could cost approximately $200 million per year (Denney 2012).

To address some of these issues, Intelligent Transportation Systems (ITS) emerged in the 1990's. ITS strives to enable signal control systems to operate efficiently, reducing traffic delay and accident-producing conflicts with fewer human and financial resources to update the system (Gordon and Tighe 2005). ITS, which includes adaptive control systems, real-time data collection

and analysis, and communications systems, could reduce the substantial costs that outdated traffic signal timing may cause to drivers and pedestrians. Optimizing signal timing plans and implementing them with the ITS systems can improve vehicle performance measures, lower vehicle operating costs, and reduce vehicle emissions. However, ITS alone has not been effective at improving the inefficiency of traffic signals – as indicated by the US DOT reports on the state of traffic signal systems (Denney 2012; Mineta 2006).

This chapter introduces two traffic control systems that have been widely deployed as ITS applications: Traffic signal coordination and traffic signal priority control. The introduction of connected vehicles is also provided, which has emerged as a significant technology in ITS system.

1.1.1 Traffic signal coordination

Coordinated signal control systems synchronize adjacent signals to improve the operation of one or more directional movements in a traffic network system (Denney 2012). The objective of coordination is to provide smooth flow of traffic along a corridor and highways. Coordination has been widely implemented in traffic control systems for many years, especially in urban areas during peak hours. Coordination is believed to perform better than other signal control strategies, including fully actuated control, if the intersections are adjacent to each other and the traffic volumes are sufficiently large (Koonce et al. 2008).

To achieve the efficient operation of coordination and smoother progression, it is important to determine appropriate traffic signal coordination plans (Yin et al. 2007). Many signal timing software packages and algorithms have been developed to optimize coordination plans. One category of coordination optimization is to minimize a performance index, such as average delay, number of stops, or travel time. Alternative approaches to creating coordination plans are based

on the concept of a green band. This approach attempts to improve the progression along arterials by maximizing the width of a progression band. The merit of the bandwidth approach is that it is not necessary to know traffic flow in detail and it works well when traffic flow is not heavy and is highly directional (Robertson 1986). The most significant shortcoming of optimizing coordination plans to maximize bandwidth is that residual queues are often overlooked in the bandwidth approach (Roess et al. 2011). In the case of heavy traffic demand, queues can disrupt the bandwidth progression significantly.

1.1.2 Transit signal priority control

In order to encourage the use of public transportation, numerous approaches have been to improve transit service. Transit Signal Priority (TSP) has been one of the candidates that can improve transit service by reducing average delay or number of stop of transit vehicle by giving traffic signal priority. Although many enhancements have been achieved in TSP strategies, the effective implementation of TSP is still a challenging and complicated task for traffic engineers since there are many factors to be considered. System-wide evaluation should be conducted before making the final decision on implementation of TSP.

A transit detection system to generate and receive priority requests is important in TSP. The detection system can be based on a number of technologies such as loop detectors, video cameras, radar, infrared transmitters, and radio. Recently, TSP detection systems have begun to use Global Positioning System (GPS). Today, connected vehicle technology starts to be deployed for TSP systems.

Priority control is not only for transit vehicles. Emergency vehicles have benefited from traffic signal preemption for the past fifty years (Paniati and Amoni 2006). Generally, preemption

allows a single emergency vehicle to signal an intersection that it is on an approach and special algorithms in the signal controller will terminate the current phase, in a safe manner, to serve the emergency vehicle. Emergency signal preemption (EVP) has been widely deployed, but the traffic control algorithms have primarily focused on one single vehicle, and have not considered the fact that there may be several emergency vehicles responding to an emergency call. Similarly, the use of traffic signal priority has been investigated for trucks (Sunkari et al. 2000).

1.1.3 Connected vehicles

Traditional data sources for ITS applications including system detectors, GPS, Bluetooth, or cellular data, have not been used to assess the system-wide effect of traffic signal control system, and to optimize signal timing plans based on the evaluation. Connected vehicle technology (CVT), which uses 5.9 GHz dedicated short range communication (DSRC) radios, enables the systematic evaluation of traffic signal control and signal optimization by providing high fidelity data. CVT includes several useful DSRC messages including a Basic Safety Message (BSM), a Signal Phasing and Timing Message (SPaT), a MAP Message (MAP), a Signal Request Message (SRM), and other messages. The messages, which are defined in Society of Automotive Engineers (SAE) J2735 standard (SAE International 2016), can be exchanged among vehicles (V2V) and between vehicles and infrastructure (V2I). CVT provides high resolution vehicle data that provides a rich characteristic of each vehicle state and the impact of the traffic signals. For example, BSMs are broadcast by an On-board Unit (OBU) installed in each vehicle ten times per second that are received by an infrastructure Roadside Unit (RSU) where vehicle trajectories are constructed over time. Data elements in the BSM include vehicle speed, heading, GPS position, size, mode, and other vehicle information. Through the high-fidelity data, mobility applications, such as the multi

modal intelligent traffic signal system (MMITSS), enable traffic controllers at each intersection to make smarter decisions. In addition, multi-modal performance assessment and optimization can be performed through the data since the mode of each vehicle is contained in the data.

1.2 Research motivation and scope

First, this dissertation conducts systematic analysis of the traffic signal control strategies in a connected vehicle environment considering multi-modality through two different types of measures. Then an optimization model is presented that integrates traffic signal coordination with adaptive signal control in a connected vehicle system. Finally, peer priority signal control logic is presented that uses peer-to-peer communications as well as DSRC communication. Peer-to-peer communications provide a longer planning horizon and addresses a concern about using DSRC alone. The specific research motivation and scope of the dissertation are as follows:

- *Quantitative analysis of smooth progression in traffic signal systems*

Smooth progression is one of the key factors in traffic signal coordination. Many studies have investigated measure of the quality of progression. However, none of the studies has concentrated on measuring a smooth driving pattern of each vehicle in terms of speed as the definition of coordination implies.

This dissertation aims to address a major coordinated signal systems issue: “How can ‘smoothness’ of progression be quantitatively measured?” To deal with this question, the concept of smooth progression is introduced and a new measure of smoothness is presented. The new measure, called the Smoothness Of the Flow of Traffic (SOFT), is used to evaluate different kinds

of traffic control systems. In addition, a multi-modal analysis was conducted using the SOFT measure to determine the impact of mix-mode traffic flow on smoothness.

- *Multi-modal system-wide evaluation of traffic signal coordination*

Traffic signal coordination may not be the right solution for every corridor. There are a number of factors to be considered when determining whether coordination will be effective on a corridor. According to the Signal Timing Manual (Koonce et al. 2008), coordination would be beneficial in cases where the intersections are adjacent to each other and the traffic volumes are sufficiently large. The MUTCD (FHWA 2010) suggests that adjacent intersections within 0.5 miles should be coordinated. Another factor to be considered, which may be related to the intersection spacing and traffic demand mentioned above, is the vehicle arrival pattern. If platoons are formed over the corridor, then the intersections should be coordinated. Coordination may not be effective on a traffic network with random vehicle arrival patterns.

Although the corridor could be ideal for coordinated operation, a coordination plan is generally optimized for a specific traffic volume and may not remain optimal at all times. In some instances, the wrong coordination plan may cause significant delay (Abbas et al. 2001; HCM 2010). Synchronizing several traffic signals along a corridor is a complex procedure that requires consideration of many factors, including distance between intersections, traffic demand, and multi-modality. Little research has been conducted to investigate overall system performance of coordination for different traffic volumes and different route flow scenarios, including coordinated and non-coordinated movements. In addition, most research has only addressed the unimodal coordination plan. Due to different vehicle dynamics, including vehicle speed, acceleration (deceleration), and reaction time to traffic signal, the impact of vehicle mode and dynamics on

performance of traffic signal control is likely to be significant. Through an investigation of the average time that vehicle spends in the traffic system, this dissertation conducts an analysis of system-wide performance based on traffic routes and volumes as well as multi-modality.

- *Adaptive optimization of traffic signal coordination*

A fixed coordinated signal plan does not always provide better performance, even with well-optimized parameters, since traffic demand fluctuates stochastically during the coordination period; thus, the offset and phase splits may not remain optimal because of the traffic pattern changes. For both coordinated and non-coordinated phases, it is important to change the coordination plan dynamically to accommodate demand variability and to improve coordination performance. Thus, there is a need to integrate coordination with adaptive signal control to be adaptive to real-time traffic demand.

An adaptive coordination optimization algorithm that integrates coordination with adaptive signal control in a connected vehicle environment is developed to address this need. The model consists of two levels of optimization. At the intersection level, an adaptive control algorithm allocates the optimal green time for each phase in real time using dynamic programming while considering coordination constraints. At the corridor level a mixed integer linear program is formulated based on data from the intersection level to optimize offsets along the corridor. After the corridor level algorithm solves the optimization problem, the optimized offsets are sent to the intersection level algorithm as updates to the coordination constraints. The intersection level optimization determines the best green allocation for each phase given the predicted arrival flow.

- *Peer-to-peer priority signal control strategy*

A signal priority algorithm was developed as part of the Multi-Modal Intelligent Traffic Signal System (MMITSS) project (University of Arizona, University of California PATH Program, Savari Networks, Inc., Econolite 2016) that receives signal request messages from vehicles as they enter the range of the DSRC radio – about 300 meters. Due to the DSRC (and MAP) range constraints, the horizon over which the mathematical model solves for priority requests is about 20 seconds with a 30 ~ 40 mile per hour (13.4 ~ 17.9 m/s) speed limit. Implementing the resulting near-term priority plan may not be very effective when trying to minimize delay. The arrival time may be too short to grant any effective treatment for the priority vehicle. This is due to the phase sequences that need to be followed and the required minimum green time for the preceding phases as well as traffic demand for the non-priority phases.

A peer-to-peer priority control model that allows requests to be forwarded from upstream intersections was developed to address this shortcoming. In the peer priority framework, the planning horizon is extended significantly, depending on the estimated travel times between adjacent intersections. The basic structure of the mathematical optimization in this research follows the signal priority control model (Zamanipour et al. 2016) in MMITSS. An improvement in the signal priority control model was created to integrate the implementation algorithm into the mathematical model. A peer-to-peer priority control platform, which implements the peer priority control strategy, was developed and tested using simulation.

1.3 Dissertation organization

The remaining chapters of the dissertation are organized as follows:

Chapter 2 provides a literature review of the two traffic signal control systems of interest: traffic signal coordination and transit signal priority control.

Chapter 3 presents a new measure to quantify smooth progression. This chapter presents an analysis of the speed variation of vehicles traveling along a corridor. Using a VISSIM simulation model and the Multi Modal Intelligent Traffic Signal System (MMITSS), where vehicle trajectory data is available for computing the measure, a new measure is used to evaluate different traffic control systems.

Chapter 4 introduces an overall system analysis approach using a new concept that addresses all traffic flows in a traffic network using data from a connect vehicle environment. The average time that vehicles spend in the traffic system is defined and utilized as the assessment measure.

Chapter 5 focuses on an adaptive optimization algorithm that integrates coordination control with adaptive signal control. The model is compared with actuated-coordinated signal control using VISSIM simulation.

Chapter 6 presents the peer priority signal control logic. To validate the strategy, a simulation experiment was designed to compare: Fully actuated control, coordination, and MMITSS priority control using two different VISSIM simulation networks: Arizona and Utah.

Chapter 7 summarizes the research presented in the dissertation, and provides a summary of the contributions of the dissertation and ideas for further research.

Chapter 2 Literature review

This chapter presents a comprehensive literature review of two traffic signal control systems: traffic signal coordination and transit signal priority. Significant research has focused on the advancement of these systems as new mathematical approaches and technologies have emerged.

2.1 Traffic signal coordination

Traffic Signal Coordination, as one of the most prevalent traffic control strategies, often provides a good solution in urban areas because it can provide progression to platoons on coordinated movements, which mostly accommodate a heavy traffic volume (Roess et al. 2011).

2.1.1 Objective of coordination

The main objective of coordination is to provide smooth progression for platoons on signalized arterials to enhance performance measures such as travel time, number of stops, and delay (Koonce et al. 2008). Many optimization models focus primarily on a performance index assuming the effectiveness of coordination is directly related to the index. However, the Traffic Signal Timing Manual (Koonce et al. 2008) states that the coordination effectiveness is also determined by the driver's experience and their perception of signal timing. Therefore, it is important to consider both objectives. It is not easy to measure the driver's perception since it is highly subjective.

In order to improve drivers' perception of a signal timing plan, many studies have proposed measures of progression quality. Day et al. (2010) developed the Purdue Coordination Diagram (PCD) to visualize the quality of progression using the arrival patterns on the coordinated movements on a cycle-by-cycle basis. Similarly, arrival types (HCM 2010) have been developed

as a measure of progression quality for traffic flowing on coordinated routes. Arrival types are characterized by the platoon ratio (ratio of the number of vehicles arriving during green to the g/C ratio). Bandwidth (Little et al. 1981; Tian and Urbanik 2007) has been used to facilitate the progression of platoons within a limited green band. Efficiency of bandwidth, which is defined as a ratio of the bandwidth to the cycle length, has been used to measure the progression quality (Robertson 1986; Roess et al. 2011). TRANSYT-7F (Wallace et al. 1984) provided another measure, Progression Opportunities (PROS), which is defined as the number of successive green signals traffic flow can pass through without any stops based on the desired speed.

2.1.2 Optimization of coordination

There are three fundamental parameters in traffic signal coordination are offset, phase splits, and cycle length. Using these parameters, coordination synchronizes signal phases over several intersections to provide progression to approaching vehicles. There are two major categories of optimization methodology used to develop coordination timing: improving quality of progression and optimization of a performance index.

In terms of improving the quality of progression, several optimization models to maximize green bandwidth along a corridor have been proposed. Morgan and Little (1964) synchronized traffic signals using bandwidth based on travel times between adjacent signals using mixed integer linear programming (MILP). Little (1966) expanded the MILP-based model to solve more general problems with new decision variables, design speed between signals and signal period (phase duration), for maximizing the bandwidth. MULTIBAND (Gartner et al. 1990) and PASSER-II (Messer et al. 1973) belong to this category of optimization models. MULTIBAND extends

MAXBAND by considering variable bandwidth progression based on changes in traffic volumes along a corridor. PASSER-II includes phase sequence optimization and a queue clearance option.

In terms of optimization of a performance index, such as delay, travel time, and number of stops, Gartner et al. (1975) developed the Mixed Integer Traffic Optimization Program (MITROP) to minimize the average delay of platoons on coordinated routes using a link performance function and a platoon flow model. Offset values were optimized using a piece-wise linearization model of platoon delay. Köhler et al. (2005) extended the original model by simplifying the formulation for a faster computation. TRANSYT-7F (Robertson 1986) is one of the most well-known models in this category. TRANSYT-7F uses a weighted sum of vehicle delay and stops as the objective function to optimize coordination plans over a network. The objective function was extended to other functions including progression opportunity, queue length, and throughput. Shoup and Bullock (1999) used individual vehicle travel times from vehicle re-identification equipment to optimize offset values. Hu and Liu (2013) presented an arterial offset optimization algorithm to minimize total delay using high resolution loop-detector data. SYNCHRO (Trafficware 2013) and VISTRO (PTV 2014a) are popular optimization tools that optimize plans based on a weighted combination of stops and delay.

Liu (1988) tried to combine the two approaches in the optimization framework. In his paper, a signal timing plan optimized by MAXBAND is used as the initial plan for TRANSYT-7F. Then, TRANSYT-7F handles optimization of offset values and phase splits at each intersection. The result showed that the model significantly outperformed MAXBAND (the bandwidth-only approach) by 9.4% in the Performance Index (PI) although the PI of the model was worse than TRANSYT-7F. Vasudevan and Chang (2006) integrated the two strategies by dividing the optimization process into two levels. At the progression or network level, MULTIBAND was used

to maximize variable bandwidth based on real-time traffic data. At the intersection level, a weighted combination of delays, stop, and queue length was minimized while keeping bandwidth constraints from the network level. The model was compared with the actuated signal control and MULTIBAND plan, and the result showed that the model outperformed both control plan in terms of performance measures including delays, stop time, queue, and speed. Tian and Urbanik (2007) also proposed a two-level framework that divides the entire system into subsystems and optimizes coordination plans for maximized progression and minimized performance index. They compared the model with PASSER II, and showed that the travel speed of the model was better than PASSER II.

Genetic Algorithm (GA) based optimization has also been another popular approach in the same optimization category. Park et al. (1999) developed a GA-based program to optimize cycle length, splits, offset, and phase sequence using a mesoscopic simulator and compared the results to the performance from TRANSYT-7F. The result showed that the GA-based model outperformed TRANSYT-7F in terms of queue time. Later, they enhanced the model to deal with oversaturated traffic conditions (Park et al. 2000). Stevanovic et al. (2007) introduced a VISSIM-based genetic algorithm optimization (VISGAOST), which optimizes timing plans for fully actuated signal control as well as coordination signal control. The results showed that timing plans optimized by the GA model performed better than Synchro plans in terms of delay and stops. The biggest challenge of the genetic algorithm is that an optimization process can only be fully solved by complete enumeration, which is computationally hard to deploy in real traffic networks where traffic patterns fluctuate stochastically.

In order to respond to variation in traffic demand, coordination was integrated with an adaptive traffic signal system which can adjust the coordination plans in real-time. SCOOT

(Robertson and Bretherton 1991) optimized coordination parameters in real-time based on current traffic data by using the TRANSYT platoon dispersion model. SCATS (Lowrie 1982; Luk 1984; Sims 1979) is another adaptive signal control system that optimizes the three coordination parameters based on a the degree of saturation, which is defined as the ratio of the effectively used green time to the total available green time. OPAC (Gartner 1983; Gartner et al. 2001) used dynamic programming in the adaptive optimization process and provided optional cycle length and offset optimization. ACS-Lite (Abbas et al. 2001) also belong to real-time adaptive signal control systems. The adaptive traffic control systems discussed above have been shown to be effective in the literature, but the systems have only been deployed in limited areas that constitute less than 1 percent of existing traffic signals.

Most of the existing traffic signal control systems are based on data from infrastructure-based sensors and detectors. With the advent of connected vehicle technology, connected vehicle-based signal control can provide significant benefit over conventional signal control systems. Feng et al. (2015a) developed an adaptive control algorithm using trajectory data from connected vehicles to optimize signal phase sequence and duration simultaneously. Later, they integrated the adaptive control algorithm with signal priority and coordination (Feng et al. 2016) in which coordination was considered as fixed priority requests. The offsets were assumed to be fixed, and the integrated framework was evaluated at only one-intersection in a network. He et al. (2012) introduced platoon-based arterial multi-modal signal control using connected vehicle technology. In their approach, they tried to achieve progression for platoons by considering potential queue delay and signal delay at the next downstream intersection along an arterial.

2.2 Transit signal priority control

Policies and strategies have been conceived to attract people to use public transportation by improving transit service in terms of punctuality and regularity (Furth and Muller 2000). Transit Signal Priority (TSP) strategy has been considered as one of the options that can improve transit service in terms of reducing delay, improving travel time, and reducing the number of stops.

2.2.1 TSP impact

Although transit signal priority provides a significant benefit to specific vehicle modes such as emergency vehicles, transit, and trucks, it does not always provide better performance for the entire network including other modes of vehicles. The system-wide impact of TSP should be investigated over the entire network prior to implementation of TSP. Delay at traffic signals has been estimated to be the most significant cause for bus delay (Sunkari et al. 1995). Due to the high cost of field evaluation, it has not been easy to perform system-wide assessments of an entire network or arterial system (Dion et al. 2004). Most of the research have been conducted to evaluate the effect of TSP using microscopic traffic simulation models, such as AIMSUN (Liao and Davis 2007a), TRANSYT-7F (Skabardonis 2000), TRAF-NETSIM (Abdelfattah and Khan 1998; Garrow et al. 1997; Khasnabis et al. 1996), CORSIM (Mirchandani and Lucas 2004; Skabardonis 2000), PARAMICS (Lee et al. 2005), OPNET (Ma and Yang 2008), and VISSIM (Byrne et al. 2005; Ekeila et al. 2009; Ghanim and Abu-Lebdeh 2015; He et al. 2014; Kim and Rilett 2005; Ngan et al. 2004; Wahlstedt 2011; Zamanipour et al. 2016; Zlatkovic et al. 2012b; a).

Analytical models have also been developed for estimating the delay impact of TSP strategies (Abdy and Hellinga 2010; Hongchao et al. 2008). Sunkari et al. (1995) evaluated the benefit of TSP operation by using the delay equation for signalized intersections in the Highway

Capacity Manual (Manual 1985). These methodologies can be a useful tool for transit agencies and traffic engineers to investigate the effect of TSP implementation. Chang et al. (2003) presented a TSP evaluation framework and plan that can provide useful information for stakeholders to make a decision on TSP deployments. The framework can be used to assess alternative TSP strategies while the evaluation plan includes performance measures that can be chosen appropriately for specific network systems to be evaluated.

There are several factors that should be considered for successful deployment of transit signal priority such as transit interval (headway), transit route, type of traffic control system in operation, pedestrian presence, traffic demand, location of bus stop (far-side or near side), uncertainty in transit arrival time, and intersection geometry (Abdy and Hellinga 2010). Ngan et al. (2004) examined the impact of traffic signal parameters on the performance of TSP under a number of traffic conditions. The results showed that a TSP strategy would be most effective when traffic volume on the transit route are relatively heavy and the bus headway is approximately 10 minutes. The results also illustrate that TSP has significant adverse impacts on cross street performance with a volume/capacity (v/c) ratio above 0.9, while the impact was minimal at low v/c ratios. For the bus stop location, the results showed that a far-side bus stop was better than a nearside bus stop in terms of transit delay. The paper also included other impact factors on TSP performance such as bus check-in detector location, left turn conditions, and coordination.

2.2.2 Types of TSP strategy

There are three major categories of signal priority: passive TSP, active TSP, and adaptive TSP. The type of TSP should be selected based on the traffic conditions at each network. Passive TSP tries to improve performance of TSP operation by using pre-determined signal timing plans

(Sunkari et al. 1995). Stevanovic et al. (2008) presented a transit priority control strategy to adjust basic signal timing parameters, including cycle length, offset, splits, and phase sequences. The results showed that the adjustment of the signal settings can significantly improve transit operations. Estrada et al. (2009) developed an optimization tool to determine the optimal set of offsets to minimize travel times for transit. Passive TSP may be beneficial only if transit frequency is relatively high (Ma and Yang 2008). Active TSP accounts for these limitations by detecting and responding to transit vehicles in real time through green extension, red truncation, and phase skipping. Active TSP strategies may sacrifice the service of other traffic movements when serving requests. Active priority may be conditional based on lateness and occupancy criteria that determines when a request can be sent (or served) (Furth and Muller 2000; Hu et al. 2015; Skabardonis and Geroliminis 2008). To address limitations of active and passive TSP, Ma and Yang (2008) integrated both active and passive strategies into one system, and showed that the integrated model can improve both variation and average bus delay.

Adaptive TSP controls signal timing for transit vehicles with the goal of using phase time more effectively. SCOOT (Robertson and Bretherton 1991) is an online adaptive signal control system that optimizes coordination parameters in real-time based on current traffic data. The signal timings are optimized for transit priority by either extension of green or red truncation. SCATS (Lowrie 1982; Luk 1984; Sims 1979) is another real-time adaptive signal control system that tries to grant tram priority by and active priority strategy based on estimated tram arrival. UTOPIA (Nelson et al. 1993) can grant priority to transit by optimizing phase duration and green start time through on-line traffic data from upstream detectors. Mirchandani and Lucas (2004) built the framework that integrated TSP and preemption in an adaptive signal control architecture based on PREDICT algorithm (Head 1995). Ling and Shalaby (2004) used a Reinforcement Learning

method to find the optimal phase duration for transit vehicles taking into consideration transit headway and elapsed green time for the requested phase. Lee et al. (2005) developed a TSP operation model that selects the best plan among various priority plans in a library according to a transit arrival prediction model. Adaptive TSP systems have been effective to minimize negative impact on other traffic to a certain extent by balancing the benefits for transit and negative impacts on other traffic. Most of the adaptive TSP systems are coupled with adaptive signal control systems. Thus, it can take high cost and time for field implementation and maintenance of the adaptive system since most of the signals in the United States are still based on closed-loop actuation with the dual-ring structure (Li et al. 2011).

Active and adaptive TSP requires a transit detection systems to generate priority requests. The detection system can be based on a number of technologies such as loop detectors, video cameras, radar, infrared transmitters, and radio. Global Positioning System (GPS) has also been popular tool for TSP detection systems. Koonce at al. (2002) and Liao et al. (2007b) developed signal priority control models based on Automated Vehicle Location Systems (AVL) using GPS-based data. Shalaby and Farhan (2004) and Skabardonis and Gerolominis (2008) also presented their own model based on an AVL systems using GPS data. However, the accuracy of GPS data can be limited due to the characteristics of the surroundings including buildings and trees in urban areas. Instead of GPS, Ma and Yang (2008) adopted Wireless Sensor Network (WSN) technology which consist of nodes that can measure and process transit data, as well as communicate between nodes in the wireless range.

Through the emergence of connected vehicle technology, connected vehicle based signal priority control can provide significant benefit over traditional TSP strategies. Hu et al. (2015) developed a person-delay-based optimization approach for an intelligent TSP strategy using

connected vehicle technology, assuming that the connected vehicle market penetration rate was 0%, except for transit. He et al. (2011a, 2014) and Zamanipour et al. (2016) developed multi modal priority control strategies that consider requests from transit as well as trucks and emergency vehicles.

Although TSP has been implemented over the past decades, challenges still exist. One of the challenges that has been observed in conventional TSP strategies is an uncertainty in transit travel time and the lack of accuracy in estimated travel time. If the travel time is estimated to be later than the actual arrival at the downstream intersection, the vehicle may not receive the desired benefit of the priority plan. On the other hand, if the arrival time was forecasted to be too early, it could force off competing phases too early, leading to unnecessary delay for other traffic. Lee et al. (2005) presented an online simulation-based TSP model to improve accuracy of prediction in travel time of transit. Shalaby and Farhan (2004) presented a Kalman filter-based algorithm using Automatic Vehicle Location (AVL) based on GPS position and Automatic Passenger Counting (APC) systems. Ekeila et al. (2009) presented a linear transit arrival prediction model based on data from an AVL system.

Another shortcoming in TSP strategies is the difficulty in dealing with multiple conflicting priority requests. Since most of the rule-based TSP strategies (Balke et al. 2000; Conrad et al. 1998; Dion and Hellinga 2002) are based on if-then structures that assumed a first-come, first-served priority logic. They have difficulties managing multiple conflicting priority requests at the same time. Head et al. (2006) presented an analytical model-based priority strategy based on a precedence graph structure that captures the ring-phase-barrier structure of a North American traffic controller. The paper showed that a rule-based first-come, first-serve policy can lead to more delay than a model that considers multiple requests simultaneously. A similar result was

found by Ma et al. (2013a), who formulated a dynamic programming model for multiple priority requests by optimizing phase sequence. Hu et al. (2015) and Zamanipour et al. (2016) used a mixed integer linear programming model to minimize vehicle delay for multiple priority requests and the result showed that vehicle delay could be significantly improved. Instead of a model-based approach, Zlatkovic et al. (2012a) used a logic processor to resolve conflicting multiple requests and tested the model in a VISSIM simulation. The result showed that the first-come, first-served policy for conflicting priority requests could result in worse performance than a policy that does not provide priority.

2.2.3 Integration of TSP and coordination

Priority eligible vehicles can benefit on coordinated routes that have been set up for regular vehicles due to the preference provided through coordination. There has been some research that attempts to integrate TSP with coordination to minimize adverse impact on general vehicles. However, it is not easy to implement transit priority strategies successfully in coordinated signal systems, where the green waves may be disrupted and cause a transition period after the priority request(s) has (have) been served (Wahlstedt 2011). When TSP is in operation during peak hours, coordination may be interrupted to provide priority to transit and it could take a long time to return to the normal coordinated cycle, which can significantly interrupt smooth progression to regular vehicles (Cohen et al. 2007).

To preserve progression and maintain coordination over a corridor while operating priority logic, Skabardonis (2000) formulated both passive and active transit priority models and performed the evaluation of the strategies with coordinated signal control. Wahlstedt (2011) tested the impact of transit and other traffic in coordination using a conditional active priority strategy

with a software-in-the-loop signal controller simulator, while Estrada et al. (2009) used a passive priority strategy in a coordinated traffic system by adjusting offset values at each intersection. Duerr (2000) tried to maintain coordinated progression for general vehicles over a corridor while allocating green times for transit dynamically based on a Genetic algorithm approach. Koonce at al. (2002) implemented a rule-based TSP logic and applied the constraints that the requested phase length changes should remain within the coordinated cycle length. Ghanim and Abu-Lebdeh (2015) used a genetic algorithm and a neural network model for the integration of TSP and coordination. Ma et al. (2010) tried a new priority control method, called Coordinated and Conditional Bus Priority (CCBP), to prevent transit that passed an upstream intersection through early green start from having extra delay at the downstream in coordination mode. Later, they presented another coordinated TSP strategy that can provide coordinated bus priority at each signal between two bus stops using a linear program model (Ma et al. 2013b). Hu et al. (2014) also developed TSP logic (TSPCV), which uses green time reallocation and transit speed adjustment based on connected vehicle data. Later, they advanced the logic, called it TSPCV-C, to operate with coordination and overcome the previous shortcoming (the intersection spacing issue) that requires enough distance between intersections to adjust speed of transit (Hu et al. 2015). Assuming coordination as a special type of virtual priority, Zamanipour et al. (2016) tried to minimize both priority request and coordination request delay in the objective function. Most of the integrated coordination-TSP methodologies discussed above have tried to provide progression for transits that run in coordinated routes (only in a major corridor). Another challenge is that transition to normal coordination cycle still could take a long time or have a negative impact on other traffic by manipulating the signal inefficiently.

2.3 Summary

There have been many improvements in traffic signal control systems over the past decades. This chapter reviewed two major traffic signal control systems that have been most widely implemented in real world: Traffic signal coordination and transit signal priority control.

There are many factors to be considered to determine which control system will be effective for a particular traffic network including traffic pattern, volume, intersection spacing, and multi-modality. Considering these factors, a system-wide assessment should be conducted to decide on the best traffic control system. However, little research has been conducted to investigate the overall system performance of traffic signal control system when strategies such as coordination and priority are implemented. In addition, most of the traffic signal coordination strategies are not adaptive to real-time traffic demand. Since traffic demand fluctuates during the coordination period, coordination parameters may not remain optimal.

The literature review of TSP strategies has shown that the difficulty in dealing with multiple conflicting priority requests has been addressed through analytical model-based priority algorithms, but the impact to other traffic in the network when serving transit priority requests remains unaddressed although there has been research to minimize adverse impact of other traffic while granting priority for transit vehicles.

Chapter 3 Quantitative analysis of smooth progression in traffic signal systems

This chapter introduces a concept of smooth progression in terms of vehicle speed variation and presents a new measure of smoothness, which can evaluate the quality of progression quantitatively using connected vehicle technology. In the Multi Modal Intelligent Traffic Signal System (University of Arizona, et. al. 2016) a vehicle trajectory awareness software component (Feng et al. 2015a) that runs on the RSU receives the BSMs and decodes them into individual data elements including vehicle speed, heading, and GPS position. The BSM data is collected into vehicle trajectories that can be used to compute control and performance measures based on the path that each vehicle travels. This connected vehicle capability has been replicated in simulation using the VISSIM microscopic traffic simulation tool (Feng et al. 2015b) and the drivermodel.dll to simulate equipped vehicle BSMs. The vehicle awareness component provides the ability to compute new performance measures to help answer the question about assessment of smooth progression. This capability can be implemented in field deployments and in traffic simulation.

3.1 Methodology

In order to quantify smoothness, an analysis of speed variation of vehicles traveling along the coordinated route(s) was conducted. Figure 3-1 illustrates the network used in this dissertation and is based on a section of El Camino Real in San Mateo, CA., where the Multi-Modal Intelligent Transportation Signal System (MMITSS) impacts assessment (Ahn et al. 2016; US DOT 2015) was conducted.

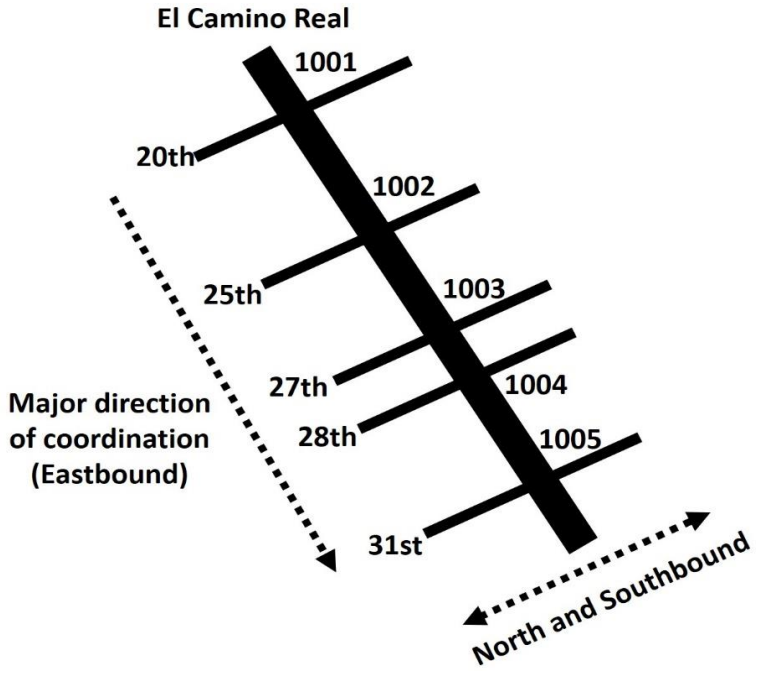

Figure 3-1 Study network based on a section of El Camino Real in San Mateo, CA

Visually, examining speed profiles, or time-space diagrams (Gazis 1965; HCM 2010) reveals the idea of smooth flow as illustrated in Figure 3-2. Figure 3-2(a) shows the progression of a vehicle that traveled through four intersections without having to stop. This would be considered smooth flow since the vehicle has almost constant speed. The speed profile shown in Figure 3-2(b) illustrates a vehicle that has significant speed variation due to the traffic signals, queues, and other traffic dynamics. One might be inclined to define the sum of squared errors (SSE) between the free flow speed and the actual vehicle speed as a measure that would differentiate between these two cases. However, when Figure 3-2(c) is compared with Figure 3-2(d), Figure 3-2(d) has a smaller SSE value although the speed pattern in Figure 3-2(c) might be considered better in terms of smoothness. The SSE from a vehicle speed profile does not necessarily reflect the smooth progression of that vehicle. To address this deficiency, a new metric is defined that better characterizes the smoothness of a vehicle's movement.

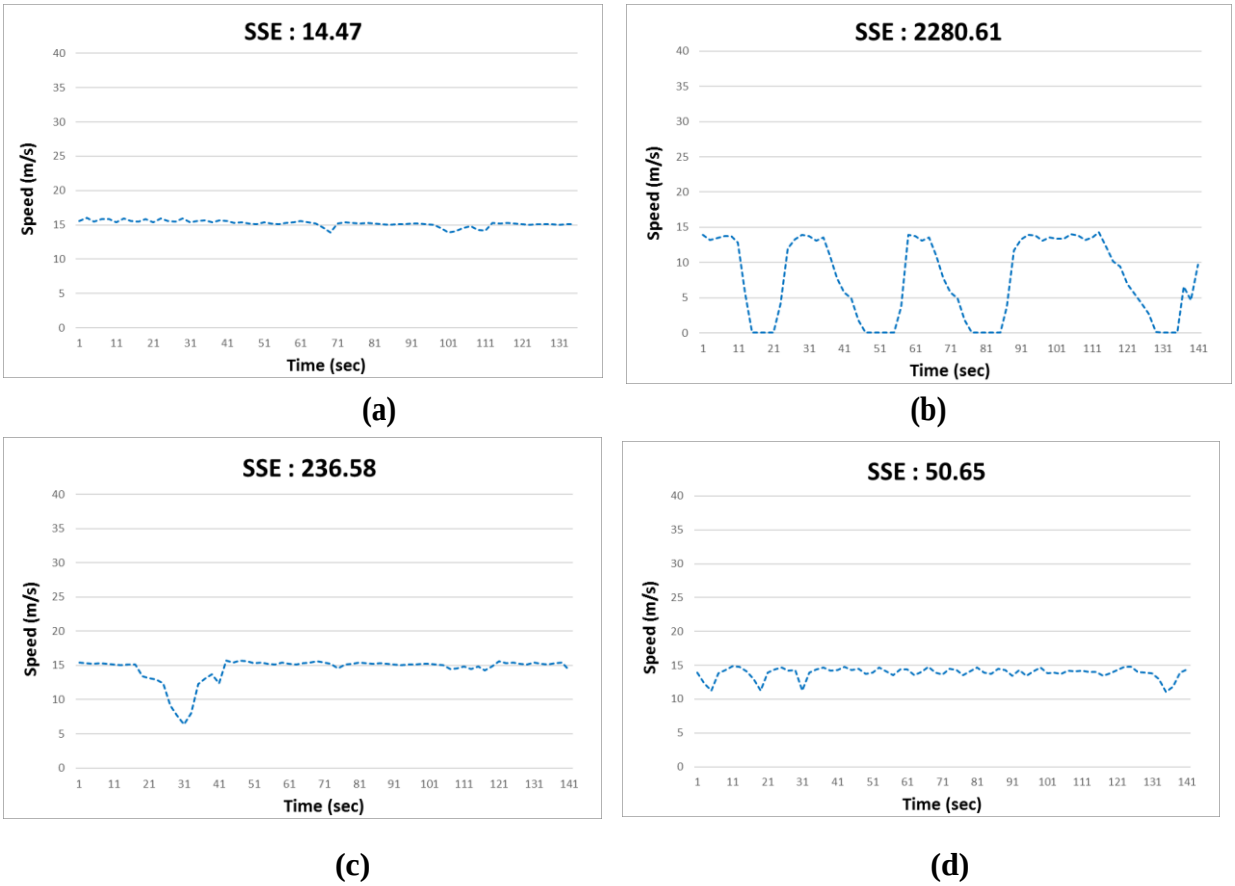

Figure 3-2 Speed profile: (a) a vehicle that does not stop, (b) a vehicle that has to stop several time, (c) a vehicle that slows once, and (d) a vehicle that exhibits a start-stop pattern

3.1.1 Smoothness Of the Flow of Traffic (SOFT)

The Smoothness of the Flow of Traffic (SOFT) is defined as a measurement of the ability to provide continuous travel for vehicles through multiple intersections with less variation in vehicle speed. The measure of smoothness is based on the frequency content of a vehicle's speed over time. If a vehicle's speed is constant, then there is no high frequency variations of speed. If a vehicle accelerates and decelerates, repeatedly in a cycle of acceleration and deceleration, then the speed will vary and contain more power at higher frequencies. Frequency content of a signal, such

as the speed profile, can be measured using the Fourier Transform (Welch 1967), which is defined as:

$$S(f) = \int_{-\infty}^{\infty} s(t) \cdot e^{-2\pi \cdot i \cdot f \cdot t} dt \tag{1}$$

If $s_v(t)$ is the speed profile of the v^{th} vehicle and the speed is sampled every T_0 seconds, then $\{s_v(nT_0), n = 0, \ldots, N\}$ is the set of speed samples for the v^{th} vehicle. T_0 is the sampling interval and should be selected small enough to ensure the speed characteristic of each vehicle is adequately captured (Jerri 1977). In the connected vehicle architecture (SAE International 2016), vehicle data is sampled and communicated every 100 ms (10 Hz). In most modern microscopic traffic simulation models (PTV 2014b; TSS-Transport Simulation Systems 2014) vehicle positions can be updated 10 times per simulated second. In this chapter, it is assumed that speed samples are available every 2 seconds.

The discrete Fourier Transform (Welch 1967) is used to estimate the spectrum and is defined as:

$$X_k^v = \sum_{n=0}^{N-1} s_v(nT_0) \cdot e^{-2\pi knjt/T_0} \qquad \text{for } k = 0, \ldots, N-1 \tag{2}$$

where X_k^v is the contribution of the k^{th} frequency harmonic of the speed profile (signal) of the v^{th} vehicle.

As the variation of speed increases, the power (contribution) at the higher frequencies increases. Using the ratio of the power at low frequency to the power at high frequency, "smoothness" is defined as follows:

$$SOFT(v) = 100 \times \left(1 - \sqrt{\sum_{k=1}^{N-1} \left(\frac{P_k^v}{P_0^v} \right)^2} \right) \tag{3}$$

Where $P_k^v = \left| X_k^v \right|^2$.

SOFT(v) is defined as the ratio of the sum of the total power distributed over the higher frequencies to the power at zero frequency (P_0^v) which is average vehicle speed. The new measure is expressed in root sum square (RSS) of power as a percentage value. The fundamental concept of *SOFT(v)* is similar to Total Harmonic Distortion (THD), which has been used to identify the linearity of audio systems and the power quality of electric power systems. THD is defined as the ratio of the sum of the powers of all harmonic components to the power of the fundamental frequency (Shmilovitz 2005). However, fluctuating speed is different from distortion which is the alteration of the original signal or waveform. Speed profiles with more variations have larger values of power at the higher harmonics; hence, smooth progressed vehicles have higher SOFT measures.

Figure 3-3 shows an example of the transformations for two cases: a vehicle that does not have to stop when traveling the coordinated route and a vehicle that has to stop 4 times on the same route. The top graph of each case is the speed profile for one vehicle in the time domain, and the lower graph is the power spectral density in the frequency domain. Vehicle speed is represented by dots in time domain (top graph), which represents the speed samples received every two seconds. It is observed that power amplitude at the higher frequencies (e.g. 0.01 to 0.1 Hz) is very low in Figure 3-3(a), while it is higher in Figure 3-3(b). These figures demonstrate that the plots in each frequency domain facilitate the variation of speed in the time domain.

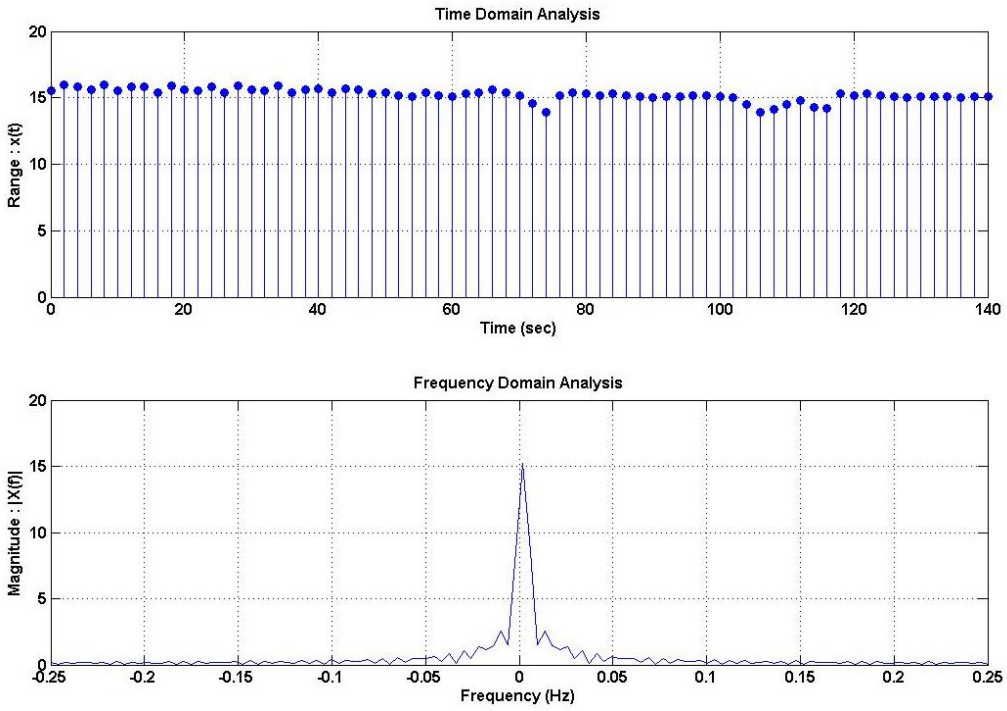

(a)

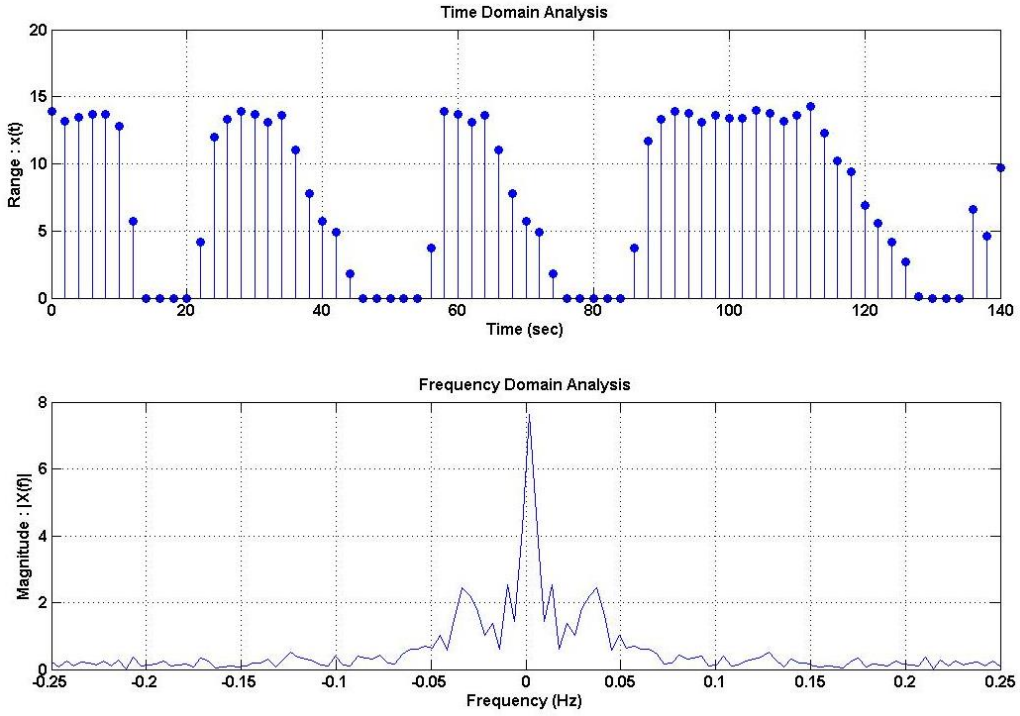

(b)

Figure 3-3 Transformation of speed profile from time domain to frequency domain: (a) Green rest on coordinated route, (b) Free operation on coordinated route

SOFT(v) is a measure of smooth progression for a single vehicle, *v*. To assess the performance of a signal timing plan over a corridor or route, the average SOFT value over all vehicles is computed. A simulation study was conducted to demonstrate the ability of average SOFT as a measure of traffic signal coordination performance that captures the drivers' experience.

3.2 Case study

To examine the quality of progression, the Purdue Coordination Diagram (Day et al. 2010, 2012) is first generated for two traffic control strategies and then compared with the new measure – average *SOFT*. As mentioned earlier, a network consisting of five intersections on El Camino Real in San Mateo, CA was modeled in VISSIM 6.00-19. Figure 3-1 illustrates the five intersections numbered from 1001 to 1005. The length of the corridor is 1.7 miles with three lanes on the main movement and 200 feet of turn bay at each intersection. The signals are operated in fully actuated (free) mode and in coordination mode on the eastbound and westbound movements. The traffic demands are summarized in Table 3-1.

Table 3-1 Vehicle volume (veh/hr) for each movement

Main street	**Eastbound**	**Westbound**
HIGH	2200	1600
MED	1100	800
Side street	**Northbound**	**Southbound**
Int. 1001	600	600
Int. 1002	500	500
Int. 1003	250	250
Int. 1004	250	250
Int. 1005	700	700

The major direction of coordination is eastbound since it has more demand than westbound. The HIGH volume on the main street is used for most of the analysis in this chapter except for multi-modal (truck and regular vehicle) analysis, which uses the MED volume data. As shown in Table 3-1, the HIGH volume scenario consists of 2200 vph in the eastbound direction (phase 2), 1600 vph in the westbound direction (phase 6), and 250~600 vph on side streets. The MED volumes scenarios have less demand on the major street with the same demand on side streets.

Traffic control in the simulation model is based on a dual-ring barrier control structure with eight phases. The traffic signal control is simulated using the Econolite ASC/3 SIL virtual signal controllers in VISSIM. VISTRO is used to generate coordination plans for each intersection based on the HIGH and MED demand scenarios respectively (Table 3-2). VISTRO uses a weighted sum of total vehicle delay and number of stops as the objective function (PTV 2014a). VISTRO identified 100 seconds as the optimal cycle length for all intersections.

Table 3-2 Optimized coordination parameters from VISTRO

Each intersection		Offset	Phase split							
			1	2	3	4	5	6	7	8
HIGH volume	Int. 1001	0	13	35	27	25	13	35	-	-
	Int. 1002	42	15	45	-	-	15	45	20	20
	Int. 1003	61	11	49	20	20	11	49	-	-
	Int. 1004	70	13	53	17	17	13	53	-	-
	Int. 1005	97	13	39	24	24	13	39	-	-
MED volume	Int. 1001	0	17	23	28	32	12	28	-	-
	Int. 1002	42	18	31	-	-	13	36	24	27
	Int. 1003	61	13	37	25	25	19	31	-	-
	Int. 1004	70	15	35	25	25	11	39	-	-
	Int. 1005	97	13	33	24	30	12	34	-	-

The system is simulated under both coordination and free operation. In both cases, the side street signals are actuated, which means phases will be skipped if there is no demand; will gap out if there is no vehicle arrival for three seconds gap; or, will max out if the phase split from Table 3-2 is reached.

The Purdue Coordination Diagram (PCD) is an innovative tool to evaluate the quality of progression. This diagram is useful to visualize vehicle arrival patterns during coordination and to evaluate the performance in terms of the percentage of arrivals on green, called Percentage of Green (POG). In this chapter, a modified PCD is generated, called CV-PCD, to visually demonstrate the progression using vehicle trajectories created by connected vehicle technology. Instead of using advance detectors, per the original PCD technique, the CV-PCD is generated using connected vehicle data. The original PCD is generated based on event data from detectors on the approach to an intersection. The arrival events may be impacted by a queue that extends beyond the detector, hence there could be some bias in the visualization. The CV-PCD can be generated more accurately based on the exact vehicle arrival based on connected vehicle data. In addition, a multi-modal CV-PCD is possible since the SAE J2735 BSM contains information about vehicle mode.

In Figures 3-4 and 3-5, the vertical axis is time in cycle, while the horizontal axis is simulation time. The green-diamond and red-square marks represent the beginning of green and the end of green at each cycle, respectively. The arrival time of each vehicle at a stop bar in the major coordinated phase is marked as a grey dot on the graph. If a vehicle is not able to pass through the stop bar due to a residual queue even after a green light, the time that the vehicle joins the back of the queue is marked as the arrival time on the graph. Figure 3-4 demonstrates the CV-PCD of the first three intersections (Int. 1001 ~ 1003) respectively during free operation, while

Figure 3-5 shows the CV-PCDs of the same three intersections during coordination. To draw the CV-PCD for free operation without a fixed cycle length, the time in cycle (x-axis on the CV-PCD) is reset to zero at the end of phase 2 (Ø2) green, which is a similar way to be drawn in the PCD. As the CV-PCDs from Figure 3-4 display, both green-diamond and red-square marks fluctuated every cycle due to the free operation which does not have a fixed cycle length. As shown in Figure 3-4(c), the arrival pattern at Int. 1001 was randomly scattered since vehicles were inserted into the intersection from upstream by the VISSIM simulation input flow with a random distribution. However, Figures 3-4(a) and 3-4(b) show that dense platoons exist during most of the cycles. The graph also illustrates that most of the observed vehicles arrived before signals turned green, meaning poor progressions. Average POG of each cycle in Figures 3-4(a) and 3-4(b) were 11.9% and 24.1% respectively, while the POG in Figure 3-4(c) was 39.4%, which means that the quality of progression is degraded in terms of POG during free operation. Comparing Figures 3-4(a) and 3-4(b) with Figures 3-5(a) and 3-5(b), it can be observed that coordination improves POG from 11.9% to 84.9% and 24.1% to 84.1%, respectively. Based on the traffic demand, the CV-PCDs obviously indicate that this corridor should be coordinated in terms of POG. In addition, Figures 3-5(a) and 3-5(b) reveal that the offset from VISTRO was well optimized since most of the arrivals occurred during a green interval.

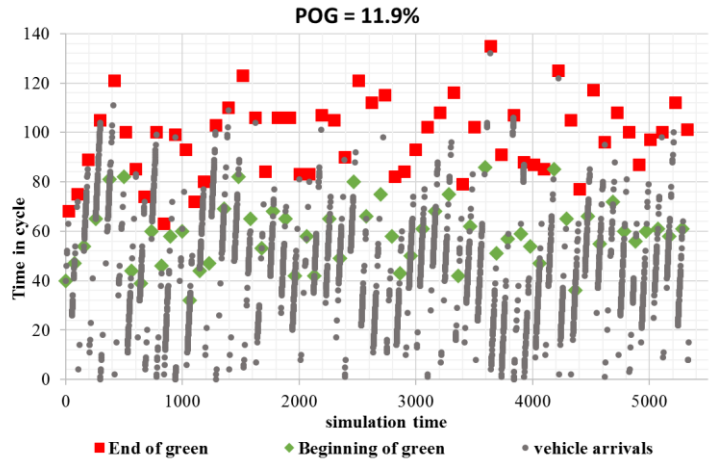

(a)

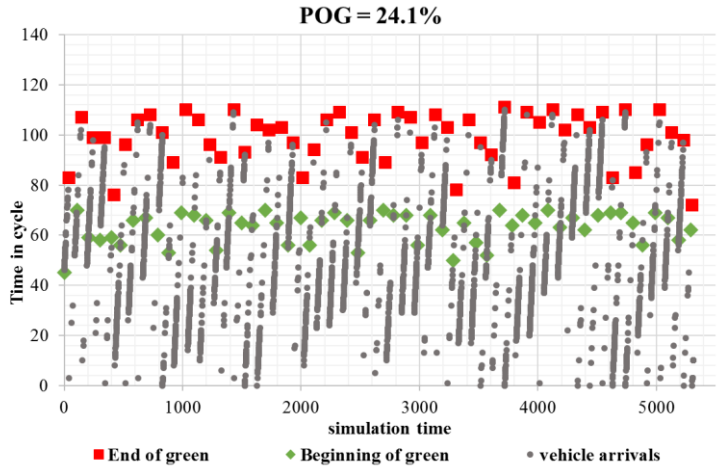

(b)

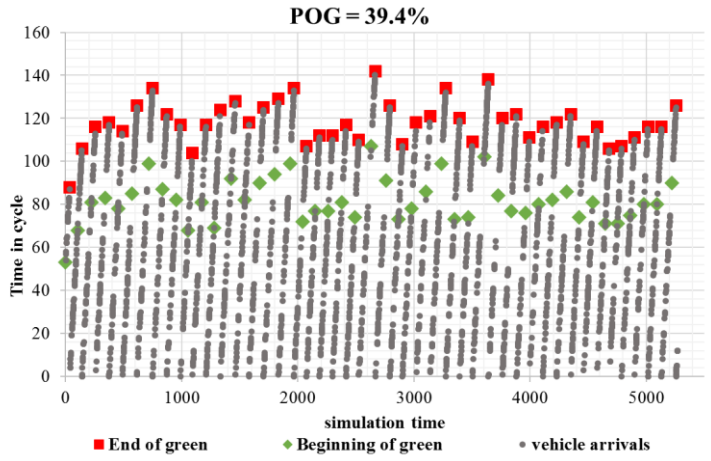

(c)

Figure 3-4 Purdue Coordination Diagram for free operation: (a) Int. 1003, (b) Int. 1002, (c) Int. 1001

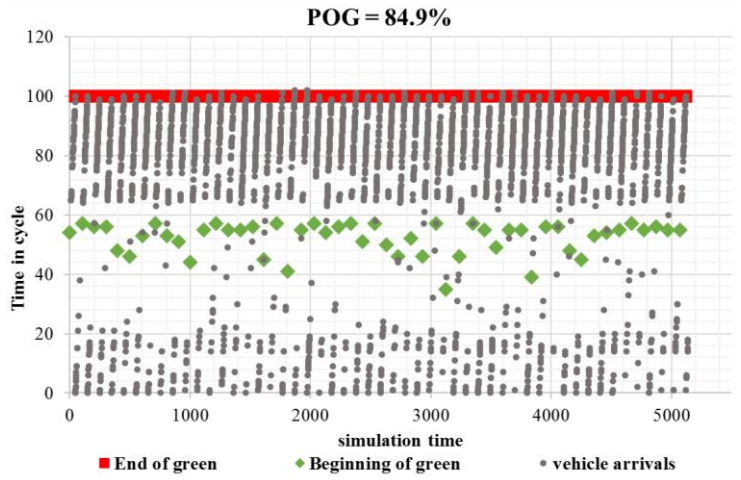

(a)

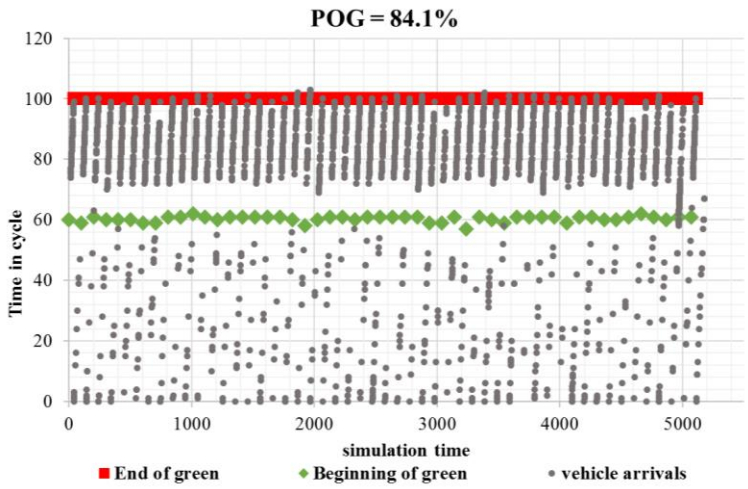

(b)

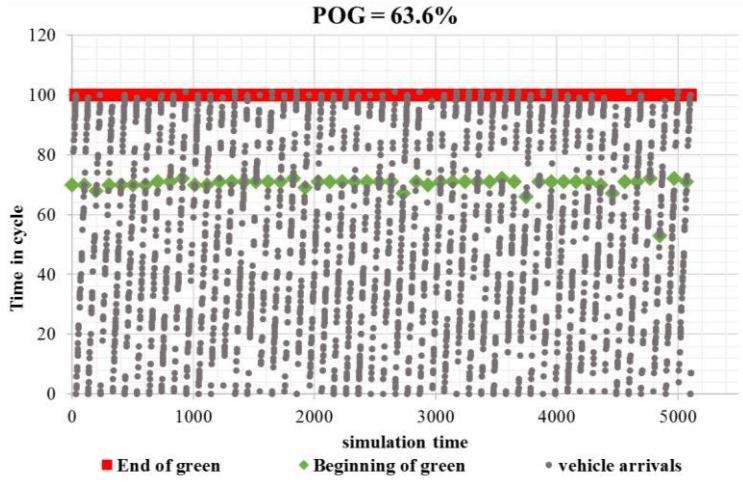

(c)

Figure 3-5 Purdue Coordination Diagram for coordination: (a) Int. 1003, (b) Int. 1002, (c) Int. 1001

By analyzing vehicle arrival patterns from the CV-PCDs, useful information on traffic signal performance can be obtained. For example, the presence of groups of vehicles (or platoons) that progress through the signal during the green interval each cycle shows good progression. This information can help traffic engineers understand traffic signal performance and adjust coordination parameters according to the traffic demand. However, POG does not guarantee the smooth driving that drivers desire. Even within good platoon progression after the start of the green interval, each driver may face a fluctuating vehicle speed over corridor due to interactions with the other vehicles. Therefore, it is not possible to identify a specific (or continuous) smooth pattern of each vehicle's speed over a corridor using the CV-PCD visualization tool.

3.2.1 Measure of average SOFT

The SOFT measure can capture the speed variation that the CV-PCD did not reveal. To demonstrate an example of the SOFT measure for the coordinated traffic signal plan, the vehicle speed profiles from the simulation are used to estimate the average SOFT over all vehicles. Figure 3-6 illustrates the speed profiles for all vehicles that traveled through the corridor. Figure 3-6(a) was generated when free operation was used for control and shows that many vehicles were stopped or delayed at most of the intersections. Figure 3-6(b) was generated when coordination was in operation, which has fewer stops after the second intersection. In Figure 3-6(c), the traffic signals along the coordinated route were in green rest during the simulation time. The speed of vehicles was essentially constant since most of the vehicles did not accelerate or decelerate throughout the corridor.

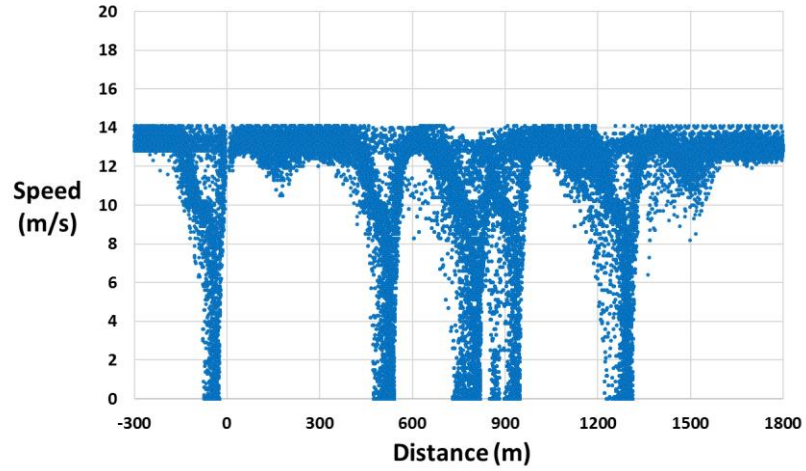

(a)

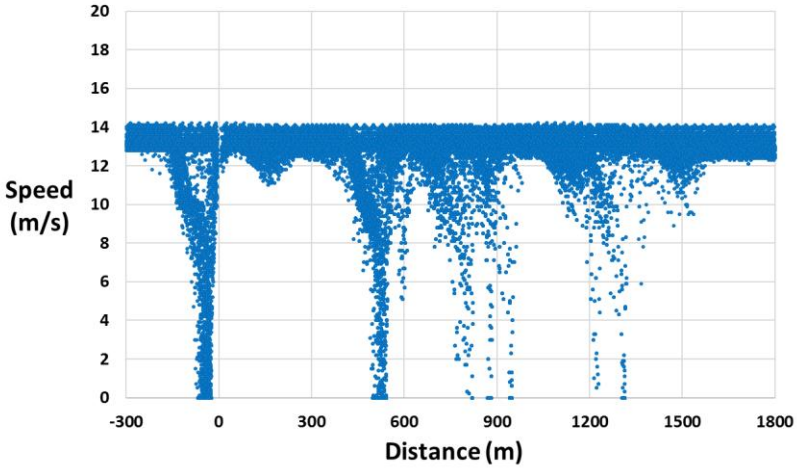

(b)

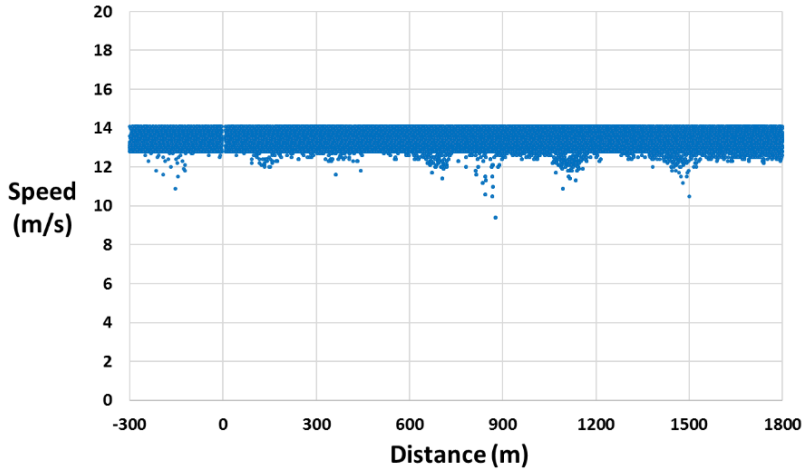

(c)

Figure 3-6 Speed profile: (a) Free operation, (b) Coordination, (c) Green Rest

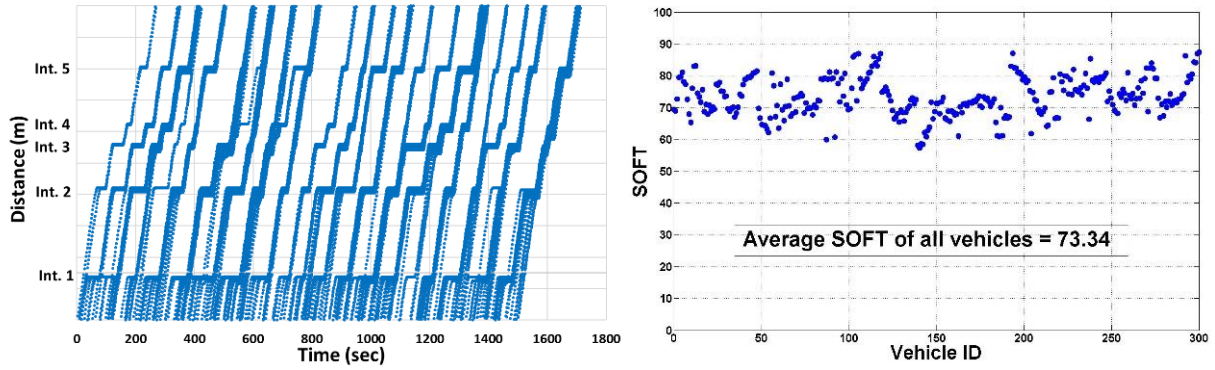

(a)

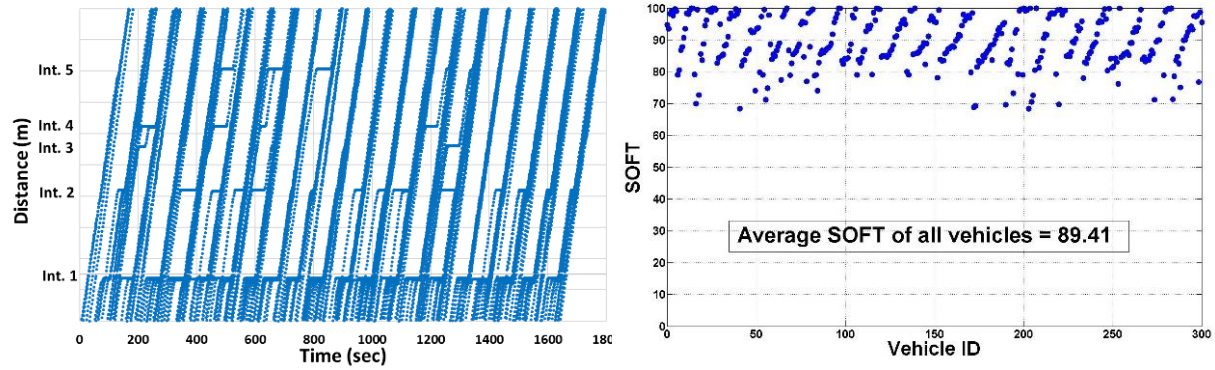

(b)

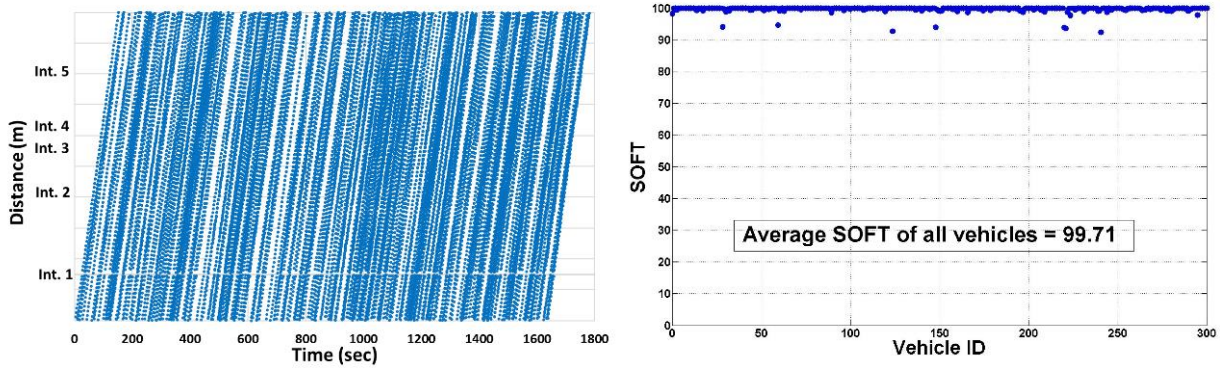

(c)

Figure 3-7 Comparison of the trajectories in time-space diagram and average of the SOFT: (a) Free operation, (b) Coordination, (c) Green rest

To measure SOFT, the speed profile of each vehicle from Figure 3-6 is transformed into a power spectrum in the frequency domain then used to calculate SOFT as described Equation (3). Figure 3-7 presents the time-space trajectory (left) and the SOFT measure (right) for all vehicles that passed through the coordinated route. Each blue dot on the right graph represents the SOFT value of a vehicle, and the average SOFT of all vehicles is shown at the middle of the graph. Free operation (Figure 3-7(a)) has the most speed variations in the time-space diagram resulting in the lowest average SOFT value. As shown in Figure 3-7(b), the impact of coordination is observed by the smooth progression in time-space diagram, and the average SOFT value is higher than during free operation. In Figure 3-7(c), the time space trajectories are essentially constant, and the average SOFT value is almost one hundred since most of the vehicles did not have any variation in speed. The standard deviation of SOFT values in the green rest case was 0.95, which is significantly small comparing to free operation and coordination, 6.14 and 7.70, respectively. The standard deviation in free operation was rather slightly smaller than in coordination.

3.2.2 Analysis of SOFT for different vehicle modes

Smooth progression may be affected by other factors such as combination of vehicle modes (e.g. truck, bus, and regular vehicle) and drivers' behavior in addition to the traffic signal timing plans. To investigate the impact of vehicle mode on smooth progression, another vehicle mode (truck) was inserted into the VISSIM traffic stream. The MED volume case from Table 3-1 and coordination parameters optimized by the volume were used for this analysis (Table 3-2). The ratio of trucks among all vehicles input on the coordinated route was increased for each case: 0%, 20%, 40%, and 60%. Figure 3-8 presents the SOFT diagrams that demonstrate the differences between the four cases. The blue dots represent regular vehicles, while the red squares represent trucks. As

Figure 3-8 indicates, the average SOFT was significantly impacted by the ratio of trucks. As the ratio of trucks increased to 60%, the average SOFT value decreased to 76%, which was almost as low as the observed during free operation in Figure 3-7(a).

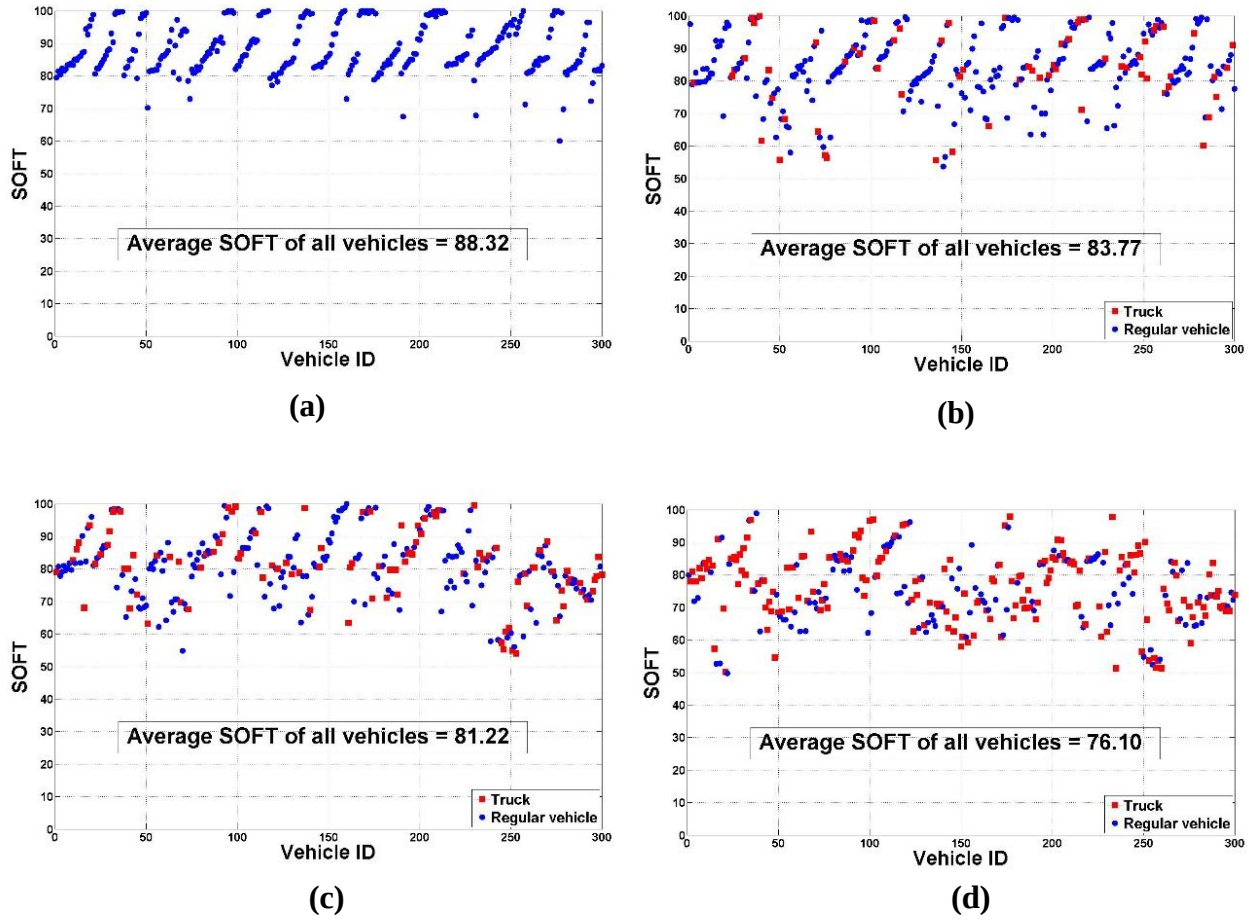

Figure 3-8 The average SOFT of coordination by different ratios of trucks among all vehicle input: (a) 0%, (b) 20%, (c) 40%, (d) 60%

Box plots of individual vehicle SOFT values were generated to graphically compare the distribution between the four cases (Figure 3-9). The case based on 60% trucks displayed the largest range of SOFT values and the largest variation.

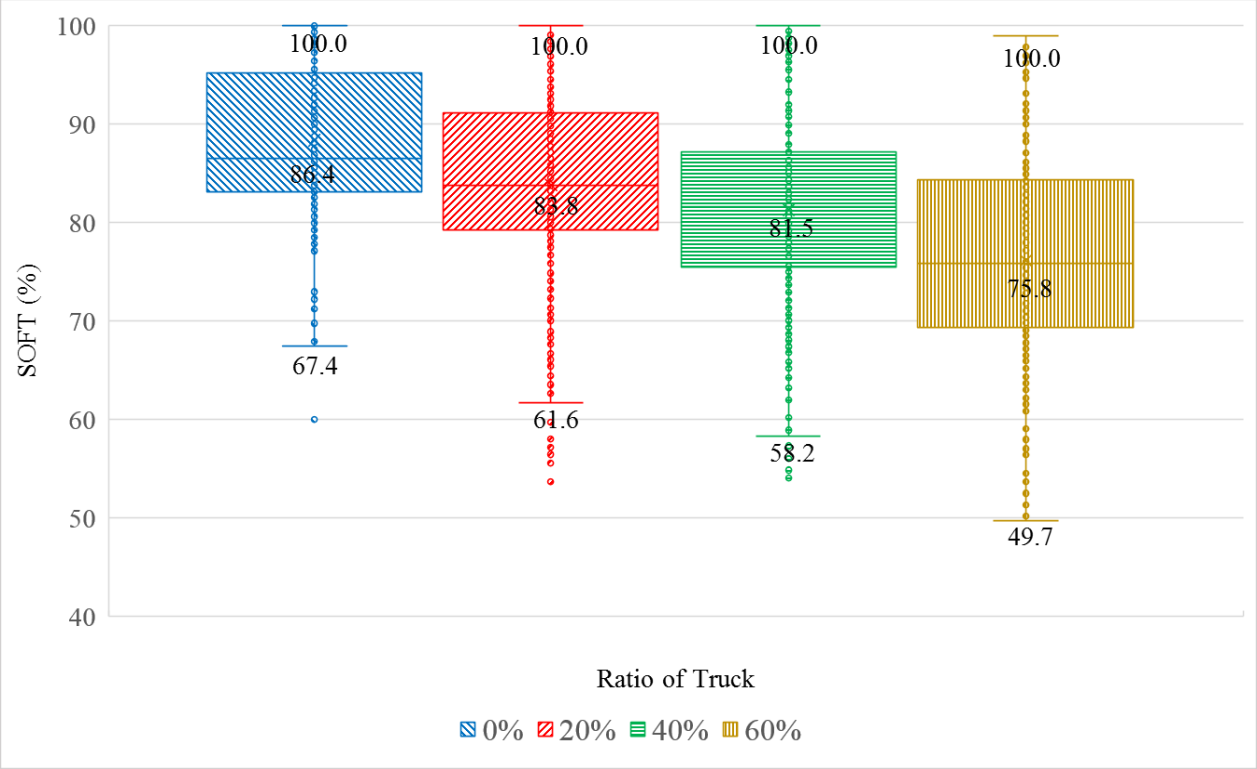

Figure 3-9 Box plot for the SOFT of coordination by different ratios of trucks among all vehicle input

Considering the lower demand volume assumed ("Medium") in this analysis, the ratio of trucks can have a critical effect on the smoothness of traffic flow and the impact can be as significant as the signal control strategy. This impact is due to the different dynamics of trucks, or transit vehicles, that can interfere with smooth progression of regular vehicles causing acceleration and deceleration. The differences in vehicle dynamics significantly impacts the traffic flow.

Further statistical analysis was conducted to compare the performance of each vehicle mode separately. The average SOFT values for each mode were compared using a paired-t test under different ratios of trucks. The null hypothesis of the test was that the mean SOFT values of each mode were equal. For a significance level of α = 0.05 (confidence level of 95%) with approximately 320 sample points, the p-values for each case are shown in Table 3-3. The results

indicate that the null hypothesis for all cases is rejected at the 5% significance level, which means that the mean values of two vehicle modes are significantly different regardless of the ratio of trucks.

Table 3-3 T-test for each case with 95% confidence level

Statistical result		20% of truck	40% of truck	60% of truck
Mean ($\bar{x}$)	Truck	82.691	81.247	76.561
	Regular vehicle	84.064	81.209	75.416
Standard deviation	Truck	12.300	10.712	10.576
	Regular vehicle	9.621	10.254	10.487
P-value		7.3156e-66	7.6681e-26	1.8773e-16
Result		Reject the null hypothesis	Reject the null hypothesis	Reject the null hypothesis

3.3 Summary

This chapter presented a quantitative analysis of smooth progression in terms of the speed variation of vehicles. A new measure, Smoothness Of the Flow of Traffic (SOFT), was used to evaluate how smoothly a vehicle, or platoons of vehicles, progresses through a corridor based on the frequency content of the vehicle speed. This new measure can be computed using data from Connected Vehicle and can help determine the quality of progression along a coordinated route. In addition, a multi-modal investigation into the impact of vehicle mode was conducted. The results showed that as the percentage of trucks in the traffic stream increased, the average SOFT value became significantly lower indicating the impact of mixed mode operations. This indicates the potential

need for traffic signal coordination plans that consider the different modes and possibly other traffic control measures to help smooth the flow of the traffic stream. The analysis and measurements were conducted using microscopic traffic simulation (VISSIM) and Connected Vehicle technology that will be deployable in the very near future.

Chapter 4 Multi-modal system-wide evaluation of traffic signal coordination

A systematic investigation of traffic signal coordination is conducted to analyze the benefits and impacts on the entire system using the vehicle time spent in the system as the basis of the analysis. The system-wide evaluation in this chapter is two-fold. First, this chapter conducts an analysis of system-wide performance based on traffic routes and volumes. The analysis addresses systematic consideration of the performance of coordinated signal systems as viewed by vehicles on the coordinated route(s) and those on the non-coordinated routes. The relationship between the optimization performance index and the actual impact on vehicles that are served by the coordinated phase(s) and those that are served by the non-coordinated phases is studied. Secondly, the chapter investigates how multimodal traffic composition systematically affects the performance of coordination. In order to conduct both analyses, the average time that vehicles spend in the traffic system is defined and utilized as the assessment measure.

Section 4.1 introduces the concept of "time spent in the traffic system" using Little's Theorem and Section 4.2 introduces the results of two analyses, including analysis of route and volume and analysis of multimodality.

4.1 Methodology

4.1.1 Little's theorem in a traffic system

Queueing theory deals with system operations when customers may have to wait before obtaining service (Bertsekas et al. 1992). In the context of a traffic signal system, vehicles traveling along

an arterial that have to wait for a green indication at a signalized intersection are analogous to customers in a queueing system. At a single intersection, service time depends on several factors including the phase green time of the signal, queueing dynamics of vehicles including slowing or stopped time, and start up and acceleration time. When an arterial is considered as a system, the expected time spent in the system will include both the travel time and travel dynamics.

Let $\alpha(t)$ represent the number of vehicle arrivals to the system up to time t. $N(t)$ represents the number of vehicles in the system at time t, and T_i represents the time spent in the system by the i^{th} vehicle. The average number of vehicles in the system observed up to the time *t* is:

$$N_t = \frac{1}{t}\int_0^t N(\tau)d\tau \tag{1}$$

When the system is in steady-state, N_t can be considered as the steady-state average, N, defined as,

$$N = \lim_{t\to\infty} N_t \tag{2}$$

The average time spent in the system per vehicle in the interval [0, t], T_t, is defined as

$$T_t = \frac{\sum_{i=0}^{\alpha(t)} T_i}{\alpha(t)} \tag{3}$$

The steady-state time average of each vehicle is similarly defined as

$$T = \lim_{t\to\infty} T_t \tag{4}$$

The time average arrival rate of vehicles to the system in the interval [0, t], λ_t, is defined as

$$\lambda_t = \frac{\alpha(t)}{t} \tag{5}$$

In the same way, the steady-state arrival rate is defined as

$$\lambda = \lim_{t \to \infty} \lambda_t \tag{6}$$

From the variables defined above, Equation 7, known as Little's theorem, is defined as

$$N = \lambda \cdot T \tag{7}$$

For a traffic queueing system in steady-state, Little's theorem enables one to determine the average vehicle time spent in the system, T, by knowing the number of vehicles in the system and the arrival rate to the system.

The key point is to determine, $N(t)$, which is the number of vehicles in the system at time *t*. Connected vehicle technology makes it possible to observe $N(t)$ on each route or for each vehicle mode with specific time steps. Of course, market penetration of connected vehicles impacts observation of $N(t)$, but 100% penetration rate will be assumed for this analysis, and partial observation, or lower market penetration rates, will be addressed in future research. In this chapter, the vehicle trajectory awareness component takes a snapshot on current vehicles' state (approach and mode) at each intersection every 5 seconds and saves them for one and a half hours. Based on GPS location and heading information of each connected vehicle, the vehicle trajectory awareness determines a current approach and the corresponding requested signal phase that each vehicle is taking, and adds the information to the trajectory of each vehicle. Next, the saved trajectory data from five intersections are processed in MATLAB. Based on the requested signal phase

information and each vehicle's ID, the path from entry to exit that each vehicle took while present in the system is obtained, and $N(t)$ is determined on each route or in the entire system. Finally, the average number of vehicles on each route, or in the entire system, N , is calculated over the entire analysis time period.

4.1.2 Time spent in the traffic system

Using connected vehicle data, the time spent in the traffic system is used to analyze the effect of coordination on a system. Many studies have been conducted to measure traditional travel time using Global Positioning System (GPS) (Quiroga and Bullock 1998) and vehicle re-identification techniques (Coifman 1998; Kwong et al. 2009). Day et al (2010) estimated travel time using midblock and intersection Bluetooth probe sensors to evaluate the effect of offset changes. Connected vehicles provide high fidelity data that make it possible to conduct a systematic analysis considering multiple vehicle routes, modes (e.g. truck, bus, and regular vehicle), and traffic volumes. The average number of vehicles and the associated time spent in the system, based on Littles' theorem, can be directly measured. This measure also makes it possible to perform a multi-modal assessment of coordination on the entire system.

To differentiate the impact of coordination on the vehicle movements, routes are categorized into three types: coordinated (eastbound in this study), uncoordinated (westbound), and side street routes. The red dotted line of eastbound direction in Figure 4-1 represents the coordinated route, which considers only vehicles that traverse through all the intersections. The other red dotted line that moves in the opposite direction is the westbound route, which is not coordinated. Other routes are considered as side street routes.

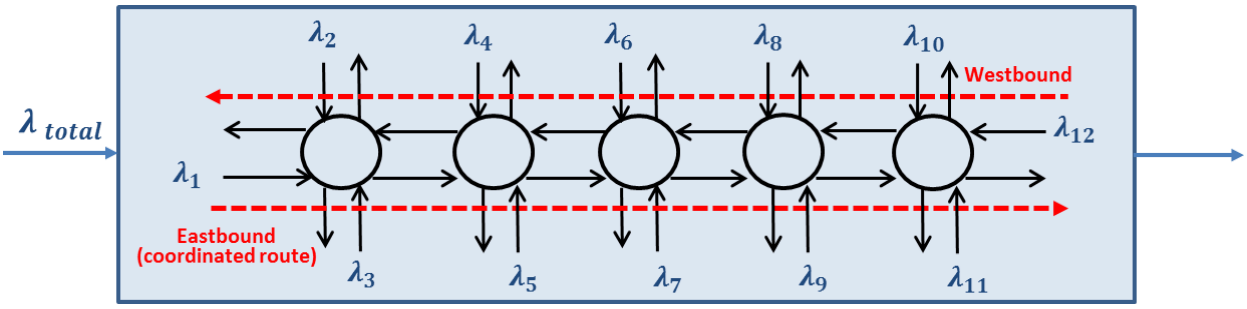

Figure 4-1 A traffic system with several intersections

As shown in Figure 4-1, λ_i represents the arrival rate (vehicle per hour) at each vehicle input (i) to the traffic system. $\lambda_1 = \lambda_E$ is the arrival rate at the eastbound route (coordinated route), while $\lambda_{12} = \lambda_W$ is the arrival rate for the westbound route. The remaining arrival rates from λ_2 to λ_{11} represent the arrival rates at each side street, respectively. Assume N_E and N_W represent the average number of vehicles on the eastbound (coordinated route) and westbound, respectively. Given the arrival rate and average number of vehicles on each route, the average time spent on both routes, T_E, T_W, can be determined by Little's theorem as follows:

$$T_E = N_E / \lambda_E \tag{8}$$

$$T_W = N_W / \lambda_W \tag{9}$$

For the case of side street routes, where vehicles arrive at n different nodes (for n = 2,…,11), the corresponding arrival rates λ_{SI}, can be calculated as follows:

$$\lambda_{SI} = \sum_{i=2}^{11} \lambda_i \tag{10}$$

Given N_{SI}, which represents the average number of vehicles on side street routes, T_{SI} can be determined similarly,

$$T_{SI} = N_{SI} / \lambda_{SI} \tag{11}$$

Since $N = N_E + N_W + N_{SI}$ and $\lambda = \lambda_E + \lambda_W + \lambda_{SI} = \lambda_E + \lambda_W + \sum_{i=2}^{11} \lambda_i$, then Little's theorem ($N = \lambda \cdot T$) yields,

$$N_E + N_W + N_{SI} = (\lambda_E + \lambda_W + \sum_{i=2}^{11} \lambda_i) \cdot T \tag{12}$$

$$N_E + N_W + N_{SI} = \lambda_E \cdot T + \lambda_W \cdot T + \lambda_{SI} \cdot T \tag{13}$$

Finally, the time spent in the entire system, T, is determined by,

$$T = (N_E + N_W + N_{SI}) / (\sum_{i=1}^{12} \lambda_i) \tag{14}$$

Note that T is not equal to $T_E + T_W + T_{SI}$.

4.2 Results of analysis

To conduct the systematic analysis, the same five intersections on El Camino Real in San Mateo in the previous chapter were modeled in VISSIM 6.00-19. The signals were controlled in fully actuated mode and in coordination mode on the eastbound travel direction with the associated traffic demands summarized in Table 4-1(a). The volume on the main street is changed from HIGH

to MED to LOW to illustrate different demand scenarios. Based on a dual-ring barrier control structure with eight phases, traffic control was implemented in the simulation model. To construct a connected vehicle environment, five virtual RSUs are installed and are connected to five Econolite ASC/3 SIL virtual signal controllers in VISSIM. The network was simulated under both coordination and free operation. The side street signals are actuated in both cases. Based on the HIGH demand scenario, a coordination plan for each intersection was generated by VISTRO as shown in Table 4-1(b). VISTRO is an optimization tool that uses a weighted sum of total vehicle delay and number of stops as the objective function. The optimal cycle length from the tool for all intersection was 100 seconds. Each simulation period was 5400 seconds with 1800 seconds of warm-up period and the simulation was replicated with ten different random seeds.

Table 4-1 Vehicle volume and Optimized coordination parameters from VISTRO

(a)

	Vehicle volume (Veh/hr)							
	Eastbound			Westbound			North bound	South bound
	HIGH	MED	LOW	HIGH	MED	LOW		
Int. 1001	2200	1100	5500	1600	800	400	600	600
Int. 1002							500	500
Int. 1003							250	250
Int. 1004							250	250
Int. 1005							700	650

(b)

	Coordination plan parameters								
	Offset	Phase split (cycle length : 100 seconds)							
		1	2	3	4	5	6	7	8
Int. 1001	0	13	35	27	25	13	35	-	-
Int. 1002	42	15	45	-	-	15	45	20	20
Int. 1003	61	11	49	20	20	11	49	-	-
Int. 1004	70	13	53	17	17	13	53	-	-
Int. 1005	97	13	39	24	24	13	39	-	-

4.2.1 Analysis of route and volume

4.2.1.1 System-wide performance by route and volume

The first analysis evaluated the effect of coordination on each route based on a single vehicle mode (regular passenger vehicles). The result shows the performance of coordination is changed by vehicle volume on the major street. Table 4-2 shows the performance of optimized coordination on the coordinated route for 10 simulation replications. With HIGH demand (Table 4-2(a)), the average time spent in the system on the eastbound direction decreased by 34.83% (where improvement percentages are shown in green and degradations in red) when comparing coordination with free operation. For the westbound route, the travel time in the system was reduced slightly from the free operation (-3.74%). Even for the side street routes, coordination reduced the time spent in the system by -5.51% over free operation. This improvement will be discussed in the next section. In the MED and LOW demand scenarios (Table 4-2(b) and 4-2(c)), coordination demonstrated superior performance along the coordinated route showing 26% to 29% improvement. However, the side street routes resulted in 8.09% and 16.96% increase in the average time in the system, respectively, which is a result of the reduced demand on the

coordinated movement when the signal is held green for the coordinated movement. Actuated operation can be more adaptive to fluctuation in traffic demand than coordination.

Table 4-2 Time spent in the system: (a) HIGH demand, (b) MED demand, (c) LOW demand
(a)

		Free operation			Coordination		
		Coordinated route (Eastbound)	Westbound	Side street	Coordinated route (Eastbound)	Westbound	Side street
λ (veh/sec)		0.39	0.19	1.76	0.39	0.19	1.76
Rep. 1	N (veh)	114.37	53.01	206.58	73.69	51.22	194.57
	T (sec)	296.92	304.52	115.58	191.30	294.25	108.87
Rep. 2	N (veh)	115.01	48.46	206.00	73.68	47.94	195.72
	T (sec)	298.57	278.36	115.26	191.28	275.37	109.51
Rep. 3	N (veh)	121.07	56.29	202.63	77.17	53.75	188.14
	T (sec)	314.32	323.38	113.38	200.34	308.79	105.27
Rep. 4	N (veh)	110.04	56.23	205.10	73.87	52.22	192.85
	T (sec)	285.68	323.04	114.76	191.78	300.00	107.91
Rep. 5	N (veh)	112.81	55.51	197.28	73.77	51.43	190.78
	T (sec)	292.87	318.88	110.39	191.51	295.41	106.75
Rep. 6	N (veh)	113.78	54.16	203.75	72.39	53.26	190.31
	T (sec)	295.39	311.11	114.01	187.94	305.97	106.49
Rep. 7	N (veh)	109.80	56.35	206.25	73.63	51.87	192.49
	T (sec)	285.07	323.68	115.40	191.15	297.99	107.71
Rep. 8	N (veh)	110.23	49.82	207.32	73.74	49.85	193.63
	T (sec)	286.17	286.21	116.00	191.45	286.37	108.34
Rep. 9	N (veh)	115.86	54.65	198.35	76.04	50.27	191.70
	T (sec)	300.80	313.93	110.98	197.41	288.80	107.26
Rep. 10	N (veh)	114.09	50.13	199.49	73.05	52.81	190.57
	T (sec)	296.20	287.95	111.62	189.64	303.35	106.63
Avg	**N (veh)**	**113.71**	**53.46**	**203.28**	**74.10**	**51.46**	**192.08**
	T (sec)	**295.20**	**307.11**	**113.74**	**192.38**	**295.63**	**107.47**
	Ratio				**-34.83%**	**-3.74%**	**-5.51%**

(b)

		Free operation			Coordination		
		Coordinated route (Eastbound)	Westbound	Side street	Coordinated route (Eastbound)	Westbound	Side street
λ (veh/sec)		0.20	0.09	1.52	0.20	0.09	1.52
Rep. 1	N (veh)	52.42	23.23	144.54	35.29	23.04	157.30
	T (sec)	267.48	251.11	95.28	180.09	249.13	103.68
Rep. 2	N (veh)	47.89	24.94	148.79	34.15	23.06	159.91
	T (sec)	244.36	269.62	98.08	174.29	249.28	105.41
Rep. 3	N (veh)	52.43	25.48	146.54	35.56	23.68	156.97
	T (sec)	267.52	275.50	96.59	181.45	256.00	103.47
Rep. 4	N (veh)	50.37	24.68	146.17	34.62	23.60	159.05
	T (sec)	257.01	266.79	96.35	176.67	255.18	104.84
Rep. 5	N (veh)	49.02	22.95	144.18	33.70	24.38	158.43
	T (sec)	250.15	248.05	95.04	171.97	263.55	104.43
Rep. 6	N (veh)	48.34	25.08	143.70	35.10	23.65	154.59
	T (sec)	246.67	271.10	94.72	179.12	255.73	101.90
Rep. 7	N (veh)	48.87	25.22	148.43	34.81	26.74	157.54
	T (sec)	249.37	272.70	97.84	177.65	289.11	103.84
Rep. 8	N (veh)	47.51	23.22	148.02	36.14	23.06	159.62
	T (sec)	242.45	251.06	97.57	184.42	249.25	105.21
Rep. 9	N (veh)	48.20	23.57	145.24	35.40	22.56	157.20
	T (sec)	245.98	254.83	95.74	180.63	243.84	103.62
Rep. 10	N (veh)	50.68	26.80	143.68	34.94	23.75	156.78
	T (sec)	258.62	289.69	94.71	178.30	256.79	103.34
Avg	**N (veh)**	**49.57**	**24.52**	**145.93**	**34.97**	**23.75**	**157.74**
	T (sec)	**252.96**	**265.04**	**96.19**	**178.46**	**256.79**	**103.97**
	Ratio				**-29.45%**	**-3.12%**	**+8.09%**

(c)

		Free operation			Coordination		
		Coordinated route (Eastbound)	Westbound	Side street	Coordinated route (Eastbound)	Westbound	Side street
λ (veh/sec)		0.10	0.05	1.40	0.10	0.05	1.40
Rep. 1	N (veh)	23.50	11.37	121.25	17.50	10.36	142.21
	T (sec)	239.83	245.83	86.76	178.60	223.98	101.77
Rep. 2	N (veh)	23.93	11.96	123.18	86.64	11.18	141.65
	T (sec)	244.17	258.63	88.15	169.55	241.78	101.36
Rep. 3	N (veh)	23.10	11.11	121.07	17.28	10.37	145.36
	T (sec)	235.71	240.14	86.64	176.31	224.14	104.02
Rep. 4	N (veh)	24.73	11.38	121.83	17.27	10.19	141.66
	T (sec)	252.37	245.98	87.18	176.24	220.43	101.37
Rep. 5	N (veh)	21.02	11.98	121.51	15.93	11.64	141.08
	T (sec)	214.57	259.10	86.95	162.53	251.77	100.95
Rep. 6	N (veh)	23.07	11.92	120.82	17.71	11.26	139.11
	T (sec)	235.40	257.73	86.46	180.74	243.42	99.55
Rep. 7	N (veh)	21.64	12.92	121.89	15.59	12.13	142.22
	T (sec)	220.83	279.39	87.22	159.14	262.33	101.77
Rep. 8	N (veh)	21.41	11.27	125.10	16.39	9.87	144.99
	T (sec)	218.46	243.73	89.52	167.29	213.39	103.75
Rep. 9	N (veh)	22.72	11.98	116.98	16.98	9.59	140.97
	T (sec)	231.82	259.04	83.71	173.32	207.37	100.88
Rep. 10	N (veh)	21.96	12.34	122.11	15.91	10.28	142.65
	T (sec)	224.10	266.89	87.38	162.41	222.37	102.08
Avg	**N (veh)**	**22.71**	**11.82**	**121.57**	**23.72**	**10.69**	**142.19**
	T (sec)	**231.73**	**255.65**	**87.00**	**170.61**	**231.10**	**101.75**
	Ratio				**-26.37%**	**-9.60%**	**+16.96%**

The system performance based on the original optimization is summarized in Table 4-3 and Figure 4-3. The results show that coordination outperforms free operation by 14.22% under HIGH demand. However, as the demand is lowered and the signal timing remains the same, the improvement is less and actually worse by 8.66% in the LOW demand scenario (Figure 4-3(a)). The point in Figure 4-3(a) where the coordination and free operation performance curves intersect is an indicator for traffic engineers to either stop running coordination or switch to a new coordination plan, since coordination is performing worse system-wide for demand below this point.

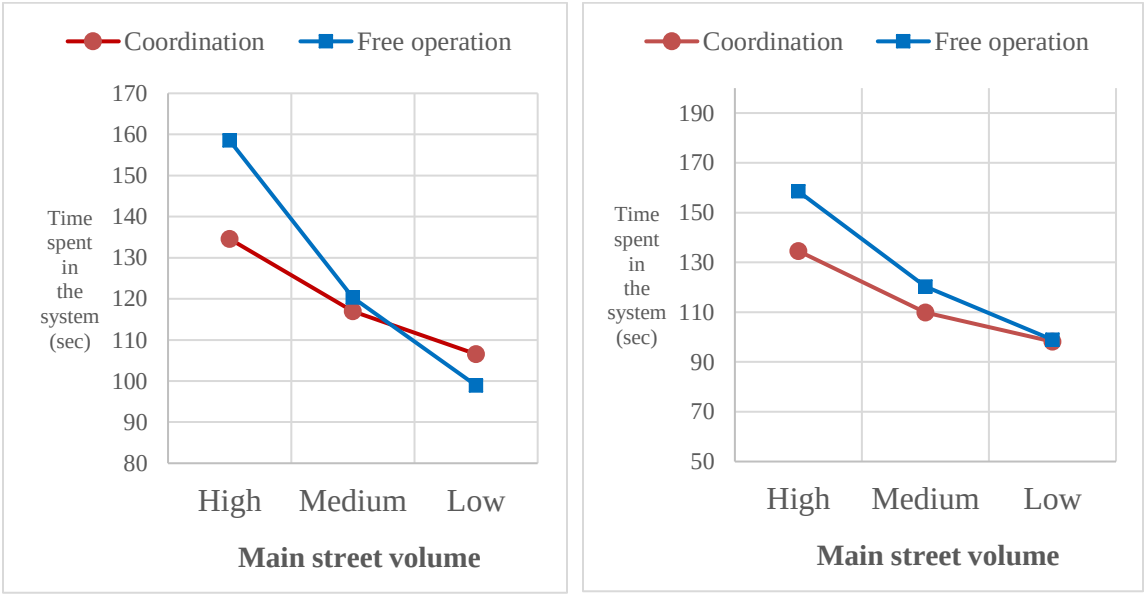

(a) **(b)**

Figure 4-2 Entire system performance: (a) Original optimization, (b) Re-optimization

Further analysis was conducted to determine the effect of coordination with re-optimized signal timing plans based on the different volumes. The signal plans, including split, offset, and cycle length, were re-optimized using the VISTRO based on each scenario volume (MED and LOW), respectively.

Table 4-3 System performance summary

Main street volume		HIGH		MED		LOW	
		Free operation	Coordination	Free operation	Coordination	Free operation	Coordination
Original optimization	N (veh)	370.17	317.53	219.90	216.37	156.00	169.51
	T (sec)	**157.76**	**135.32**	**121.79**	**119.84**	**101.19**	**109.95**
	Ratio		**-14.22%**		**-1.61%**		**+8.66%**
Re-optimization	N (veh)	370.17	317.53	219.90	202.07	156.00	155.76
	T (sec)	**157.76**	**135.32**	**121.79**	**111.92**	**101.19**	**101.03**
	Ratio		**-14.22%**		**-8.11%**		**-0.15%**

As a result of the re-optimization, the time spent in the system under the MED demand scenario, is improved from -1.61% to -8.11% (Table 4-3). Under the LOW demand scenario, re-optimization made coordination slightly better from +8.66% to -0.15%. However, it is still not superior to free operation from an overall system point of view. Figure 4-4 illustrates the performance of re-optimized coordination on each route. Under the MED demand scenario (Figure 4-4(a)) the coordinated route is slightly improved, however, the re-optimization significantly improved the side streets from 103.97 second to 87.76 second. The improvement in the LOW demand scenario is similar (Figure 4-4(b)). As mentioned before, although vehicles on the coordinated route spend less time in the system, the entire system performance does not benefit from coordination when the demand on the coordinated route is not significantly higher than on the side street routes or when the coordinated signal timing plan was developed for other demands.

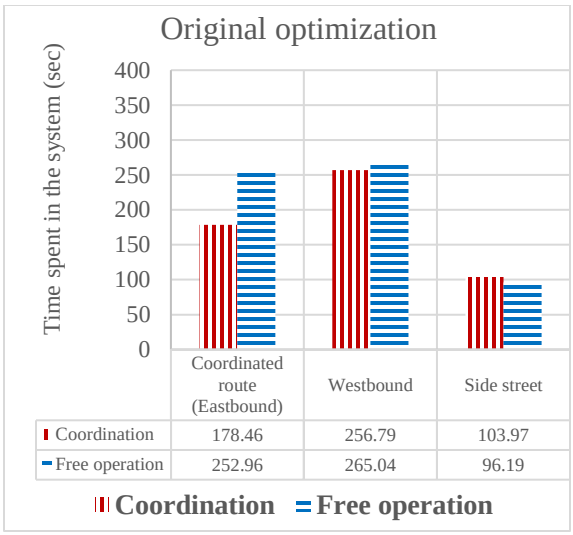

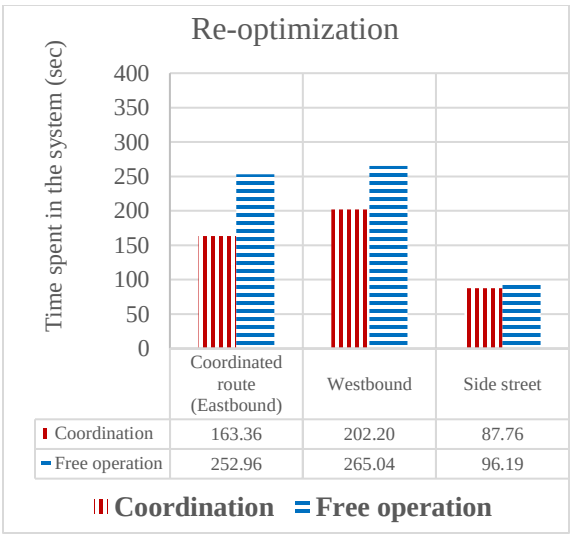

(a)

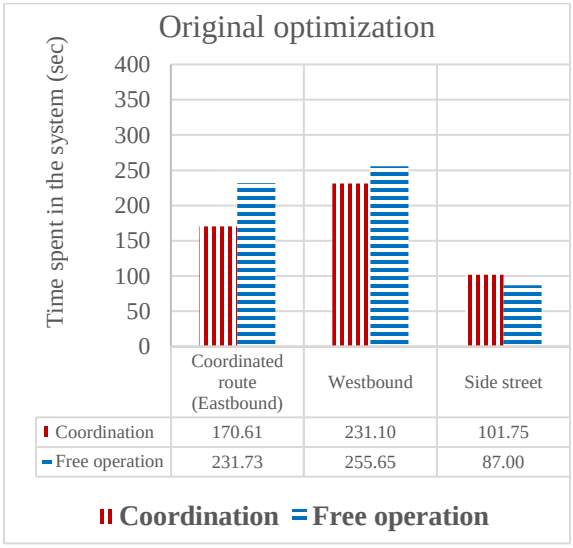

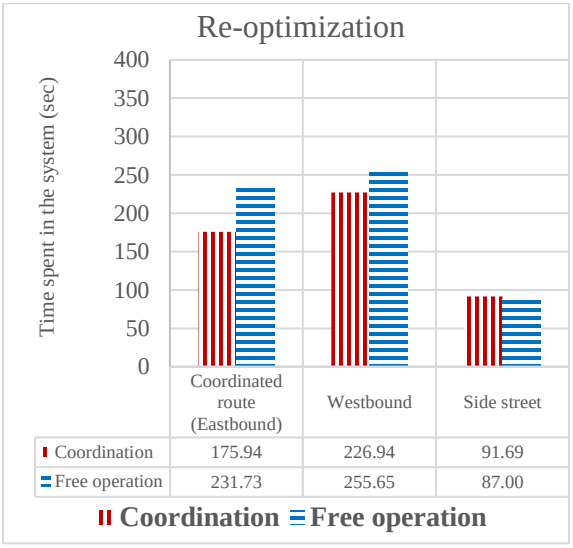

(b)

Figure 4-3 Comparison of performance of each route after re-optimization: (a) MED demand scenario, (b) LOW demand scenario

4.2.1.2 Decoupling coordinated and side street route flows

When the signals are coordinated, the performance on the side street routes is expected to be worse when compared to free operation. However, it was found that the side street routes under coordinated operation performed better by -5.51% than in free operation in the HIGH demand

scenario (Table 4-2(a)). This is due to a benefit that vehicles from the side streets gain when they join the coordinated route flow.

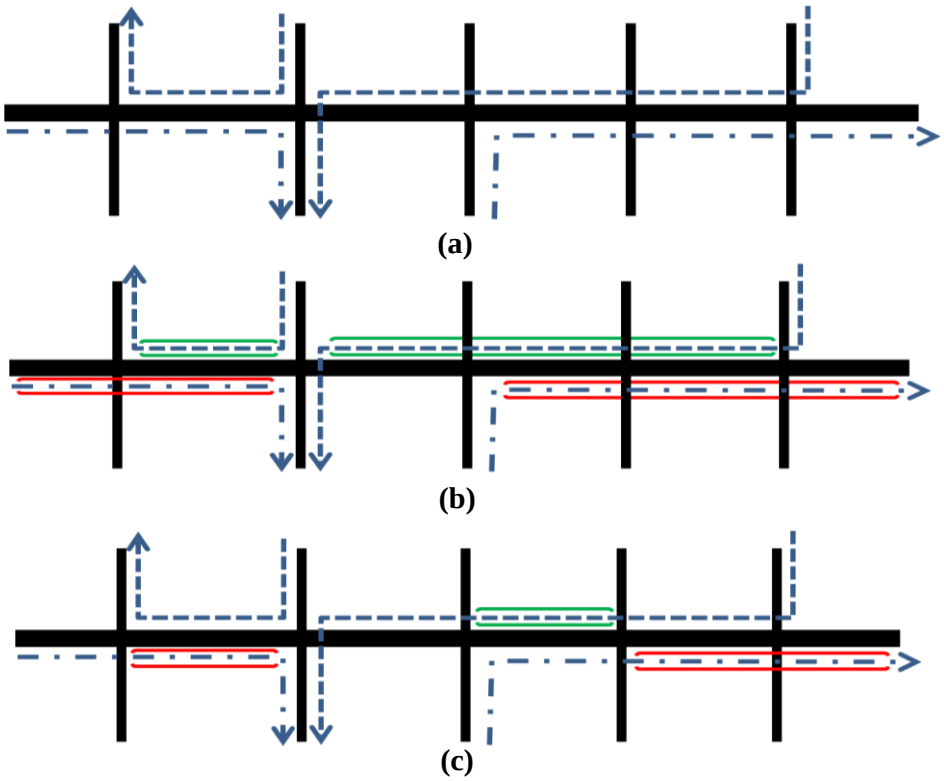

(a)

(b)

(c)

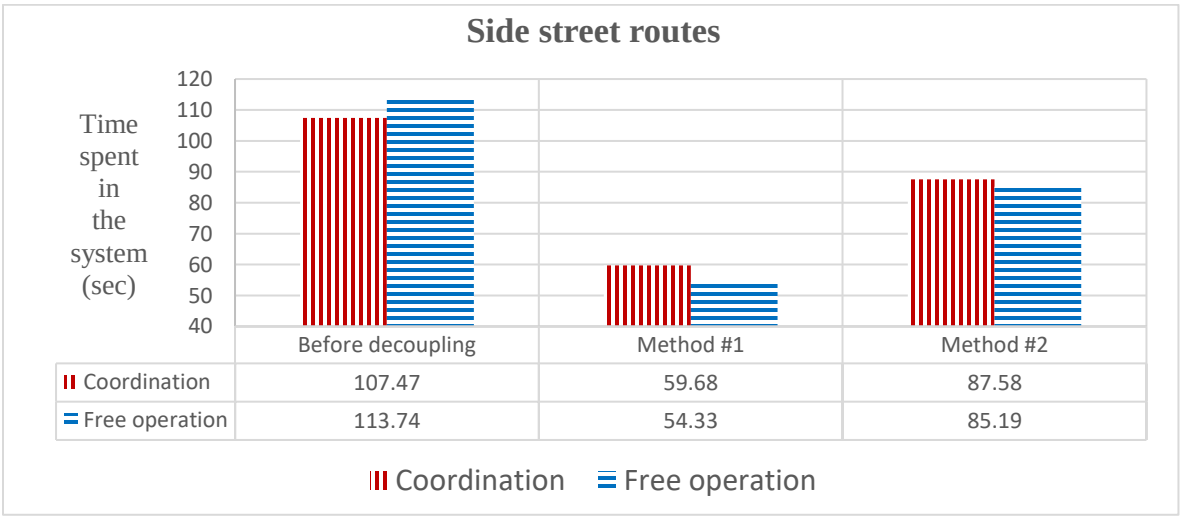

(d)

Figure 4-4 Classification by route: (a) Before decoupling, (b) Method #1, (c) Method #2, (d) Performance of the side street route(s)

Figure 4-5 shows two types of arrows to differentiate the eastbound (long-dotted arrow) and westbound (short-dotted arrow) routes. Any vehicles following routes shown as both types of arrow in Figure 4-5(a) are considered side street route vehicles in the previous analysis. The coordinated flows on the eastbound were considered to be only the vehicles that entered the coordinated phase at the first intersection and exited the coordinated phase at the last intersection. However, many of the vehicles on the side street routes benefit from the coordinated signals if the vehicles enter the coordinated route. Thus, part of the side street flows traveling the eastbound direction on the main street should be considered as part of the coordinated route flows for a more accurate analysis of the performance of coordination signal plans. Similarly, a few of the vehicles moving westbound on the main street should also be considered as part of the westbound route.

In order to account for this effect, the coordinated and side street route flows will be decoupled. The vehicles that traveled on the main street (eastbound and westbound) are categorized into two route flows: primary and secondary. All of the vehicles that were previously classified as “eastbound (coordinated route)” or “westbound” belong to a primary component. For the secondary component, two criterions were applied: method#1 and method #2.

Method #1 considers any side street vehicle that joins the eastbound or westbound route as being part of the routes as soon as it enters the main street. This behavior is illustrated in Figure 4-5(b) where the red or green sections indicate the route flow where side street vehicles are considered part of the eastbound or westbound flow, respectively.

Method #2 assumes that vehicles that start on a side street route and enter the eastbound or westbound route are not part of the route flow until they pass through at least one signal phase, respectively (Figure 4-5(c)). That is, when they turn onto the routes they are not part of the platoon flow until they pass through intersections on the same phase.

Figure 4-5(d) illustrates the differences in the time spent in the system for side street routes when the two re-classification methods are applied. The time spent in the system for the routes increases by 9.86% and 2.81%, respectively, when compared to free operation. The detailed results of the coordinated route performance including both primary and secondary component are shown in Table 4-4.

Table 4-4 Results of the decoupling methods

		Free operation			Coordination		
		Coordinated route (Eastbound)	West bound	Side street	Coordinated route (Eastbound)	West bound	Side street
Before decoupling (same as Table 4-2(a))	T (sec)	295.20	307.11	113.74	192.38	295.63	107.47
	Ratio				**-34.83%**	**-3.74%**	**-5.51%**
After Decoupling Method #1	T (sec)	325.60	336.12	54.33	214.11	321.69	59.68
	Ratio				**-34.24%**	**-4.29%**	**+9.86%**
After Decoupling Method #2	T (sec)	310.58	320.28	85.19	200.79	307.11	87.58
	Ratio				**-35.35%**	**-4.11%**	**+2.81%**

There are two ways to interpret this result. First, from a system perspective, coordination can benefit vehicles that enter the control section on the coordinated phase and vehicles that enter the control section from a non-coordinated phase of side street, but join the coordinated flow. This indicates that coordination can be beneficial to many vehicles in the control section. Second, when the route flows are decoupled so that the time in the system of the side street flow vehicles are considered, the impact of coordination of the side street vehicle flows are more correctly captured. The decision on when to use coordination would depend on the demand level, the distribution of route flows in the control section and the operating agency's policy about impact on side street, or local, traffic.

4.2.2 Analysis of multimodality

4.2.2.1 Configuration of Origin-Destination pair methodology

This section investigates the impact of multimodality on coordination by comparing it with free operation. To analyze the multimodal impact on the system, two modes of vehicle were used: regular passenger vehicles and trucks. The VISSIM simulation network that was used for the previous analysis was seeded with MED demand using an origin-destination (O-D) pair methodology instead of static route at each intersection. One hundred thirty two O-D pairs were generated in total. Table 4-5 shows each O-D pair volume, while Figure 4-6 presents node information, numbered from 1 to 12 along the corridor. As Figure 4-6 shows, only the 23 most critical O-D pairs were chosen among all O-D pairs due to space limitation. Each pair was assigned from 'A' to 'Z' according to its origin. The trucks were assumed to be traveling on the major street.

Table 4-5 Origin-Destination volume matrix (veh/hour)

Node	**1**	**2**	**3**	**4**	**5**	**6**	**7**	**8**	**9**	**10**	**11**	**12**	Vol.
1	0	110	110	22	22	38.5	38.5	22	22	27.5	27.5	660	1100
2	258	0	180	18	6	12	6	15	15	15	15	60	600
3	96	348	0	6	12	6	12	13.2	13.2	16.8	16.8	60	600
4	156	6	6	0	265	6	6	12	6	14.4	14.4	108	600
5	50	10	10	230	0	5	5	5	5	25.5	25.5	129	500
6	35	7.5	7.5	2.5	5	0	135	5	2.5	7.5	7.5	35	250
7	35	7.5	7.5	2.5	2.5	140	0	2.5	2.5	7.5	7.5	35	250
8	30	12.5	12.5	5	5	2.5	2.5	0	145	5	5	25	250
9	30	12.5	12.5	5	5	2.5	2.5	145	0	5	5	25	250
10	147	14	14	14	14	7	7	7	7	0	252	217	700
11	74.9	14	14	14	14	7	7	7	7	392	0	149	700
12	320	40	40	40	40	40	40	40	40	80	80	0	800

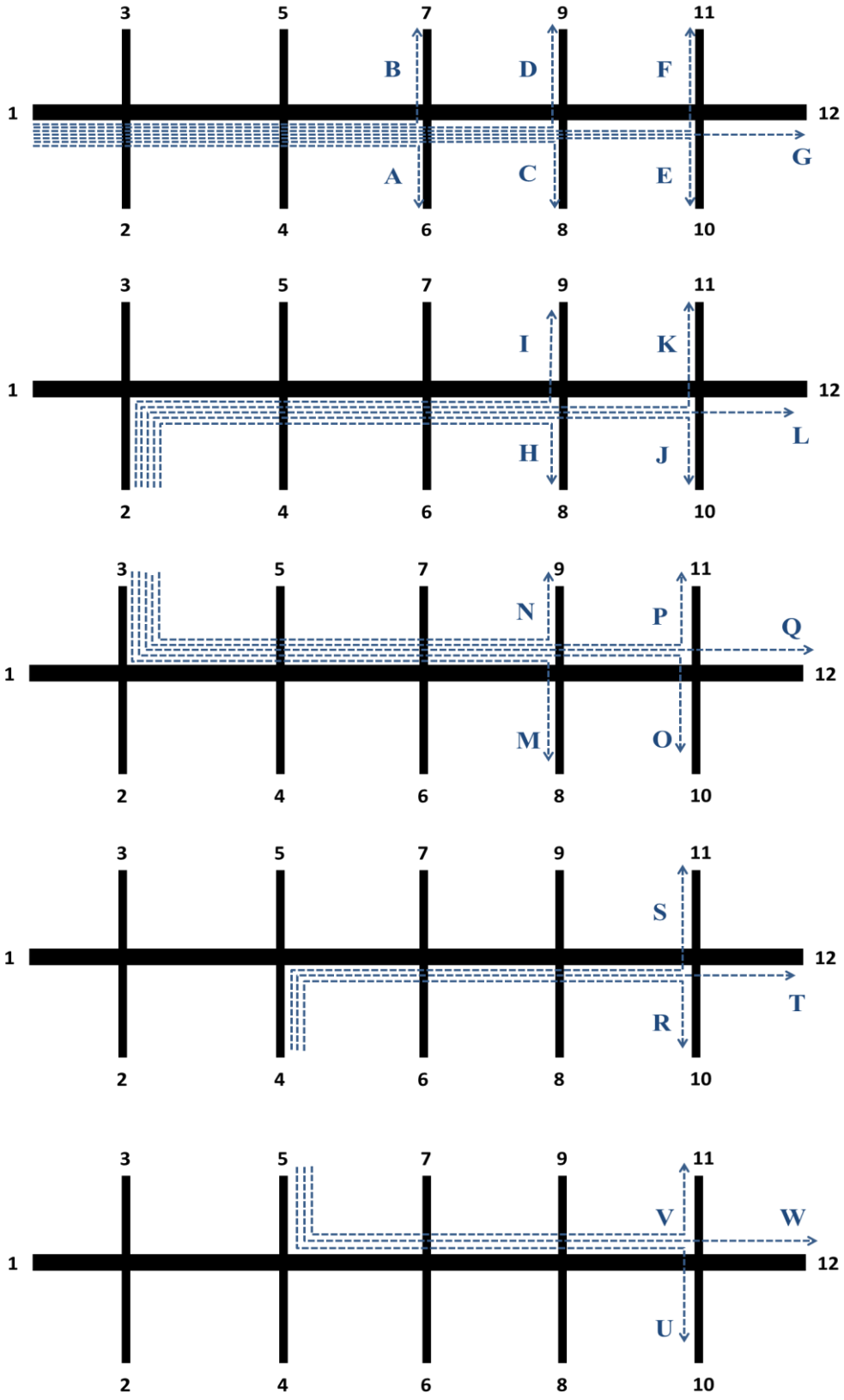

Figure 4-5 Critical O-D pairs chose from total 132 pairs

Different from the route and volume analysis, the average number of vehicles (N) by vehicle mode on each O-D pair can be obtained from connected vehicle data. Assume N_i^R and N_i^T represent the average number of vehicles for regular vehicle and truck, respectively, on each critical O-D pair (i). Given the arrival rate from the O-D matrix and average number of vehicles in the system, the average time spent in the system for each mode on each critical O-D pair, T_i^R and T_i^T can be determined by the Little's theorem.

$$T_i^R = \frac{N_i^R}{\lambda_i^R} \quad (\text{or } T_i^T = \frac{N_i^T}{\lambda_i^T}) \qquad (\text{for } i = \text{A},\ldots,\text{W}) \qquad (15)$$

4.2.2.2 Performance of critical O-D pairs

To test a variety of situations, the ratio of vehicle modes was changed under both coordination and free operation. The ratio of trucks travelling eastbound and westbound on a major street were increased in 20% increments from 0% to 60%, while the ratio of regular vehicles was decreased proportionally in the same manner. Figure 4-7 shows the performance of the critical O-D pairs under different truck ratios. It was observed that time spent in the system for both regular vehicles and trucks was increased with the increase in trucks no matter which signal control systems was operated. As expected, regular vehicle performance outperformed truck performance over all ratios. Significant performance differences between free operation and coordination in each case (ratio of trucks) still existed although the differences were reduced marginally.

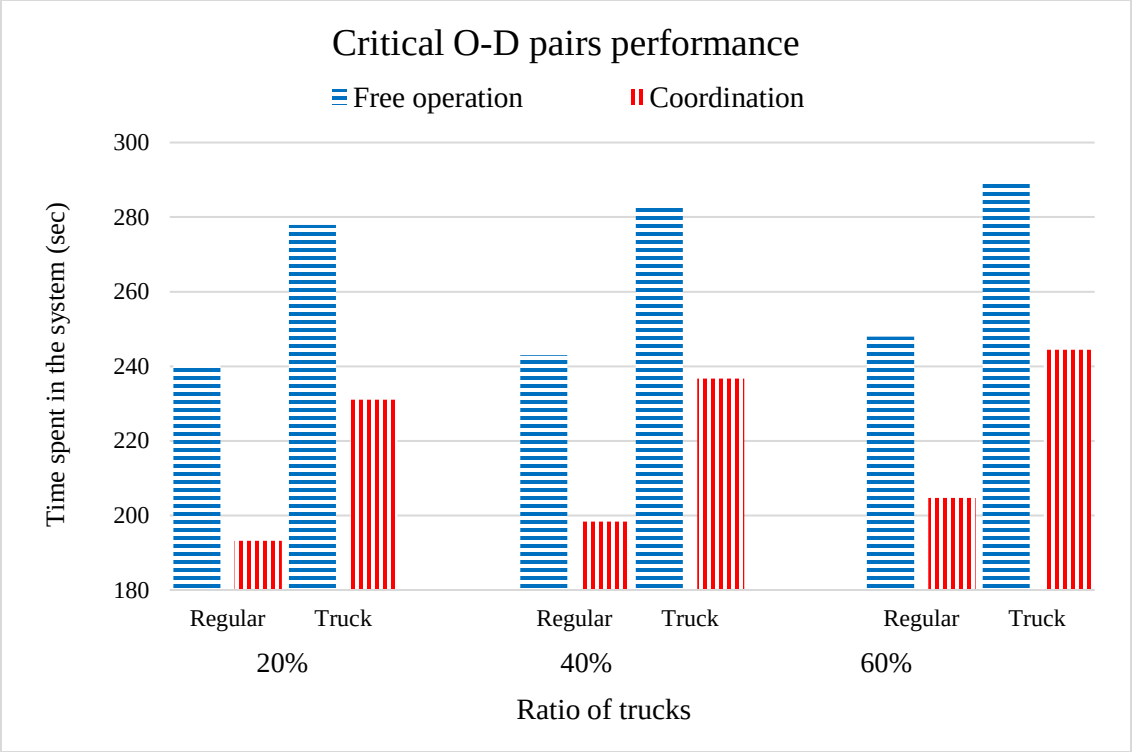

Figure 4-6 Time spent in the system for the 23 critical O-D pairs

As shown in Table 4-6(a), when the ratio of trucks increased, the difference in the performance of the regular vehicle between free operation and coordination was reduced from -21.75% to -17.44%. The same pattern was also observed in the performance of the truck. It also revealed that the modality has more impact on coordination than free operation. When comparing the performance in 20% of trucks to the performance in 60% of trucks (Table 4-6(b)), the difference in each mode during free operation was worse by +3.13% and +4.33%, respectively, while the performance during coordination was worse by +5.93% and +5.79%. The detailed performance of each critical O-D pair is shown in Table 4-7, where the performance of the truck is shown only from 'A' to 'G' because trucks traveled on the major street in the system.

Table 4-6 Comparison of time spent in the system for the 23 critical O-D pairs

(a)

		Free operation	Coordination	Difference
0% of trucks	Regular	238.86	186.91	**-21.75%**
	Truck	-	-	-
20% of trucks	Regular	240.39	193.23	**-19.62%**
	Truck	277.89	231.02	**-16.87%**
40% of trucks	Regular	242.94	198.37	**-18.35%**
	Truck	282.41	236.70	**-16.19%**
60% of trucks	Regular	247.92	204.69	**-17.44%**
	Truck	289.92	244.40	**-15.70%**

(b)

		20% of trucks	60% of trucks	Difference
Free operation	Regular	240.39	247.92	**+3.13%**
	Truck	277.89	289.92	**+4.33%**
Coordination	Regular	193.23	204.69	**+5.93%**
	Truck	231.02	244.40	**+5.79%**

Figure 4-8 demonstrates the entire system performance of both modes, including a total of 132 O-D pairs under each signal control strategy. Similar to the critical O-D pairs performance, the ratio of trucks had a significant effect on the performance of the entire system. A proportional rise in the performance of both signal control strategies was observed as the ratio of trucks was increased. An interesting observation was that the measure of coordination in the 60% of trucks ratio was almost the same as free operation without any of the trucks (0% of trucks). The coordination plan that was optimized assuming a unimodal condition does not seem to be working efficiently with a high ratio of trucks. If the trucks were assumed to be traveling on another critical O-D pair besides from ‘A’ to ‘G’, the difference would have increased.

Table 4-7 Time spent in the system on each critical O-D pair

Critical OD pair		0%	20%		40%		60%	
		Regular	Regular	Truck	Regular	Truck	Regular	Truck
FREE OPERATION	A	178.1	178.8	188.5	173.8	190.7	185.2	193.7
	B	198.1	208.3	233.9	220.0	233.9	228.6	244.7
	C	193.5	198.9	210.9	207.2	217.2	207.7	219.4
	D	205.7	213.1	232.7	213.8	232.7	231.5	246.0
	E	222.6	227.4	243.5	236.4	256.9	247.3	262.6
	F	258.7	266.4	296.0	268.8	290.0	285.4	301.8
	G	272.4	275.7	293.3	281.1	299.5	291.2	307.2
	H	205.2	204.9	-	208.5	-	218.2	-
	I	202.4	212.3	-	226.0	-	226.5	-
	J	224.2	226.4	-	238.6	-	251.4	-
	K	259.7	275.1	-	279.5	-	280.8	-
	L	270.3	276.4	-	284.2	-	293.2	-
	M	196.7	201.3	-	214.3	-	216.7	-
	N	211.3	219.1	-	224.5	-	239.8	-
	O	232.6	240.6	-	250.6	-	261.3	-
	P	254.2	270.4	-	285.1	-	288.4	-
	Q	273.3	283.5	-	290.1	-	298.0	-
	R	134.1	140.0	-	145.0	-	149.7	-
	S	168.2	174.4	-	173.2	-	190.6	-
	T	179.6	182.2	-	186.7	-	192.6	-
	U	160.6	163.3	-	173.8	-	181.6	-
	V	196.5	196.5	-	205.6	-	219.2	-
	W	204.2	206.5	-	212.9	-	222.6	-
COORDINATION	A	129.1	136.4	159.0	144.9	168.7	156.2	177.7
	B	181.5	184.3	197.1	186.4	204.6	190.5	208.3
	C	144.2	151.8	179.5	162.1	186.6	169.4	192.0
	D	180.9	185.7	211.3	196.1	220.1	205.9	229.0
	E	172.1	180.6	199.8	191.2	213.8	201.8	221.4
	F	221.3	225.4	267.5	233.9	270.4	248.0	272.9
	G	191.6	201.6	241.1	211.7	246.6	225.0	254.4
	H	164.5	166.2	-	168.1	-	174.0	-
	I	208.5	208.6	-	207.5	-	210.8	-
	J	193.5	197.7	-	200.9	-	208.0	-
	K	254.7	255.3	-	254.4	-	258.6	-
	L	213.3	216.6	-	219.6	-	226.2	-
	M	183.4	186.7	-	186.6	-	191.1	-
	N	232.9	233.2	-	231.7	-	233.7	-
	O	216.0	218.5	-	219.1	-	226.0	-
	P	273.1	273.0	-	273.4	-	275.0	-
	Q	232.1	235.2	-	238.0	-	243.9	-
	R	116.3	120.3	-	121.7	-	124.6	-
	S	170.3	173.6	-	174.2	-	177.4	-
	T	138.9	142.0	-	144.1	-	148.6	-
	U	162.6	165.5	-	168.0	-	171.5	-
	V	216.5	219.8	-	221.9	-	226.4	-
	W	184.0	187.0	-	188.4	-	192.0	-

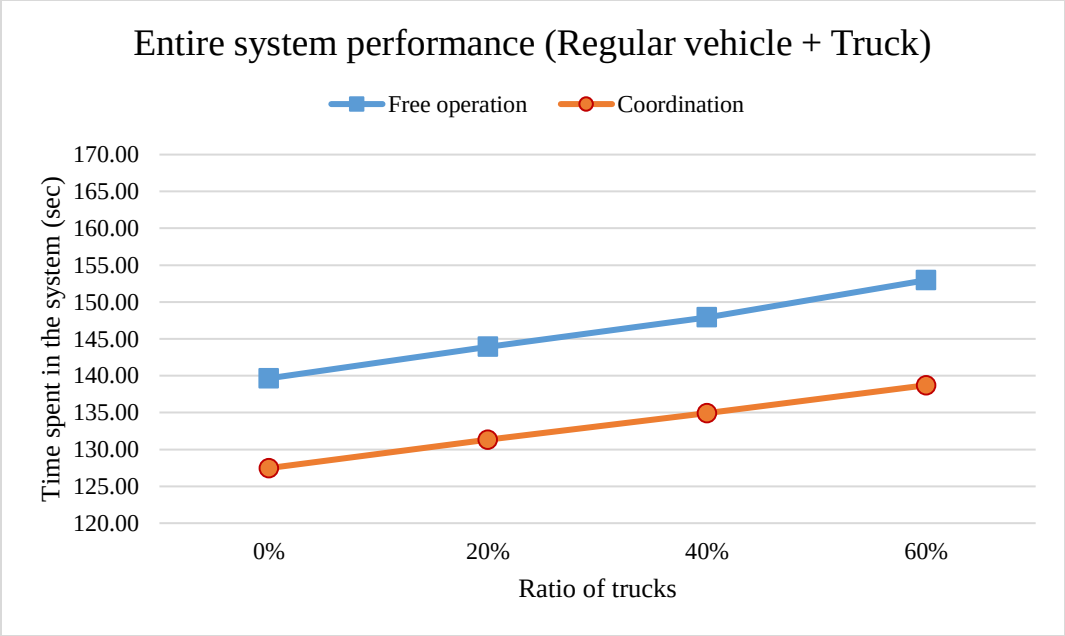

Figure 4-7 Time spent in the system for entire system including total O-D pairs (132)

4.2.2.3 Statistical analysis of O-D pairs performance

In order to compare the performance of each vehicle mode by ratio of trucks, a statistical analysis was conducted. The mean time spent in the system of each mode from ten replications was compared using a paired-sample t-test under different ratios of trucks and each signal control system. Table 4-8(a) reveals the results and shows whether the performance of two modes at each ratio of trucks is significant at the confidence level of 95% when comparing free operation with coordination, while Table 4-8(b) demonstrates the significance of the performance between 20% of trucks and 60% of trucks at each signal control system. The null hypothesis of the test was that the mean values of each mode were equal. All results in Table 4-8 indicate that the null hypothesis for all cases is rejected at the 5% significance level, which means that the difference of two vehicle modes at each case is significant. A similar result was observed in the entire system performance of both modes including all 132 O-D pairs during each signal control system (Table 4-8(c)).

Table 4-8 T-test for each case with 95% confidence level: (a) Comparison by each signal control from critical O-D pairs performance, (b) Comparison by ratio of trucks from critical O-D pairs performance, (c) Entire system performance (total O-D)

(a)

		P value	**Result** (Free operation → Coordination)
0% of truck	Regular	7.7509e-11	Reject the null hypothesis
	Truck	-	-
20% of truck	Regular	2.3107e-12	Reject the null hypothesis
	Truck	4.2224e-11	Reject the null hypothesis
40% of truck	Regular	5.2478e-10	Reject the null hypothesis
	Truck	8.1408e-09	Reject the null hypothesis
60% of truck	Regular	9.5486e-10	Reject the null hypothesis
	Truck	5.4968e-09	Reject the null hypothesis

(b)

		P value	**Result** (20% of truck → 60% of truck)
Free operation	Regular	0.0065	Reject the null hypothesis
	Truck	0.0034	Reject the null hypothesis
Coordination	Regular	3.1420e-09	Reject the null hypothesis
	Truck	9.8567e-06	Reject the null hypothesis

(c)

		P value	**Result** (Free operation → Coordination)
20% of truck	Regular + Truck	1.7450e-09	Reject the null hypothesis
40% of truck	Regular + Truck	4.6263e-10	Reject the null hypothesis
60% of truck	Regular + Truck	1.0245e-09	Reject the null hypothesis

4.3 Summary

This chapter presented a systematic analysis of traffic signal coordination in connected vehicle environment. The time spent in the system was used as the main performance indicator. First, a systematic investigation into the impact of coordination by each route was conducted when the signal timing was developed based on vehicle volume. The results showed that coordination performed system-wide better than free operation when traffic volume is medium or high on the main street. However, it was observed that there was a point below which performance of coordination is worse than free operation unless the signals were re-timed for the specific volume. The difference between free and coordinated operation was less under low volume conditions. Second, a multi-modal analysis of the performance of coordination on each O-D path was conducted. The ratio of trucks had significant effect on the performance of both coordination and free operation, and with a high ratio of trucks (60%), the coordination plan that was optimized for unimodal condition could not outperform free operation. All analyses were conducted using microscopic traffic simulation (VISSIM) and Connected Vehicle Technology (CVT).

Chapter 5 Adaptive optimization of traffic signal coordination

This chapter presents a methodology that integrates coordination with adaptive signal control using data from connected vehicles. The optimization framework consists of two levels: intersection and corridor. Section 5.1 introduces the system overview, and Section 5.2 and 5.3 introduces the intersection and corridor level control system, respectively. In Section 5.4, the performance of the model is validated by a VISSIM simulation experiment by comparing various performance measures under different market penetration rates of connected vehicles.

5.1 System overview

This section provides an overview of the model implementation. Figure 5-1 presents the platform of the adaptive coordination system, which can be implemented in both simulation and real traffic networks. In the VISSIM simulation environment, the drivermodel.dll API (Feng et al. 2015a) is used to generate BSMs. The intersection level control consists of several components including Vehicle Trajectory Awareness, Adaptive Control Algorithm, Coordinator, and Traffic Controller Interface, all of which are processed by the RSU at each intersection. The Offset refiner component is located at corridor level, and is responsible for optimization of the coordination offsets for all intersections in the control group.

First, the Vehicle Trajectory Awareness component decodes the BSMs from the OBUs and constructs vehicle arrival data including the desired signal phase, location, and estimated time of arrival of each vehicle at the stop bar. Based on the vehicle arrival data and coordination constraints

from the Coordinator component, the Adaptive Control Algorithm component optimizes the signal timing by solving a dynamic program (DP). Coordination constraints include the time left to the offset reference point in every cycle.

After running a traffic network for a certain period of time, the average traffic flow data from the Vehicle Trajectory Awareness component is sent to the Offset Refiner component, which uses an optimization solver, such as CPLEX ("CPLEX Optimizer Manual" 2015) or GLPK ("GLPK Reference Manual" 2012), to solve a MILP to get optimal offset values. The optimal offset values are sent back to Coordinator components at each intersection. Based on the optimal offsets, the Coordinator updates the coordination constraints and the Adaptive Control Algorithm applies the updated constraints to the phase allocation optimization.

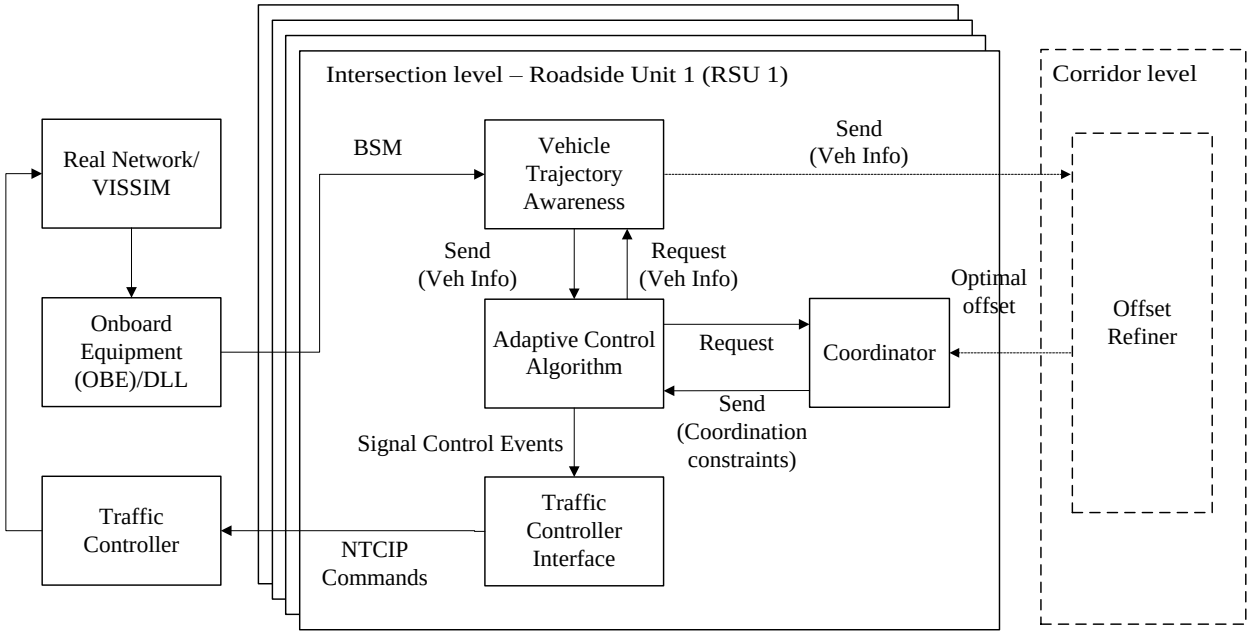

Figure 5-1 Platform overview

Every two seconds the Adaptive Control Algorithm component creates the optimal phase duration signal plan. The signal plan is sent to the signal controller through the Traffic Controller Interface

component using NTCIP (“NTCIP 1202, National Transportation Communications for ITS Protocol Object Definitions for Actuated Traffic Signal Controller (ASC) Units, v02.19. November 2005.” n.d.)commands including Vehicle Call, Force-off, and Hold.

5.2 Intersection level control system

5.2.1 Coordination-based adaptive control

The original Adaptive Control Algorithm developed by Feng et al. (Feng et al. 2015a) used total vehicle delay based on predicted vehicle arrivals as the objective of the optimization. First, an arrival table is defined as a two dimensional matrix of time and phase to serve as the input to the dynamic program. Next, based on the phase duration in each controller barrier group, the total vehicle delay was calculated as the summation of queue length of each phase over time. However, the arrival table did not consider the accumulated delay for vehicles that were already stopped in the queue. The arrival table treated all stopped vehicles the same and did not consider how long the vehicles had been stopped. Total vehicle delay may not result in a solution that is fair to all vehicles. It is possible that one phase may be delayed much longer than another because of low demand. The original algorithm was solved only once at the beginning of each barrier group.

Due to the limited DSRC range and fluctuating flow patterns, it is necessary to solve the optimization more frequently. In this chapter, instead of minimizing total vehicle delay from the arrival table, average delay of individual vehicles is considered using the stopped time of each vehicle from the connected vehicle trajectory data. The algorithm is solved every 2 seconds or at the end of each barrier, whichever occurs first.

Coordination is integrated with the Adaptive Control Algorithm and an extended delay function. The objective function of the integrated algorithm is based on fixed force-off

coordination. The coordination constraints are updated every time the optimization problem is solved. The constraints are initially based on the phase split sets and offset values optimized by VISTRO ("PTV Vistro - the traffic engineering tool" n.d.), and are updated through the corridor level optimization. VISTRO uses a weighted sum of total vehicle delay and number of stops as the objective function. A typical coordination plan is based on phase splits, which determine the force-off points for each phase. On the other hand, adaptive signal control determines the phase service durations constrained by minimum and maximum green time. To integrate coordination with adaptive signal control, minimum and maximum green times are adjusted based on the initial splits generated by VISTRO.

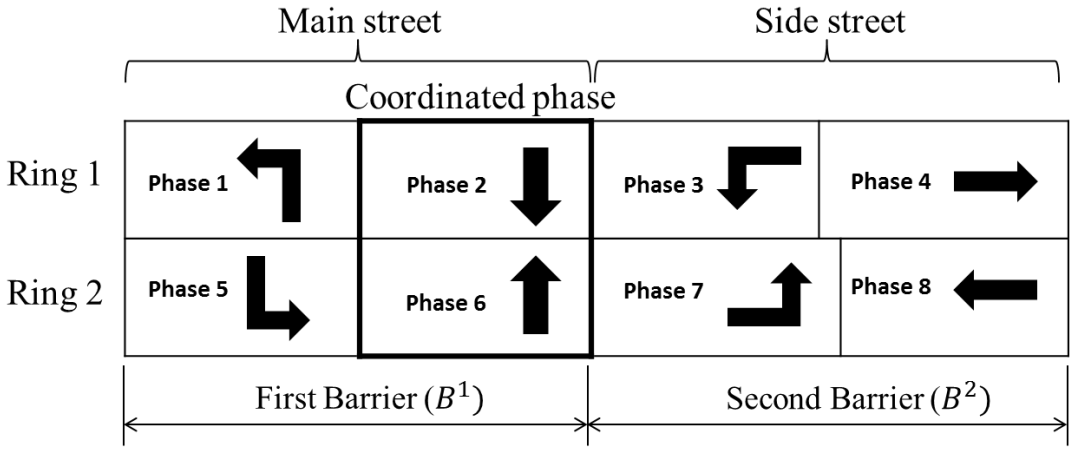

Figure 5-2 Phase and ring signal structure

As Figure 5-2 illustrates, the algorithm is designed based on a standard NEMA dual-ring-barrier structure.

The following notation is used in the model formulation:

i = Phase index

j = Index of each stage in the DP.

cp : Coordinated phase in the same ring (ncp : non-coordinated phases in the same ring)

Sp^i = Split time for phase i

B_{min}^{j} = Minimum barrier length of stage j

B_{max}^{j} = Maximum barrier length of stage j

$G_{min}^{p,r}$ = Minimum green time of phase p in ring r (G_{min}^{i} for phase $i = 1,2,3,\ldots,8$)

$R_{p,r}$ = Phase clearance interval of phase p in ring r (R_i for phase $i = 1,2,3,\ldots,8$)

$GE_{p,r}$ = Elapse Green time of phase p in ring r

$\emptyset$ **:** Offset reference point

$t_{\emptyset}$ = Time left to offset reference point

$t_{\bar{\emptyset}}$ = Time spent after offset reference point

X_j = The optimal barrier length at stage j

p' = Platoon length (sec)

q' = Platoon height (flow rate, veh/sec)

$A(t)$ = Total number of stopped vehicles at the stop bar at the input link at time t

$B(t)$ = Total number of approaching vehicles that will arrive before the queue dissipation at time t

s = Saturation flow rate (0.5 veh/sec)

l = Number of lanes

β = Travel time factor

α = Platoon dispersion factor

F = Smoothing factor

T = Time lag = $\beta \cdot t_a$

t_a = Average travel time

σ = Standard deviation of travel time

$q_a(t)$ = Arrival flow at the downstream intersection at time t

$q_d(t)$ = Departure flow at the upstream intersection at time t

γ_{mn} = Arrival time of the platoon's leading vehicle at the stop bar, measured in relative time to the start of green on the link (m, n)

δ = Residual queue clearance time

y = Ratio of platoon flow to saturation flow rate = q'/s

$Q(t)$ = Queue length of stopped platoon at time t

t_0 = Dissipating time of stopped platoon at the stop bar

$\emptyset_{mn}$ = Offset at the intersection j facing the link (m, n)

τ_{mn} = Travel time of the platoon's leading vehicle on the link (m, n)

g_{mn} = Green duration at the intersection j facing the link (m, n)

f_{mn} = Average flow on the link (m, n)

$A = \{\}$: Set of links of an arterial

K_{mn} = The number of linear segments for the link (m, n)

The minimum green times, (G^2_{min}, G^6_{min}), of the coordinated phases are assumed to be equal to the initial split (Sp^2, Sp^6) less the phase change interval. The maximum green times, (G^2_{max}, G^6_{max}), of the coordinated phases are assigned the extra time in the cycle based on the cycle length less the total of the minimum green times and phase change intervals of all non-coordinated phases (ncp) in the same ring. The minimum and maximum green times are defined in Equations 1 ~ 4. The change interval, R_j, is assumed to include the yellow change and red clearance time.

$$G^2_{min} = Sp^2 - R_2 \quad (1)$$

$$G^6_{min} = Sp^6 - R_6 \quad (2)$$

$$G^2_{max} = \mathrm{C} - R_2 - \textstyle\sum_{i \in ncp}(G^i_{min} + R_i) \quad (3)$$

$$G^6_{max} = \mathrm{C} - R_6 - \textstyle\sum_{i \in ncp}(G^i_{min} + R_i) \quad (4)$$

Under the fixed force-off option, if one non-coordinated phase gaps out, the extra time is assigned to the next phase in the sequence. Based on this logic, the non-coordinated phases have the following maximum green time.

$$G_{max}^{3} = (Sp^{3} - R_{3}) + (Sp^{4} - R_{4} - G_{min}^{4}) \quad (5)$$

$$G_{max}^{4} = (Sp^{3} - R_{3} - G_{min}^{3}) + (Sp^{4} - R_{4}) \quad (6)$$

$$G_{max}^{7} = (Sp^{7} - R_{7}) + (Sp^{8} - R_{8} - G_{min}^{8}) \quad (7)$$

$$G_{max}^{8} = (Sp^{7} - R_{7} - G_{min}^{7}) + (Sp^{8} - R_{8}) \quad (8)$$

$$G_{max}^{1} = (Sp^{1} - R_{1}) + (Sp^{3} - R_{3} - G_{min}^{3}) + (Sp^{4} - R_{4} - G_{min}^{4}) \quad (9)$$

$$G_{max}^{5} = (Sp^{5} - R_{5}) + (Sp^{7} - R_{7} - G_{min}^{7}) + (Sp^{8} - R_{8} - G_{min}^{8}) \quad (10)$$

The algorithm solves the optimization problem every 2 seconds to include recent vehicle arrivals. Barrier constraints are updated to reflect changes in the elapsed green time, denoted $GE_{r,p}$ for ring r and phase p. Equations 11 – 13 describes the barrier constraints. In the first stage (barrier) of the DP, the minimum and maximum green time can be flexible due to the elapsed green times of phases that are currently serving, Equation 11 and 12 define how the barrier constraints are calculated for the first and second phase respectively in the first stage. Equation 13 shows the barrier constraints calculation for later stages.

$$\begin{aligned} B_{min}^{1} &= \max\{\max\{0, G_{min}^{1,1} - GE_{1,1}\} + R_{1,1} + G_{min}^{2,1} + R_{2,1}, \max\{0, G_{min}^{1,2} - GE_{1,2}\} + R_{1,2} + G_{min}^{2,2} + R_{2,2}\} \\ B_{max}^{1} &= \max\{\max\{0, G_{max}^{1,1} - GE_{1,1}\} + R_{1,1} + G_{max}^{2,1} + R_{2,1}, \max\{0, G_{max}^{1,2} - GE_{1,2}\} + R_{1,2} + G_{max}^{2,2} + R_{2,2}\} \end{aligned} \quad (11)$$

$$\begin{aligned} B_{min}^{1} &= \max\{\max\{0, G_{\min}^{2,1} - GE_{2,1}\} + R_{2,1}, \max\{0, G_{\min}^{2,2} - GE_{2,2}\} + R_{2,2}\} \\ B_{max}^{1} &= \max\{\max\{0, G_{\max}^{2,1} - GE_{2,1}\} + R_{2,1}, \max\{0, G_{\max}^{2,2} - GE_{2,2}\} + R_{2,2}\} \end{aligned} \quad (12)$$

$$\begin{aligned} B_{min}^{2} &= \max\{G_{min}^{1,1} + R_{1,1} + G_{min}^{2,1} + R_{2,1}, G_{min}^{1,2} + R_{1,2} + G_{min}^{2,2} + R_{2,2}\} \\ B_{max}^{2} &= \max\{G_{max}^{1,1} + R_{1,1} + G_{max}^{2,1} + R_{2,1}\ G_{max}^{1,2} + R_{1,2} + G_{max}^{2,2} + R_{2,2}\} \end{aligned} \quad (13)$$

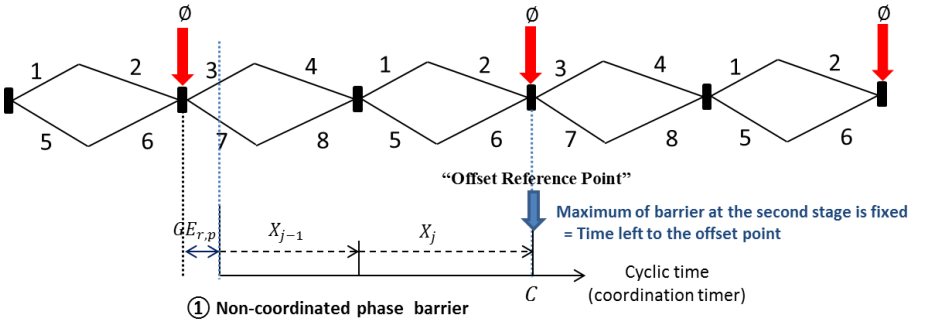

(a)

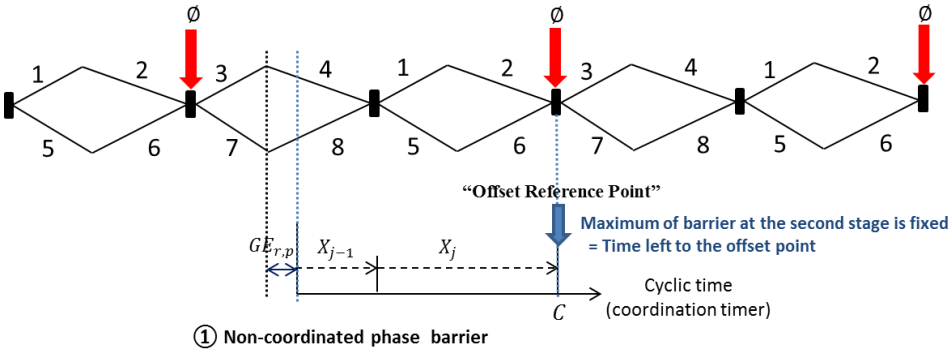

(b)

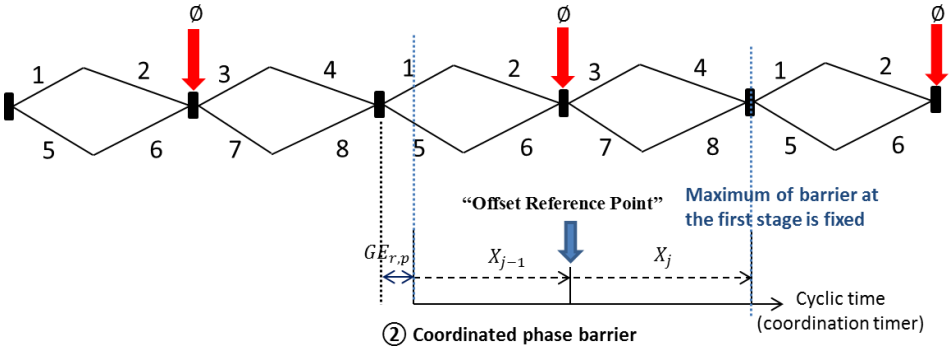

(c)

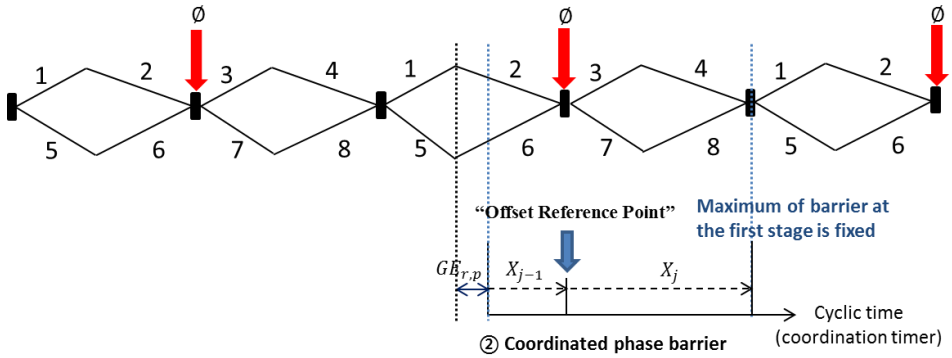

(d)

Figure 5-3 Barrier constraints by offset reference point: when current stage (barrier) only contains non-coordinated phases (a and b) and when current stage (barrier) contains coordinated phases (c and d)

These constraints should be adjusted based on the time left to the offset reference point ($t_{\emptyset}$) obtained from the Coordinator. The arrow labled as "Offset Reference Point" in Figure 5-3 represents the offset point by which the maximum of coordinated phase barrier is constrained. If current stage (barrier) only contains non-coordinated phases, such as Figure 5-3(a) and 5-3(b), each barrier has the following constraints,

$$B_{max}^{1} = \min\{\max\{Sp^{3} + Sp^{4} - t_{\bar{\emptyset}},\ Sp^{7} + Sp^{8} - t_{\bar{\emptyset}}\}, B_{max}^{1}\} \tag{14}$$

$$B_{max}^{2} = t_{\emptyset} + R_{cp} \tag{15}$$

If the current stage (barrier) contains coordinated phases, such as Figure 5-3(c) and 5-3(d), then Equations 16 and 17 are applied:

$$B_{max}^{1} = t_{\emptyset} + R_{cp} \tag{15}$$

$$B_{max}^{2} = \min\{\max\{Sp^{3} + Sp^{4}, Sp^{7} + Sp^{8}\}, B_{max}^{2}\} \tag{17}$$

These barrier constraints apply to the decision region that is illustrated by the blue-dashed verticals lines and labels with the DP decision variables X_{j-1} and X_j.

The connected vehicle market penetration rate may remain low for the next few years. To estimate non-equipped vehicle arrivals based on connected vehicle data, Goodall (Goodall et al. 2014) presented an approach that estimated the states of unequipped vehicles. The algorithm first detects potential unequipped vehicles on the roadway, inserts them into simulation, and removes if it is not correct after observing the behavior of the connected vehicles. Feng et al. (Feng et al. 2015a) extended the algorithm by estimating the location and speed of unequipped vehicles in real time. Feng's estimation algorithm is called EVLS (Estimation of Vehicle Location and Speed). They divided the road segment on the approach to an intersection into three regions and applied different estimation models in each region. Then, a complete arrival table, including all equipped

and estimated (unequipped) vehicles, is constructed. In this chapter, the EVLS algorithm is applied to estimate the states of unequipped vehicles. However, instead of constructing the arrival table for the queuing region, the stopped time of each vehicle is used to estimate delay for each individual vehicle.

5.3 Corridor level control system

5.3.1 Platoon flow model

The corridor level coordination algorithm is based on the Mixed Integer Traffic Optimization Program (MITROP) developed by Gartner et al. (Gartner et al. 1975). In the original algorithm, a rectangular-shaped periodic platoon model was constructed, which was characterized by length (time) p and height (flow rate) q. In MITROP, the platoon length (p) was assumed to be equal to the effective green time at the upstream intersection. Actual platoon length at the downstream may not necessarily be equal to the upstream green time. Flow from input links at the boundaries of each coordinated route were not considered in the optimization. Due to this limitation, the link performance function for delay calculation considered each link independently (Gartner and Deshpande 2013). Vehicle flow from the input links should be taken into account to ensure continuous progression of the platoon. The original algorithm also did not consider residual queues at the downstream links. Instead, turning flow from side streets were inserted into the major platoon as the secondary flow component.

Connected vehicle data provides an opportunity to develop a new platoon flow model that utilizes actual vehicle data. In this chapter, average platoon size on each input link is estimated from the trajectory data and the Offset Refiner utilizes the information to construct platoon flows.

Figure 5-4(a) illustrates an arterial with five intersections labeled from n^1 to n^5. Input links represent the boundaries of the coordinated route. Figure 5-4(b) illustrates flow at the input links that is divided into three components: Primary, Secondary I, and Secondary II, similar to the ELVS algorithm. Once the coordinated phase at boundary intersections turns green, the actual number of vehicles that belong to each platoon component is obtained from the trajectory data.

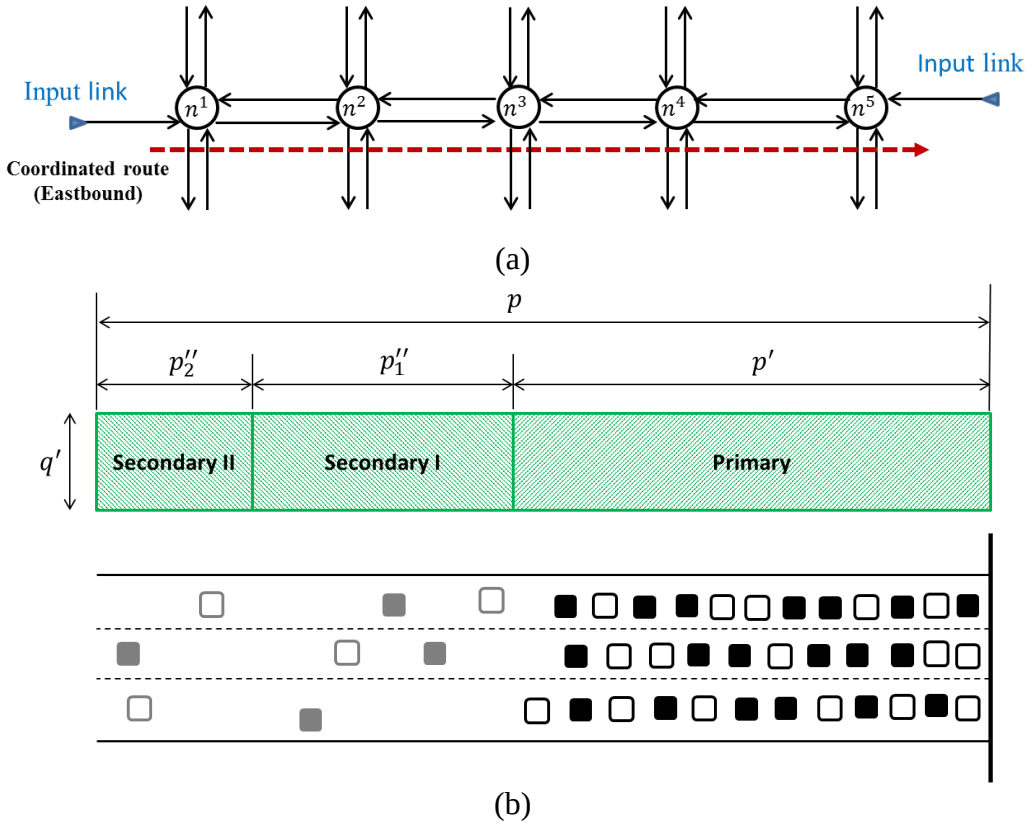

Figure 5-4 Tested network (a) and the platoon flow model (b)

The primary platoon component is the vehicles queued at the stop bar. The length (p') and platoon flow rate (q') of the primary platoon component is determined by Equation 18 where A(t) is the number of stopped vehicles at time *t*.

$$p' = \frac{A(t)}{l \cdot s}, \quad q' = \frac{A(t)}{p'} \tag{18}$$

The length and height of the primary platoon component is equal to the queue clearance time and saturation flow rate. The secondary platoon component I is a vehicle group that will join the primary component before the queue is entirely dissipated. The estimated arrival time of each vehicle in the secondary platoon component I is earlier than the primary component's dissipation time. Since a uniform square-shape platoon is maintained over the arterial, platoon flow rate (q') remains equal for all components. Therefore, using total number of unstopped vehicles ($B(t)$), the length (p_1'') of the component is calculated as follows,

$$p_1'' = \frac{B(t)}{q'} \tag{19}$$

The last vehicle group that arrives after the secondary platoon component I but before the end of green belongs to the secondary platoon component II. The length of the component (p_2'') is determined by Equation 20

$$p_2'' = (g' - (p' + p_1'')) \cdot \frac{f'}{q'} \tag{20}$$

where g' represents the green time at the boundary intersection, and f' is the average flow rate from the input link. It is assumed that vehicles in the secondary platoon component II are uniformly distributed during the remaining green time. Tuning flows from side streets are not included in these components while the flow is considered as the residual queue at the beginning of the coordinated phase. In this chapter, flow conservation is preserved, which means the total number of vehicles in the platoon ($(p' + p_1'' + p_2'') \cdot q'$) remains identical over the entire corridor.

Based on platoon flow rate, a platoon dispersion effect is applied using the calibrated platoon dispersion model by Yu (Yu 2000). Mean and standard deviation of the free flow travel time is used to calculate platoon dispersion parameters as shown in Equation 21. Table 5-1 provides the detailed results. These calibration parameters are based on the network described in

the simulation results section and are measured using connected vehicle data. Using the calibrated platoon dispersion model (Equation 22), the platoon is dispersed over the corridor as shown in Table 5-1. According to the dispersed platoon flow rate, total platoon length at each link is adjusted. The total platoon length and flow rate are used for delay calculation in the link performance function defined in the next section.

$$\beta = \frac{1}{1+\alpha},\ \alpha = \frac{\sqrt{1+4\sigma^2}-1}{2t_a+1-\sqrt{1+4\sigma^2}},\ F = \frac{\sqrt{1+4\sigma^2}-1}{2\sigma^2} \tag{21}$$

$$q_a(t) = F \cdot q_d(t-T) + (1-F) \cdot q_a(t-1) \tag{22}$$

Table 5-1 Calibrated parameters and dispersed platoon length and flow rate

		Input link	Link n^1-n^2	Link n^2-n^3	Link n^3-n^4	Link n^4-n^5
Calibrated parameters	t_a	-	43.729	21.305	9.775	27.583
	σ	-	1.856	1.266	0.712	0.873
	α	-	0.0336	0.0421	0.0393	0.0187
	β	-	0.967	0.959	0.962	0.982
	F	-	0.413	0.537	0.729	0.664
Platoon flow rate (q')		1.5	1.22	1.12	1.07	0.99
Platoon length	Primary component	18	22.21	24.18	25.29	27.36
	Secondary component I	5.5	6.76	7.36	7.71	8.33
	Secondary component II	2.11	2.59	2.83	2.96	3.19
	Total component	**25.61**	**31.56**	**34.37**	**35.96**	**38.88**

5.4 Link Performance Function (LPF)

This section provides the extended link performance function based on the platoon flow model above. Along with the average platoon size, the average queue length at the stop bar of each link, except input links, is received from the Trajectory Awareness component. Let $d(\gamma)$ be the delay which is a function of γ, the arrival time of the leading edge of the platoon at the stop-bar at each intersection. As Gardner et al. (Gartner et al. 1975) showed, the rectangular shape platoon leads to a non-linear delay function; the delay function, $d(\gamma)$, in this chapter follows the same non-linear form. To simplify the non-linear LPF, a piece-wise linear approximation is utilized. In order to perform the linearization, local minimum and maximum values of the nonlinear curve are determined and used to establish the anchor points and slope of the piece-wise linear function.

The minimal delay is determined by the green time (g) and platoon length (p) at the downstream link. Assuming that the platoon length is smaller than green time ($p \leq g$), the delay will be zero if the leading vehicle of the platoon arrives, at time γ, after the residual queue dissipates (Figure 5-5(a)). Otherwise, the platoon will be stopped (Figure 5-5(b)), and the delay (d_{min}) is calculated as follows.

$$d_{min} = \begin{cases} \frac{1}{2p} \cdot \frac{(\delta-\gamma)^2}{(1-y)} & \gamma \in [0, \delta] \\ 0 & \gamma \in [\delta,\ g-p] \end{cases} \tag{23}$$

In Figure 5-5, the residual queue clearance time is illustrated as time δ and the delay of platoon, if it is stopped, is shown by the blue shaded triangle.

If the platoon length is greater than green time ($p > g$), the minimal delay occurs when $\gamma = p - g$. Figure 5-6(c) indicates the case when there is no residual queue in front of the platoon while

Figure 5-6(d) shows the case when there is a residual queue. The average delay is attained by Equation 24.

$$d_{min} = \frac{1}{2p} \cdot \frac{(\delta-(p-g))^2}{(1-y)} \quad (24)$$

The maximum delay occurs when the leading vehicle of the platoon arrives at the downstream stop bar right after the traffic signal turns red. The local maxima from MITROP is assumed to remain the same since there is no residual queue in front of the platoon in the case.

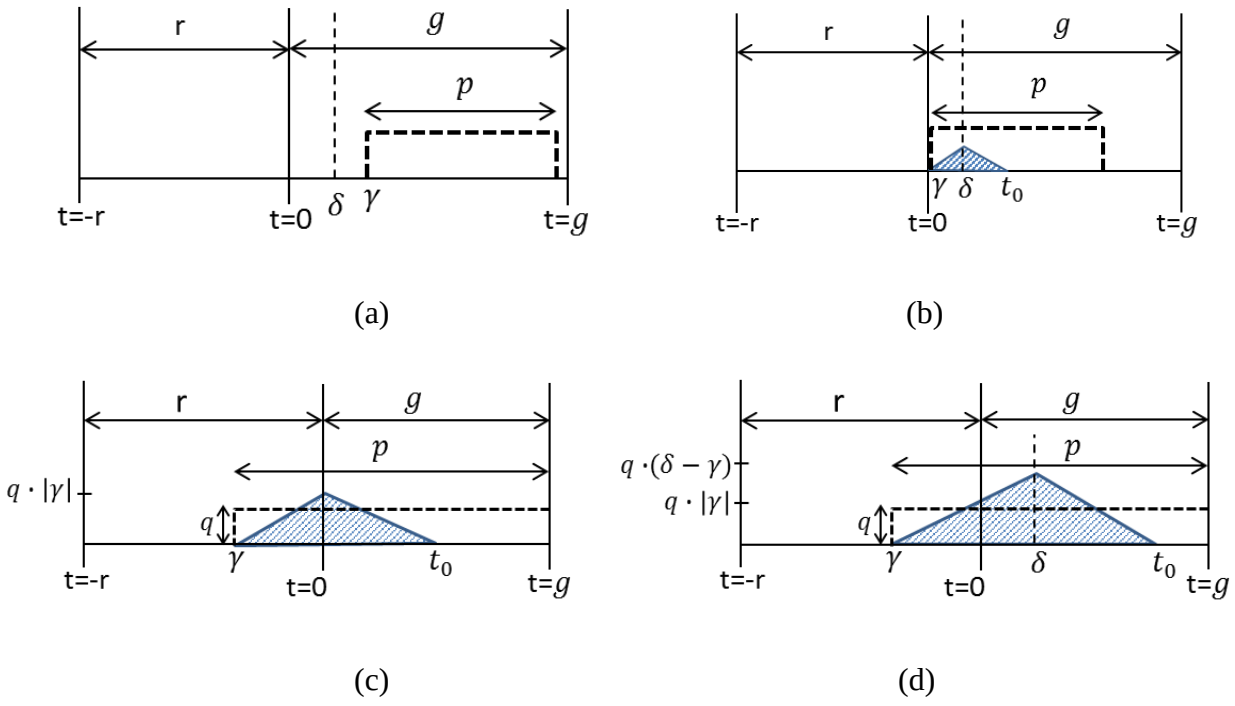

Figure 5-5 Minimum platoon delay : (a and b) platoon length (p) ≤ green time (g), (c and d) platoon length (p) > green time (g)

Based on the link performance function described above, a mixed integer linear program (MILP) is solved. For this chapter, the MILP is solved using CPLEX 12.6.3, but other solvers, such as GLPK, could be used as well. For offset optimization, the delay function $d(\gamma)$ is converted

to the function in term of offset $d(\emptyset)$ using either Equation 25 or 26. If the offset reference point is defined at the start of the coordinated green, the offset is calculated based on the travel time (τ_{mn}) of the platoon's leading vehicle less the arrival time (γ_{mn}) of the vehicle at the stop bar (Equation 25). Equation 26 is applied if the offset reference point is defined as the start of yellow.

$$\emptyset_{mn} = \tau_{mn} - \gamma_{mn} \tag{25}$$

$$\emptyset_{mn} = \tau_{mn} - \gamma_{mn} + g_{mn} - g_{nm} \tag{26}$$

Several constraints that were introduced in MITROP are applied to this algorithm. Constraint for each linear segment from the piece-wise linearization ($d_{mn}^{k}(\emptyset_{mn})$) and loop constraints ($\sum_{(m,n)\in l} \emptyset_{mn} = n_A \cdot C$) that require the sum of the offsets around a loop of the corridor be equal to an integer multiple of the cycle length are introduced. In addition, the optimal offset ($\emptyset$) remain in the interval over $[\tau_{mn} - g_{mn}\ \tau_{mn} + r_{mn}]$ because $d(\emptyset)$ is periodic with C. Finally, the objective function of the optimization is now formulated as follows,

$$\min \sum_{(m,n)\,\in\, A} f_{mn} \cdot d_{mn}$$

subject to :

$$\mathrm{d_{mn}} \geq d_{mn}^{k}(\emptyset_{mn}) \qquad (\mathrm{k} = 1, \ldots, K_{mn}, \forall (m,n) \in A)$$

$$\tau_{mn} - g_{mn} \leq \emptyset_{mn} \leq \tau_{mn} + r_{mn} \qquad (\forall (m,n) \in A)$$

$$\sum_{(m,n)\in l} \emptyset_{mn} = n_A \cdot C$$

where l : a set of links that form a loop, containing two links in opposing directions

n_A = integer

5.5 Simulation results

Five intersections along El Camino Real in San Mateo, CA, are modeled in VISSIM to evaluate the performance of the model. The coordinated direction is eastbound with 2200 vehicle per hour (vph). The demand of westbound on main street is 1600 vph while the side streets have traffic volume ranging from 250 to 700 vph. An Econolite ASC/3 virtual controller is used in VISSIM. Each simulation is run for 5400 seconds with an 1800 second warm-up period and the simulation is replicated with ten different random seeds.

A variety of performance measurements have been investigated including average time a vehicle is in the system, average delay and average number of stops. The adaptive coordination system is compared to actuated-coordinated control, for which coordination parameters including phase split and offset are determined by VISTRO based on the same vehicle demand.

To derive the average time spent in the system, Beak et al. (Beak et al. 2017) obtained the average number of vehicles (N) on each route from the connected vehicle trajectory data. Then, given the arrival rate, the average vehicle time spent in the system T, was determined by Little's theorem ($N = \lambda \cdot T$) (Little 1961). Table 5-2 show the performance of each route and the entire network respectively under 100% market penetration rate. Time spent in the system was improved by 6.57% for the coordinated route and by 3.07% for the entire network. Importantly, adaptive coordination does not have a negative impact the westbound and side street routes.

Table 5-2 Time spent in the system

(a) Each route

		actuated coordination			adaptive coordination		
		Coordinated route (Eastbound)	West bound	Side street	Coordinated route (Eastbound)	West bound	Side street
λ (veh/sec)		0.39	0.17	1.79	0.39	0.17	1.79
Rep. 1	N (veh)	75.55	44.24	220.73	69.63	41.81	216.30
	T (sec)	196.15	254.16	123.51	180.77	240.17	121.03
Rep. 2	N (veh)	75.49	42.92	217.19	70.70	39.31	217.59
	T (sec)	195.98	246.58	121.52	183.54	225.80	121.75
Rep. 3	N (veh)	78.31	47.89	211.11	72.59	42.68	212.58
	T (sec)	203.31	275.08	118.14	188.46	245.18	118.94
Rep. 4	N (veh)	74.93	45.88	213.92	70.18	43.50	213.94
	T (sec)	194.53	263.56	119.69	182.20	249.87	119.70
Rep. 5	N (veh)	74.81	45.06	218.31	70.21	42.00	215.48
	T (sec)	194.21	258.85	122.15	182.28	241.27	120.57
Rep. 6	N (veh)	73.77	43.84	222.01	69.70	40.14	216.60
	T (sec)	191.51	251.82	124.22	180.96	230.56	121.19
Rep. 7	N (veh)	73.84	45.35	221.24	69.20	41.72	218.31
	T (sec)	191.69	260.50	123.79	179.64	239.64	122.15
Rep. 8	N (veh)	74.26	46.49	217.27	70.48	42.39	214.35
	T (sec)	192.80	267.06	121.57	182.97	243.50	119.93
Rep. 9	N (veh)	73.67	46.06	217.72	68.09	41.68	214.79
	T (sec)	191.27	264.56	121.82	176.76	239.44	120.18
Rep. 10	N (veh)	75.19	44.24	214.08	69.82	42.83	214.48
	T (sec)	195.21	254.13	119.79	181.25	246.04	120.01
Avg	**N (veh)**	**74.98**	**45.20**	**217.36**	**70.06**	**41.80**	**215.44**
	T (sec)	**194.67**	**259.63**	**121.62**	**181.88**	**240.15**	**120.55**
	Ratio				**-6.57%**	**-7.50%**	**-0.88%**

(b) Entire network

		actuated coordination	adaptive coordination
λ (veh/sec)		2.35	2.35
Rep. 1	N (veh)	340.53	326.95
	T (sec)	145.12	139.34
Rep. 2	N (veh)	335.60	327.30
	T (sec)	143.02	139.48
Rep. 3	N (veh)	337.34	327.53
	T (sec)	143.76	139.58
Rep. 4	N (veh)	334.52	327.42
	T (sec)	142.56	139.54
Rep. 5	N (veh)	338.18	327.38
	T (sec)	144.12	139.52
Rep. 6	N (veh)	339.30	326.14
	T (sec)	144.60	138.99
Rep. 7	N (veh)	340.30	329.23
	T (sec)	145.02	140.31
Rep. 8	N (veh)	338.02	327.21
	T (sec)	144.06	139.45
Rep. 9	N (veh)	337.45	324.37
	T (sec)	143.81	138.23
Rep. 10	N (veh)	333.06	327.13
	T (sec)	141.94	139.41
Avg	**N (veh)**	**337.43**	**327.07**
	T (sec)	**143.80**	**139.39**
	Ratio		**-3.07%**

Other measurements from the VISSIM evaluation results were collected to investigate the performance for each application. Table 5-3 shows the improvement in terms of average delay and average number of stops in both the coordinated route and the entire network.

Table 5-3 Performance measure from VISSIM

(a) Coordinated route (eastbound)

		actuated coordination	adaptive coordination
Average Delay (sec)	Rep. 1	49.88	35.87
	Rep. 2	48.75	37.53
	Rep. 3	52.35	38.26
	Rep. 4	48.42	37.24
	Rep. 5	48.93	37.82
	Rep. 6	52.55	41.30
	Rep. 7	52.07	38.63
	Rep. 8	46.93	37.00
	Rep. 9	49.23	39.63
	Rep. 10	47.59	38.26
	Avg	**49.67**	**38.15**
	Ratio		**-23.19%**
Average number of stop	Rep. 1	1.32	1.00
	Rep. 2	1.25	1.11
	Rep. 3	1.35	1.08
	Rep. 4	1.31	1.15
	Rep. 5	1.26	1.08
	Rep. 6	1.42	1.11
	Rep. 7	1.31	1.14
	Rep. 8	1.18	1.06
	Rep. 9	1.34	1.08
	Rep. 10	1.18	1.09
	Avg	**1.29**	**1.09**
	Ratio		**-15.45%**

(b) Entire network

		actuated coordination	adaptive coordination
Average Delay (sec)	Rep. 1	60.34	55.22
	Rep. 2	59.16	55.39
	Rep. 3	59.52	55.55
	Rep. 4	58.91	55.72
	Rep. 5	59.29	55.47
	Rep. 6	61.22	55.67
	Rep. 7	60.71	56.10
	Rep. 8	59.46	54.95
	Rep. 9	59.56	54.97
	Rep. 10	58.27	55.58
	Avg	**59.64**	**55.46**
	Ratio		**-7.01%**
Average number of stop	Rep. 1	1.63	1.54
	Rep. 2	1.59	1.54
	Rep. 3	1.64	1.53
	Rep. 4	1.61	1.56
	Rep. 5	1.64	1.55
	Rep. 6	1.65	1.54
	Rep. 7	1.64	1.57
	Rep. 8	1.66	1.54
	Rep. 9	1.63	1.55
	Rep. 10	1.58	1.55
	Avg	**1.63**	**1.55**
	Ratio		**-5.00%**

Further statistical analysis was conducted to determine the statistical significance of the results. The mean values of each replication (10) were compared using a paired-sample t-test at the significant level of α = 0.05 (confidence level of 95%). The null hypothesis of the test was that the mean values of each application were insignificant. As Table 5-4 shows p-values for all measures, the result indicates that all of the null hypothesis are rejected at the 5% significance level, which means that the improvement of the adaptive coordination is significant.

Table 5-4 T-test for each case with 95% confidence level

		Time spent in the system		Performance measure from VISSIM			
				Delay		Number of stop	
		Coordinated route	Entire network	Coordinated route	Entire network	Coordinated route	Entire network
Mean ($\bar{x}$)	adaptive coordination	181.88	139.39	38.15	55.46	1.09	1.55
	actuated coordination	194.67	143.80	49.67	59.64	1.29	1.63
p-value		4.06e-09	5.19e-07	6.80e-09	9.75e-08	2.64e-05	1.38e-05
Result		Reject the null hypothesis	Reject the null hypothesis	Reject the null hypothesis	Reject the null hypothesis	Reject the null hypothesis	Reject the null hypothesis

Results of average vehicle delay and average number of stops under different market penetration rates are shown in Figure 5-6. As shown in Figure 5-6(a), for the coordinated route, under 75% penetration rate the adaptive coordination outperforms actuated coordination by 19% in average delay and 16% in average number of stops, respectively. For the entire network, the performance under the same penetration rate is better than actuated coordination by 5% in average

delay and 3% in average number of stops as shown in Figure 5-6(b). Under 50% penetration rate, the adaptive coordination still outperforms actuated coordination for the coordinated route by 18% in average delay and 12% in average number of stops, respectively. However, under the 50% penetration rate, the entire network performance becomes worse than actuated coordination by 4% in average delay and 3% in average number of stops, respectively. Since the individual vehicle delay is constructed from connected vehicle trajectory data in the objective function, the results are more sensitive to the market penetration rate. Since cycle length in adaptive coordination is assumed to be 100 seconds (as determined by VISTRO for the traffic demands), even one cycle failure due to errors in the EVLS prediction under a low penetration rate can easily cause oversaturation which is challenging to overcome.

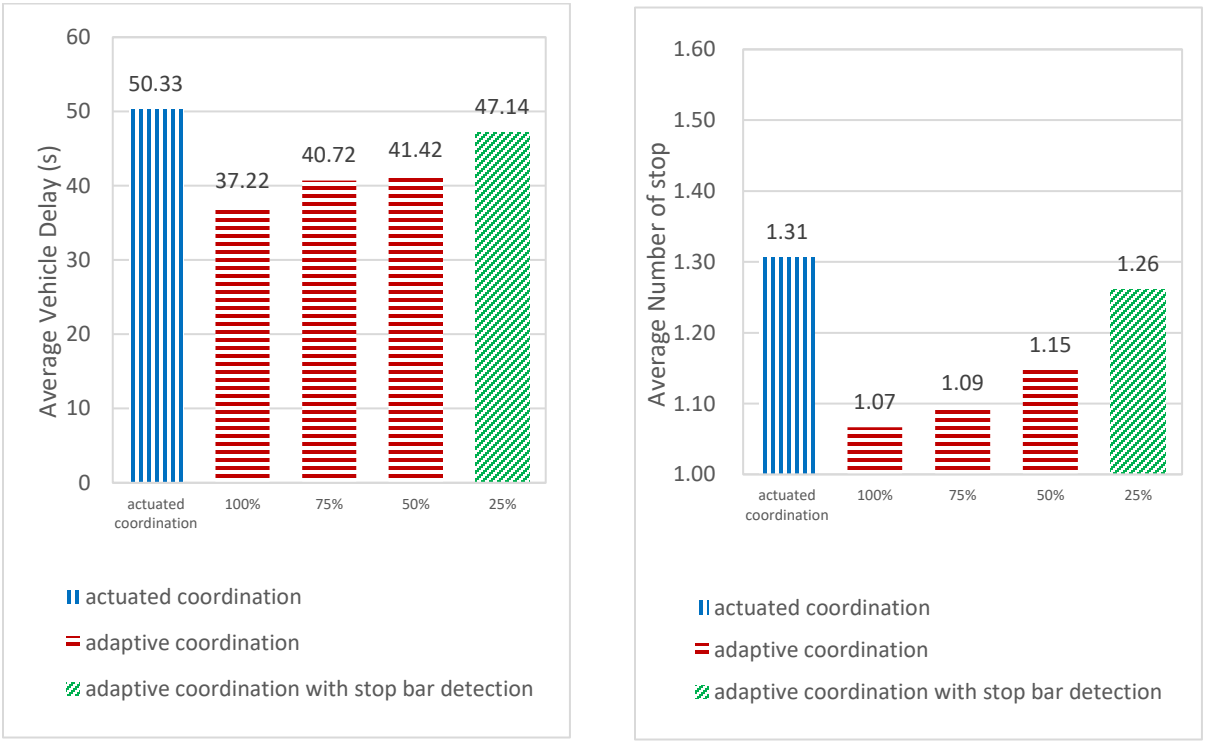

(a)

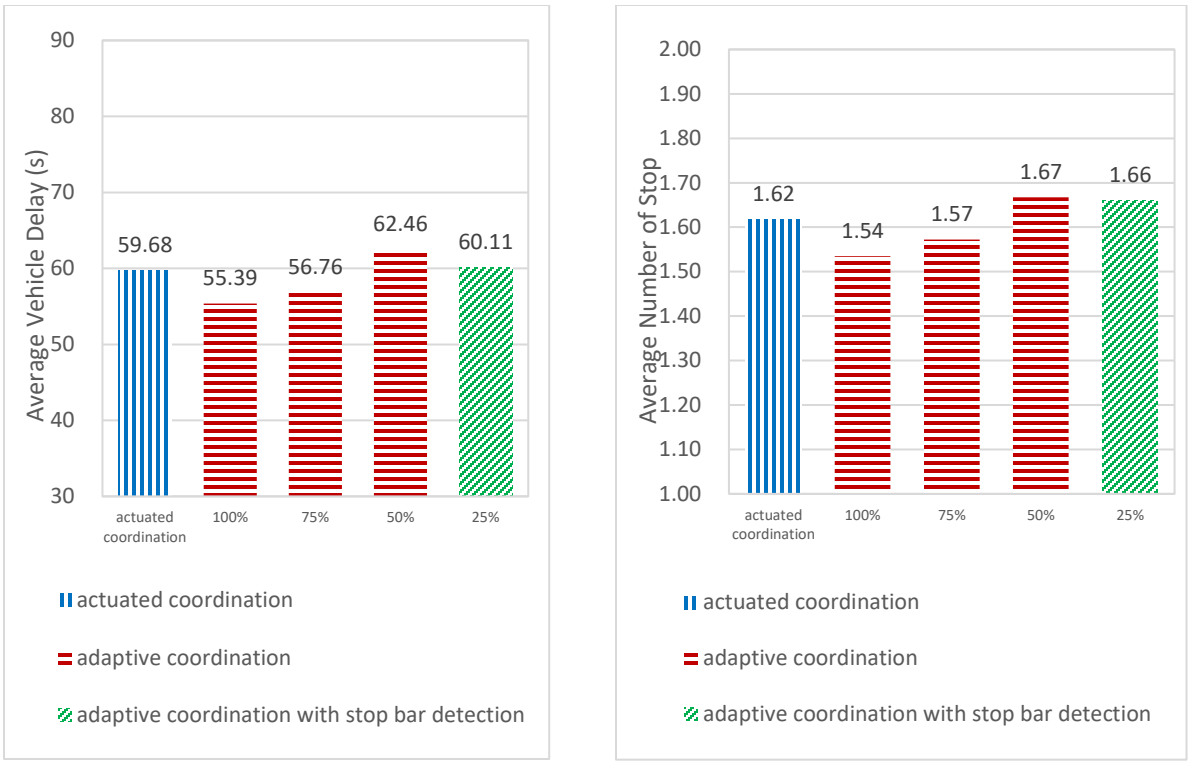

(b)

Figure 5-6 Performance measures under different penetration rates: (a) Coordinated route (eastbound), (b) Entire network

To address the low penetration rate challenge, stop bar detector actuation is integrated into the adaptive coordination algorithm. As Figure 5-6(a) shows, under 25% penetration rate, the performance of coordinated route in average delay and average number of stops are still better than actuated coordination by 6.3% and 3.4% respectively. The performance of the entire network for the integrated algorithm is almost same as actuated coordination, -0.72% and -2.56% difference in average delay and average number of stops respectively.

5.6 Summary

This chapter presented a methodology that integrated coordination with adaptive signal control based on connected vehicle technology. Two levels of optimization were used for different

objectives. Adaptive signal control generates the optimal timing plan for individual intersections while offset refiner synchronizes the offset over the entire corridor. The model has been tested in a VISSIM simulation environment based on a model of an arterial in San Mateo, CA. Adaptive coordination was compared with actuated-coordinated control. The results indicated that the model can reduce average delay and average number of stops for both coordinated routes and the entire network. To improve system performance under low market penetration rates, data from stop-bar detector has been integrated.

Chapter 6 Peer-to-peer priority signal control strategy

This chapter presents an enhancement to the signal priority algorithm that is part of the Multi-Modal Intelligent Traffic Signal System (MMITSS) project. Due to the limited range in the connected vehicle architecture, the signal priority algorithm in MMITSS can only accommodate priority requests received in the near-term (e.g. 10 ~ 20 seconds). Through this near-term priority planning, the signal controller has a limited time window to adapt for the priority request, which may lead to priority request delay. A number of studies have already revealed that the active priority policy based on such short notice can have adverse effects on other traffic (Furth and Muller 2000; Ma et al. 2010). As the time between transit vehicle detection and actual arrival time at the signal increases, the flexibility in signal adjustments is significantly increased (Duerr 2000).

A peer priority control logic is presented to provide a long-term priority plan using peer-to-peer (P2P) communications. P2P is based on the backhaul network between adjacent traffic signals. The basic structure of the mathematical optimization in this chapter follows the signal priority control model (Zamanipour et al. 2016) in MMITSS. An improvement in the priority algorithm in (Zamanipour et al. 2016) is created to integrate an implementation algorithm into the mathematical model. A platform is presented, which implements the peer priority control strategy based on the peer-to-peer priority request data from connected vehicles.

6.1 Methodology of peer-to-peer priority signal control

6.1.1 Peer priority control framework

The peer priority control framework has been designed to address the limitation of the effective range of DSRC and the extent of the MAP message. DSRC has a minimal range of 300 meters, but experience shows that signals can receive beyond 800 meters. However, a priority vehicle

approaching an intersection won't be aware of the intersection until it receives a valid MAP message and is located within the extent of the MAP. The MAP message provides a description of the intersection geometry, including approaches, lanes, stop bar, cross walks, etc. The MAP description of each approach is based on GPS waypoints used to describe the lanes. Due to a limitation in the MAP message size, the extent – distance from stop bar, is limited. Experience has shown that this is about 300 meters for relatively straight approaches and shorter distances for curved approaches. Once the priority requesting vehicle determines that it is inside the MAP extent, it can form a valid Signal Request Message (SRM) that includes the in-lane (as defined in the MAP) and the time of desired service. Figure 6-1 illustrates the scenario when P2P priority control will be effective.

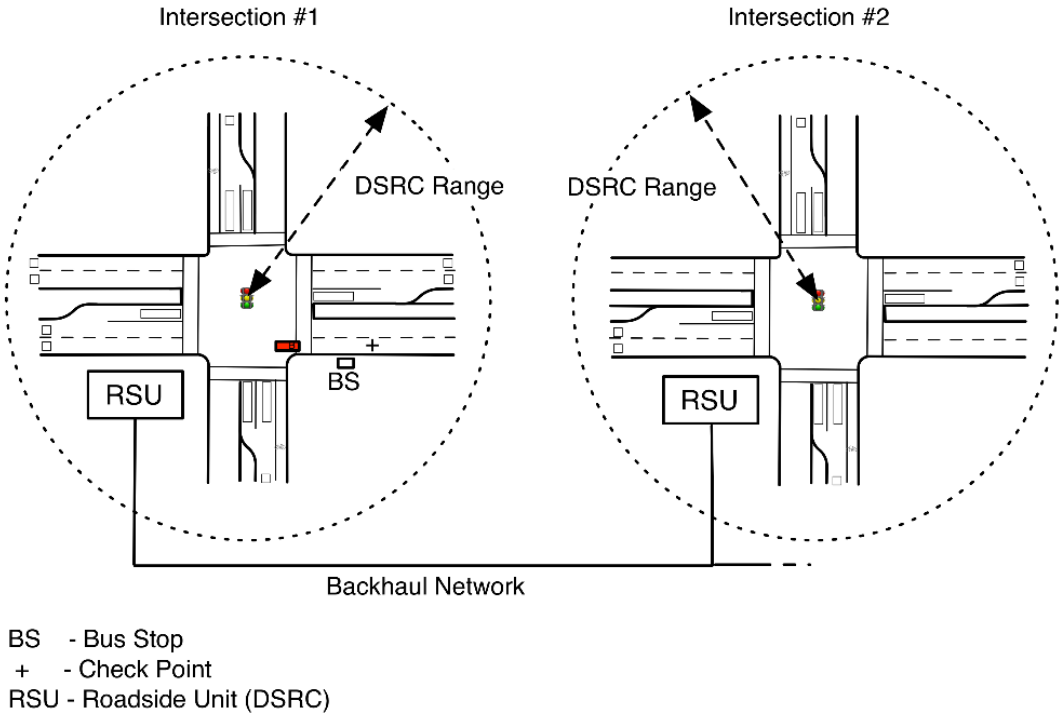

Figure 6-1 Illustration of peer priority request initiation

When a prioritized vehicle passes a stop bar at upstream intersection (intersection #1), a near-term priority request is canceled since the vehicle has been served. A peer priority request is initiated when the cancel message is received. The peer control component monitors the vehicle position until it passes one of the defined exit Check Points, which is the first GPS waypoint on an egress approach lane after the stop-bar if there is no far-side bus stop. If there is a far-side bus stop (shown as BS in Figure 6-1), the GPS waypoint after the bus stop, which is denoted as '+' symbol in Figure 6-1, becomes the check point. When the vehicle passes the exit Check Point, a Peer Priority Request, including the requested signal phase, in-lane, and estimated arrival time to the stop bar at the downstream intersection, is sent to the designated intersection (intersection #2) through the backhaul network. The estimated arrival time is calculated based on an average travel time between the exit Check Point and the stop bar at the downstream intersection. In this dissertation, an average of free flow travel time for transit vehicles from VISSIM simulation was used. The peer request makes it possible for the traffic signal controller at the downstream intersection to have a long term priority planning horizon, which can reduce delay and number of stops for transit with more flexibility for other traffic. The system architecture of the P2P priority control system is shown in Figure 6-2.

The control system consists of several software components including the Priority Request Generator, Priority Request Server, Priority Solver, Vehicle Trajectory Awareness, Traffic Control Interface, and Long Term Planning, all of which are implemented in both simulation and real traffic networks. All of the components reside at roadside, either on a Road Side Unit (RSU) or on a co-processor at each intersection.

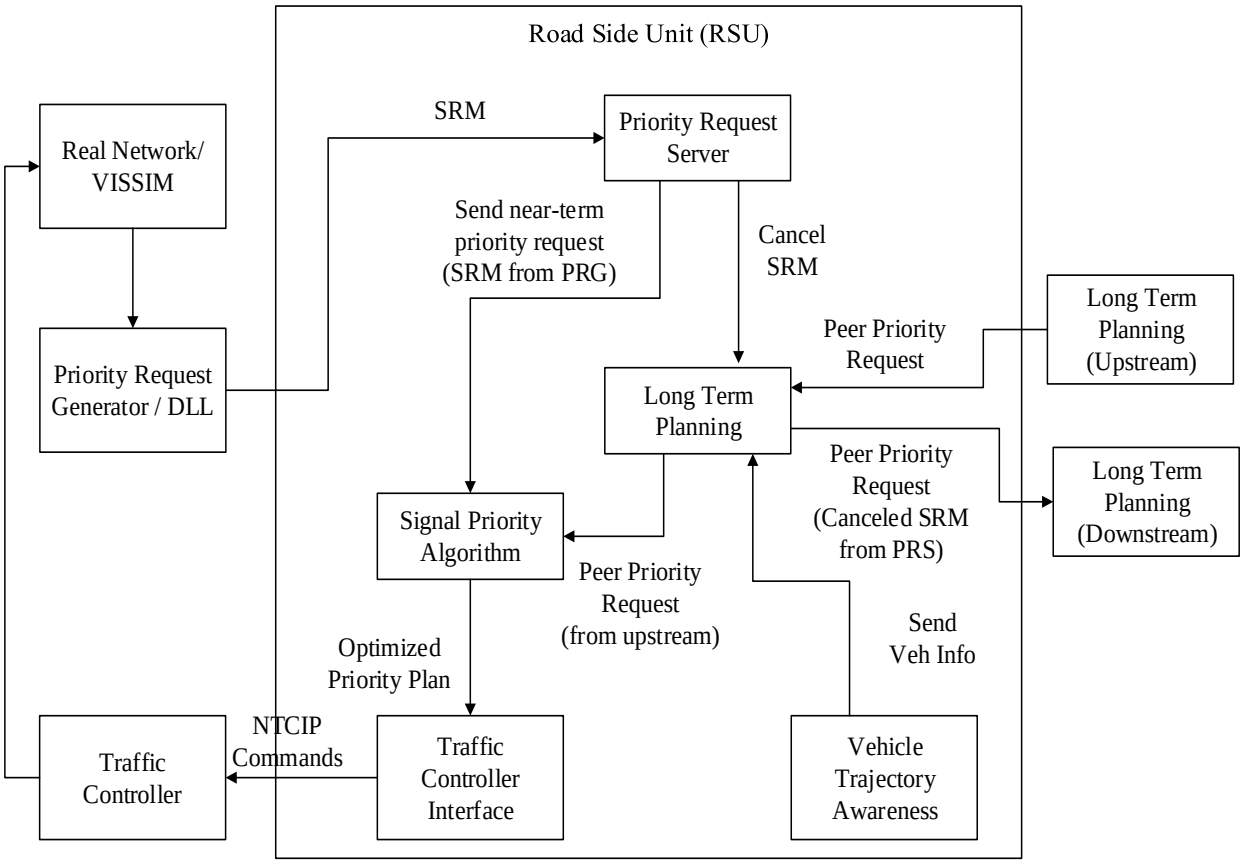

Figure 6-2 Architecture of peer-to-peer priority control system

When a priority vehicle enters in the DSRC range of the intersection, the Signal Request Message (SRM) broadcast from the Priority Request Generator on the On Board Unit (OBU) is received by the Priority Request Server (PRS) through DSRC communication. Once the PRS adds a new near-term priority request to the active requests table, a unified MILP model, which resides in the Priority Solver, creates an optimal near-term signal priority plan. The signal plan is sent to the Traffic Signal Controller through the Traffic Controller Interface, using the NTCIP ("NTCIP 1202, National Transportation Communications for ITS Protocol Object Definitions for Actuated

Traffic Signal Controller (ASC) Units, v02.19. November 2005." n.d.) commands, which include Vehicle Call, Force-off, and Hold.

When the prioritized vehicle passes the stop bar, the OBU broadcasts a cancel SRM message. The cancel SRM is received at the intersection and the PRS cancels the active signal request and checks to see if peer priority control is enabled for the downstream intersection. If it is enabled, the PRS sends a peer priority request to the Long Term Planning (LTP) component. The LTP component continues checking the vehicle position to see if it has passed one of the defined exit Check Points. When the vehicle passes the exit Check Point, the LTP sends a Peer Priority Request to the designated downstream intersection. Once a LTP at a downstream intersection receives a peer priority request, it adds the request to the active peer request table and sends it to Priority Solver. If there is no priority request in the DSRC range of the downstream intersection, the Priority Solver solves the MILP only for the peer request and sends a feasible solution to the Traffic Controller Interface. If there are priority requests that are currently being served in the DSRC range of the downstream intersection, the peer priority request is solved along with them in the same optimization process.

A detailed procedure of the peer priority control algorithm can be found in Figure 6-3. Figure 6-3(a) demonstrates how a peer priority request is initiated at an upstream intersection, while Figure 6-3(b) shows how the peer request is processed once received at the downstream intersection.

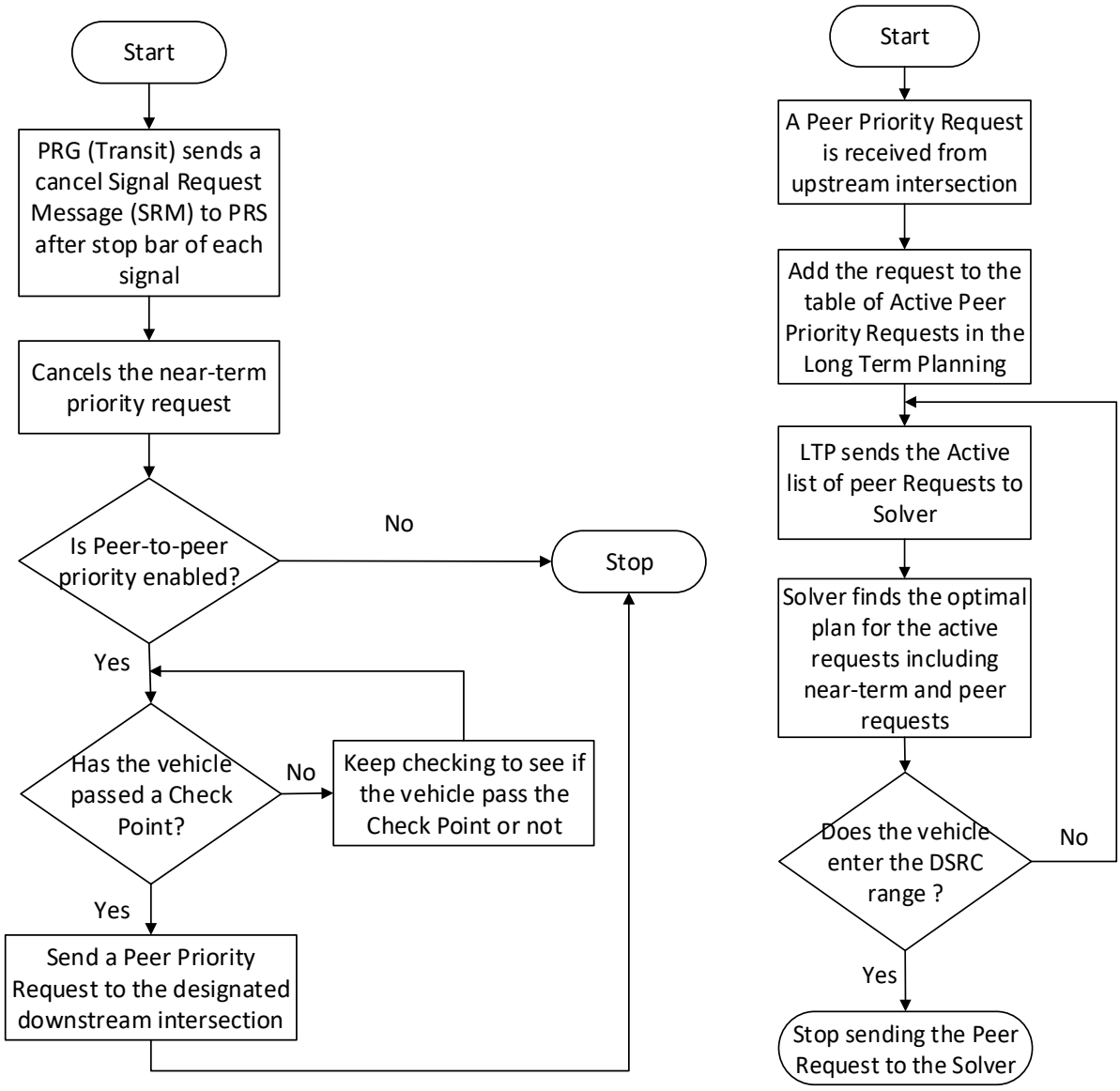

(a) Upstream **(b) Downstream**

Figure 6-3 Flow chart of peer-to-peer priority control model

Figure 6-4 shows two examples using a time-phase diagram (He et al. 2011b), which explain the necessity of P2P priority control strategies. A priority signal plan can be visualized in the diagram, which is a useful tool to analyze the optimized plan, verify if the schedule is feasible, and evaluate priority delay given the signal plan and priority request arrival times.

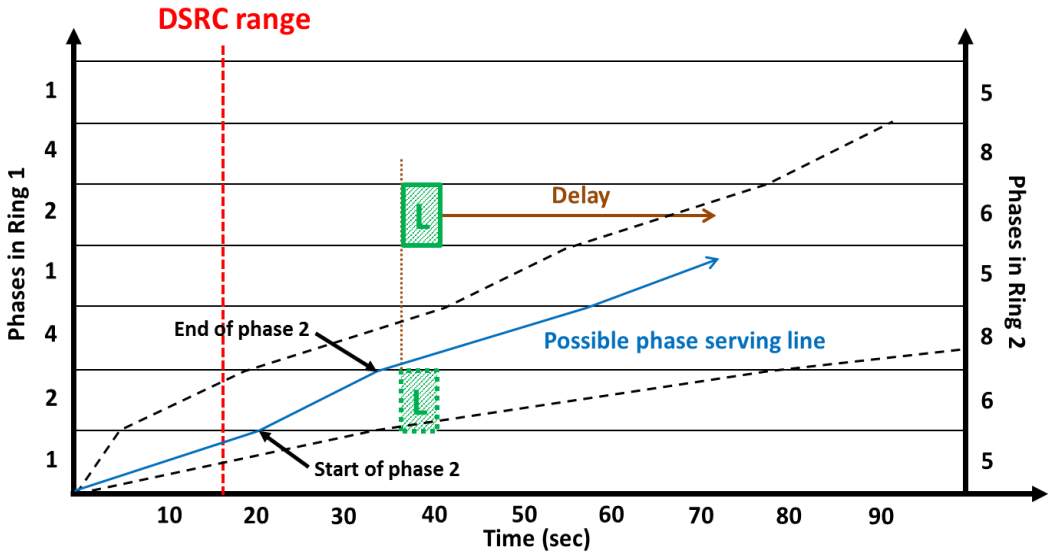

(a)

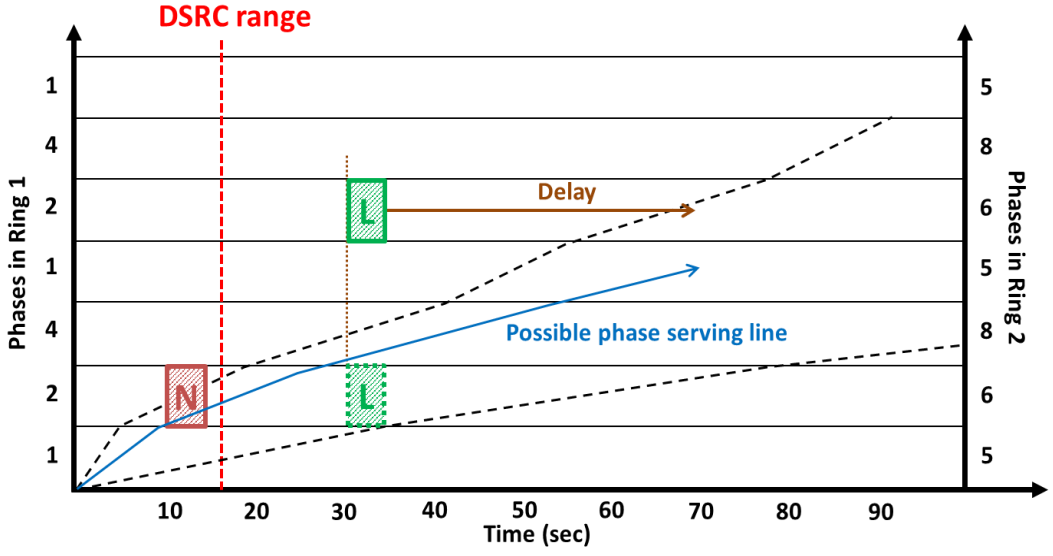

(b)

Figure 6-4 Two long term priority request scenarios: (a) without near-term request, (b) with near-term request.

A priority request (box) with an arrival time interval is shown in Figure 6-4, where the x-axis is time and the left and right y-axes are showing phases in rings 1 and 2, respectively. The box with the letter 'L' represents a priority request that is out of DSRC range and is not currently observed at the intersection. The box with the letter 'N' represents a near-term priority request that has already been detected at the intersection. The DSRC range is shown at 17 seconds. Two black dotted lines starting from the origin, which denotes current time and current phase, represent the shortest path (minimum green times for each phase) and longest path (maximum green times) over the planning horizon. A signal control plan must reside in the cone-shaped area between the two lines. The solid arrow shows a phase-serving path that the controller may possibly take within the feasible area based on actuation logic. This could be based on coordination plan splits. As shown in Figure 6-4(a), the priority request may not be served in the current cycle because it is not observed by the local server (inside DSRC range) before the signal completes the service phase (phase 2). Figure 6-4(b) shows, even with a near-term priority request being served, the long term priority request may not be served after the near term request passes the intersection. This may results in a significant delay to the priority eligible vehicle.

6.1.2 Unified mathematical optimization model

Zamanipour et al. (Zamanipour et al. 2016) developed a signal priority algorithm that includes two parts: a mathematical optimization model and a flexible implementation algorithm. Based on the standard North American NEMA dual-ring structure, the mathematical optimization model was formulated as a Mixed Integer Linear Programming (MILP) problem to minimize a weighted summation of multiple priority requests delay.

The model is shown as follow:

$$Minimize \sum_{m \in M} w^m d^m$$

$$s.t$$

$$Precedence\ Constraints$$

$$Phase\ Duration\ \&\ Interval\ Constraints$$

$$Priority\ Request\ Delay\ Evaluation\ Constraints$$

where d^m is the total priority request delay of mode m, w^m is the mode m weight determined by the multi-modal policy.

First, based on the precedence graph model (Head et al. 2006), the precedence constraints include a set of relationships between each phase in the standard NEMA dual-ring structure. In addition, phase duration and interval constraints include minimum and maximum green time for each phase and consider the current phase's elapsed green time. These two sets of constraints determine when the green time at each phase starts and how long it can last. Based on the allocated green time, the cycle that each priority request will be served is selected. The priority request delay evaluation constraints calculate the delay for each request based on the cycle that it will be served and the signal timing. Considering a multi-modal priority policy that determines the relative importance between modes, the optimization model provides one of the feasible optimal solutions, which can deal with multiple priority requests simultaneously.

In order to reduce the negative impacts on regular vehicles that may be caused by granting priority to priority-eligible vehicles, a flexible implementation algorithm was developed, which allows the non-priority phases to be actuated to cope with variation in traffic demand in real-time.

This flexible optimized signal plan ensures that the signal controller can better serve non-prioritized vehicles on the phases that precede the requested phase, while minimizing the priority request delay. As shown in Figure 6-5, a feasible region is created by two piecewise lines starting from the origin to the priority request arrival time. The left dotted piecewise line represents a set of "HOLD" points for each phase, which denotes when the signal controller should hold a phase green. The right long-dashed piecewise line represents a set of "FORCE-OFF" points that provide less, or zero, delay to the priority request. Within the flexible region between the two lines, the controller is allowed to actuate the signal phase, which means that if there is no vehicle detection (call), the phase will gap out. Otherwise, the phase will extend until the "FORCE OFF" point.

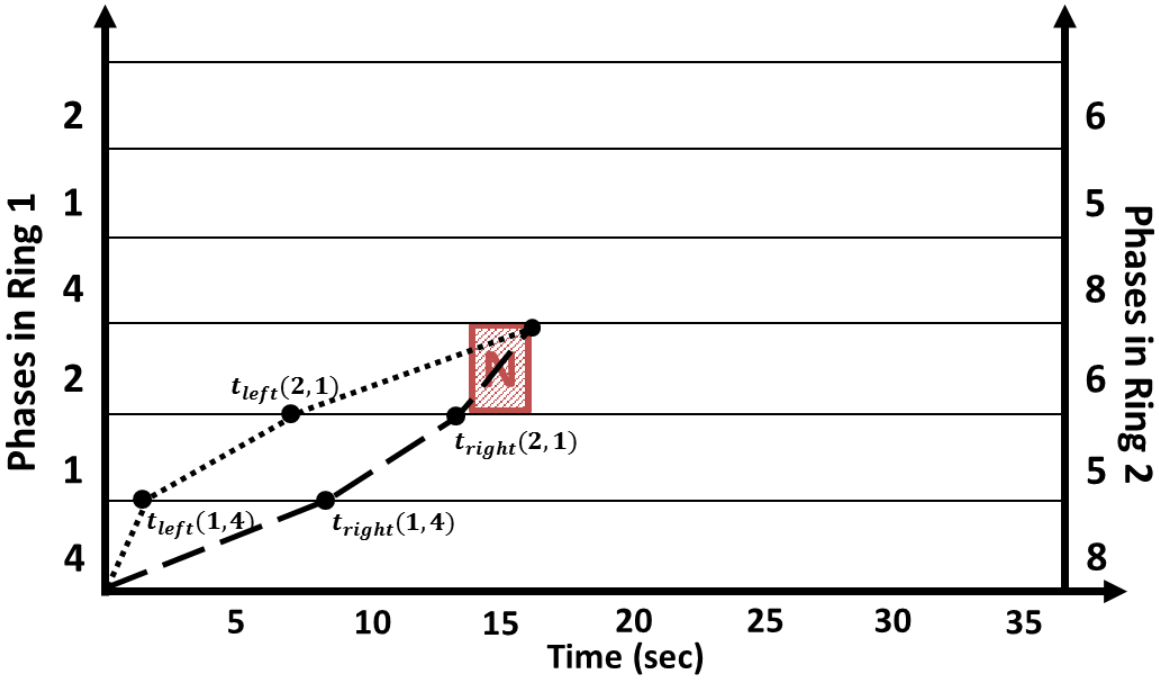

Figure 6-5 Flexible feasible signal plan in time-phase diagram

The original flexible implementation algorithm was revised to directly address signal flexibility, considering two critical points as additional decision variables in the mathematical model. The revised model is:

$$Min_{\,t_{left},\,t_{right}} \sum_{m\in M} w^m d^m - \sum_{p\in P,k\in K} (t_{right}(k,p) - t_{left}(k,p))$$

$$s.t$$

Precedence Constraints

Phase Duration & Interval Constraints

Priority Request Delay Evaluation Constraints

where d^m is the total priority request delay of mode *m*, w^m is the mode *m* weight determined by the multi-modal policy. $t_{left}(k,p)$ is the left crical point of phase *p* in cycle *k*, while $t_{right}(k,p)$ is for the right critical point, as shown in Figure 6-5. To maximize the feasible region, a negative term is added to the objective function, which is the summation of time intervals between "FORCE-OFF" point and "HOLD" point. One set of precedence constraints are considered for each ring to find the left and right critical points. The *Phase Duration & Interval Constraints* and *Priority Request Delay Evaluation Constraints* also hold for both left and right points independently. The other variables defined in (Zamanipour et al. 2016) remain the same.

Figure 6-6 shows several priority plans that the peer priority control model creates for multiple priority requests, including both near-term and peer requests, based on the revised optimization model. Each signal plan in Figure 6-6 was drawn based on actual log data from the Priority Solver component. As shown in Figure 6-6(a), the flexibility from current phase to the

requested phase is possible when there is only one peer request. The delay for the peer request will be zero, and the signal controller has significant flexibility to serve for other traffic. Figure 6-6(b) shows the priority plan for the same request approximately 10 seconds later, which still maintains a large flexible region.

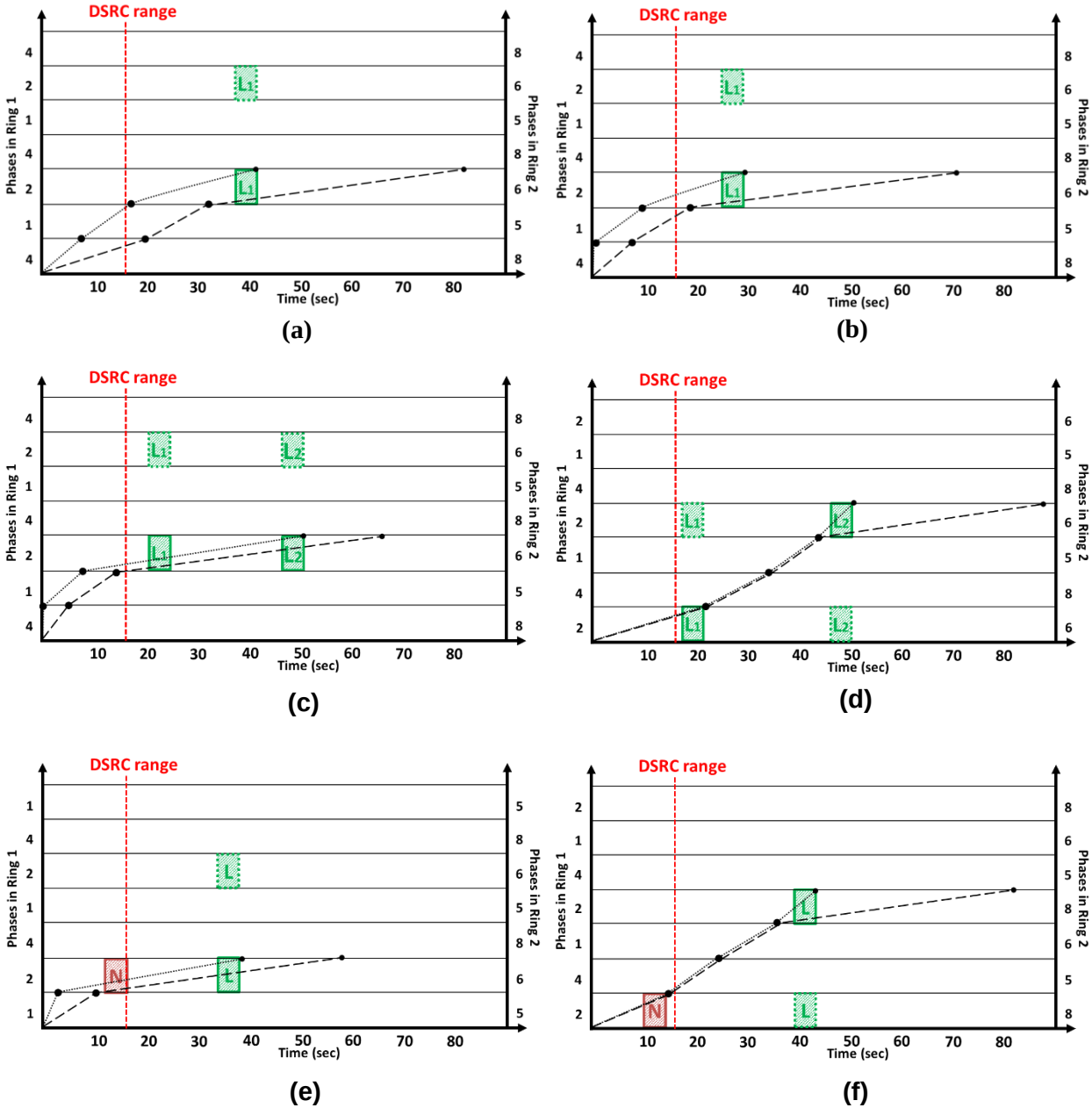

Figure 6-6 Time-phase diagram with peer priority requests and feasible plan

Even with multiple peer requests, a flexible plan can exist as shown in Figure 6-6(c). Sometimes, the flexibility can be limited to serve multiple requests as demonstrated in Figure 6-6(d). According to the arrival interval of each peer request and traffic signal status, which includes current phases served and elapsed green times of the phases, peer requests can be served in one cycle (Figure 6-6(c)), or they can be served in different cycles (Figure 6-6(d)). Figures 6-6(e and f) illustrate the same case of Figures 6-6(c and d), when the first peer requests enter the DSRC range. After the near-term request (N) passes the stop-bar, the signal controller can hold the signal green for phase 2 because a peer request (L) exists that can be served within the maximum green time of phase 2 (Figure 6-6(e)). On the other hand, if the peer request cannot be served in current cycle, the controller could force off the phase 2 right after the near-term request and follow the non-flexible line (a set of minimum green times for phases 4 and 1) up to the peer request (L) to have zero delay for the peer request (Figure 6-6(f)).

6.2 Experimental design

The peer priority control strategy has been tested on two different VISSIM simulation networks: Daisy Mountain Drive in Anthem, Arizona and Redwood Road in Salt Lake City, Utah. As Figure 6-7 shows, the Daisy Mountain corridor has 6 intersections over 2.3 miles, while the Redwood corridor has 13 intersections over 5.12 miles. The main street in the Arizona network has three lanes in both directions, and the side streets have two lanes, while the main street in the Utah network has two or three lanes, and the side streets have one or two lanes. The intersection spacing of both networks varies, although the Utah network has, on average, wider spacing ranging from 150 m to 1400 m than the Arizona network, which has a range of 300 to 900 m. An eastbound movement from Gavilian Peak to Anthem on Daisy Mountain Dr. was simulated as a bus route,

while a southbound movement from W 400 S to W 3800 S on Redwood Rd. was selected as a bus route.

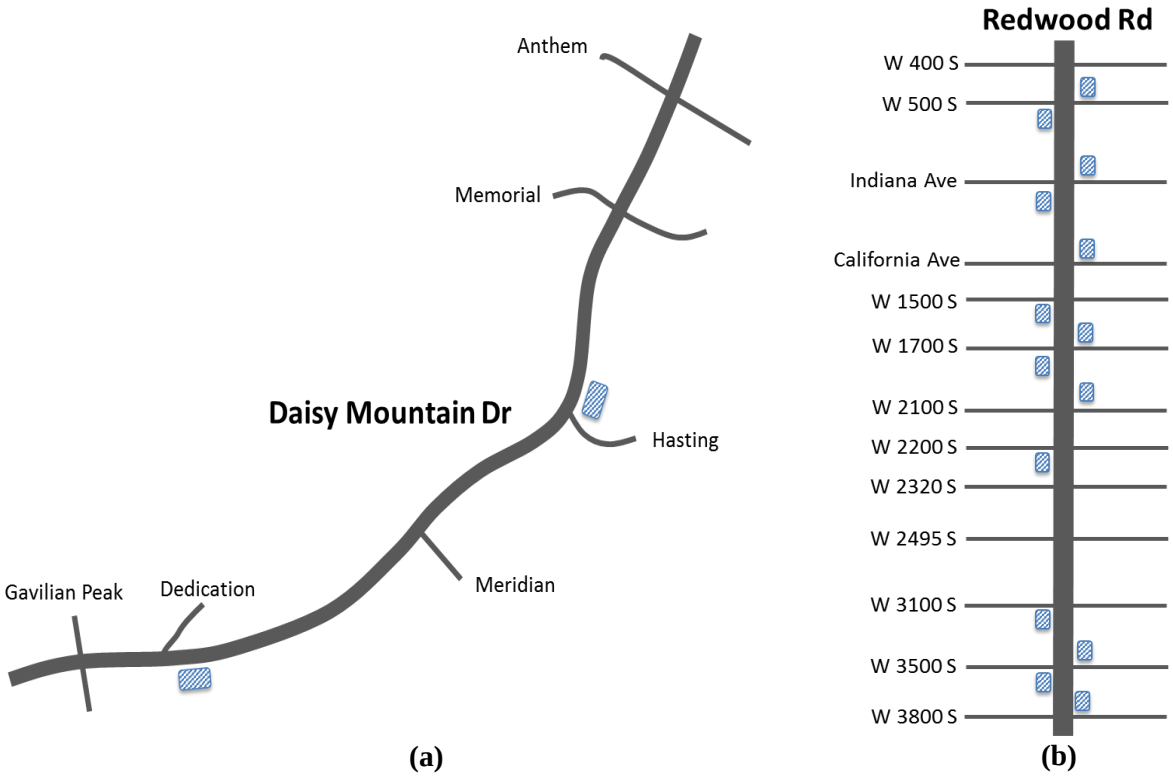

Figure 6-7 Simulation test bed layout: (a) Anthem, Arizona, (b) Salt Lake City, Utah.

The Utah Transit Authority (UTA) actually runs bus service on Redwood Rd. at approximately 10 minute intervals, while there is no public transit service running in Anthem. For the test of the P2P priority control strategy, two far-side bus stops with bus bays and located within DSRC range, shown as blue boxes in Figure 6-7(a), were simulated in the Arizona network model. As shown in Figure 6-7(b), the Utah network model has seven far-side bus stops without bus pullouts. The bus dwell time at each stop was distributed between 20 and 45 seconds for both simulation networks. The bus speed for both network was simulated as 35 miles per hour, which was slightly lower than the actual speed limit of each road.

Both simulation models were run for two and half hours, which included a thirty minute warming-up period. The bus headway for the Arizona and Utah networks were set up as five minutes and ten minutes, respectively so the experiments would include a sufficient number of buses. Both simulation experiments were replicated with ten different random seeds. Traffic demand on the main street and side streets in Anthem were 900 vehicles per hour (vph) and 200 to 400 vph, respectively. Traffic demand on the main street in Salt Lake City is 1200 vph, and side streets have traffic volume ranging from 200 vph to 500 vph. An Econolite virtual controller (ASC/3), which can support the NTCIP interface, was used in the simulation.

6.3 Evaluation results

Several measurements from VISSIM were evaluated including average vehicle delay, number of stops, and travel time. The peer priority control strategy was compared to three different signal control applications: fully actuated control (free mode), coordination control, and MMITSS priority control. The coordination parameters on the Arizona network, including phase splits, cycle length, and offsets, are determined by VISTRO (PTV 2014a) based on the vehicle demand, while the parameters for the Utah were provided by the Utah Department of Transportation.

Table 6-1 summarizes the performance of transit on a bus route for both networks in terms of average values of ten replications with different random seeds. Compared to fully actuated control in Arizona, the average vehicle delay, number of stops, and travel time from peer priority control were greatly improved by -48.35%, -94.94%, and -11.57%, respectively. Similar results were shown in the Utah network. When comparing the same measures with coordination control in both networks, peer control outperformed coordination by -41.39% ~ -42.92%, -59.85% ~ -94.03%%, and -9.49% ~ -11.80%, respectively. The results show that the improvements were

slightly reduced compared to fully actuated control. This is because signals were coordinated on the bus route, and buses benefit from the coordinated progression. However, as buses travel over a corridor, they cannot remain in the progression due to stopping and dwelling for passengers at bus stops. A comparison between peer priority control and MMITSS priority control also shows that all of the measures from the peer control were improved. In particular, the average number of stops for both networks were significantly decreased by -81.82% and -42.91%, respectively.

Table 6-1 Performance measure of transit (Average values)

Simulation network		Measurement	Average vehicle delay	Average number of stop	Average travel time
Arizona	Bus Route (eastbound)	Fully actuated control	79.673	1.317	334.735
		Coordination control	72.096	1.117	327.042
		Priority control	51.404	0.367	306.423
		Peer Priority control	41.150	0.067	295.999
	Comparison	***Peer VS Fully actuated***	***-48.35%***	***-94.94%***	***-11.57%***
		Peer VS Coordination	***-42.92%***	***-94.03%***	***-9.49%***
		Peer VS Priority control	***-19.95%***	***-81.82%***	***-3.40%***
Utah	Bus Route (eastbound)	Fully actuated control	298.417	5.150	998.802
		Coordination control	279.796	3.258	980.491
		Priority control	197.715	2.292	898.360
		Peer Priority control	163.994	1.308	864.751
	Comparison	***Peer VS Fully actuated***	***-45.05%***	***-74.60%***	***-13.42%***
		Peer VS Coordination	***-41.39%***	***-59.85%***	***-11.80%***
		Peer VS Priority control	***-17.06%***	***-42.91%***	***-3.74%***

To show the reliability of the transit service under each signal control system, the standard deviation of travel time and vehicle delay were compared in Table 6-2. Compared to fully actuated control, the peer control model significantly improved the reliability of vehicle delay by -69.12% in Arizona and -53.01% in Utah. The reliability of travel time was also improved by -63.07% in Arizona and -50.66% in Utah. In comparison to coordination and MMITSS priority control, the results show that the reliability of the peer control outperformed in both networks as shown in Table 6-2.

Table 6-2 Performance measure of transit (Standard deviation)

Simulation network		Measurement	STD of vehicle delay	STD of travel time
Arizona	Bus Route (eastbound)	Fully actuated control	27.322	28.003
		Coordination control	24.315	24.320
		Priority control	13.008	13.886
		Peer Priority control	8.437	10.342
	Comparison	***Peer VS Fully actuated***	***-69.12%***	***-63.07%***
		Peer VS Coordination	***-65.30%***	***-57.47%***
		Peer VS Priority control	***-35.14%***	***-25.52%***
Utah	Bus Route (eastbound)	Fully actuated control	50.390	49.530
		Coordination control	32.819	32.761
		Priority control	31.323	32.991
		Peer Priority control	23.677	24.440
	Comparison	***Peer VS Fully actuated***	***-53.01%***	***-50.66%***
		Peer VS Coordination	***-27.85%***	***-25.40%***
		Peer VS Priority control	***-24.41%***	***-25.92%***

Table 6-3 demonstrates how the peer priority control affects the performance of regular vehicles in the entire system. It was observed that in both networks the peer priority control does not have a negative impact on regular vehicles in terms of average vehicle delay, number of stop, and travel time, compared to fully actuated and MMITSS priority control. However, the average number of stops under coordination control in both networks was better than peer control, although vehicle delay and travel time from the peer control were better than under coordination. It turned out that the coordination plans from VISTRO and the UDOT were effective at minimizing the number of stops for regular vehicles, although it did not improve the number of stops for transit because the coordination cannot differentiate vehicle modes, as shown in Table 6-1.

Table 6-3 Performance measure (Average) of regular vehicle on entire network

Simulation network		Measurement	Average vehicle delay	Average number of stop	Average travel time
Arizona	Entire network	Fully actuated control	40.677	1.565	158.224
		Coordination control	48.600	1.290	165.929
		Priority control	40.579	1.566	158.137
		Peer Priority control	40.445	1.549	157.963
	Comparison	***Peer VS Fully actuated***	***-0.57%***	***-1.03%***	***-0.16%***
		Peer VS Coordination	***-16.78%***	***20.07%***	***-4.80%***
		Peer VS Priority control	***-0.33%***	***-1.06%***	***-0.11%***
Utah	Entire network	Fully actuated control	45.587	1.572	135.587
		Coordination control	61.623	1.415	151.562
		Priority control	45.821	1.575	135.839
		Peer Priority control	45.969	1.576	136.087
	Comparison	***Peer VS Fully actuated***	***0.84%***	***0.24%***	***0.37%***
		Peer VS Coordination	***-25.24%***	***11.32%***	***-10.21%***
		Peer VS Priority control	***0.32%***	***0.03%***	***0.18%***

A statistical analysis was performed to determine the significance of the simulation results. Using a paired-sample t-test at the confidence level of 95%, the mean value of ten replications were examined for each signal control's comparison. The null hypothesis of the test was that the mean values of each signal control were insignificant compared to peer priority control. According to p-values for all measures of transit, all of the null hypothesis are rejected at the 5% significance level, which indicates that the improvement of peer priority control on transit is significant. For the same measures of regular vehicles, the test fails to reject all of the null hypothesis except for the comparison of peer and coordination control, indicating that the mean values are insignificant. Accordingly, the results indicate that the peer priority control model does not have adverse impact on the performance of regular vehicles.

6.4 Summary

This chapter presents a methodology that enhanced the MMITSS priority control strategy based on P2P and DSRC communications in a connected vehicle environment. The peer priority control strategy makes it possible for a signal controller to have a flexible long-term plan for prioritized vehicles. The peer control model was evaluated using two VISSIM simulation networks: each an arterial in Anthem, AZ and Salt Lake City, UT. The control was compared with three different types of signal control systems: fully actuated control (free mode), coordination, MMITSS priority control. The results indicate that the model can significantly reduce average vehicle delay, number of stops, average travel time for transit in both networks. Importantly, the model does not have an adverse effect on regular vehicles for the same measures. Statistical analysis was followed to show the significance of transit performance from ten simulation replications.

Chapter 7 Summary, contributions and future research

7.1 Research summary

This dissertation researched two different approaches to systematic analysis for traffic signal control systems, and developed two methodologies that address challenges from traditional coordination and priority signal control. All of the analysis and optimization approaches have been conducted in a connected vehicle environment.

7.1.1 Quantitative analysis of smooth progression in traffic signal systems

A quantitative analysis of smooth progression in terms of the speed variation of vehicles was developed. A new measure, Smoothness Of the Flow of Traffic (SOFT), was used to evaluate how smoothly a vehicle, or platoons of vehicles, progresses through a corridor based on the frequency content of the vehicle speed. This new measure can be computed using data from connected vehicles and can be used to determine the quality of progression along a route. In addition, a multi-modal investigation into the impact of vehicle mode was conducted. The results showed that as the percentage of trucks in the traffic stream increased, the average SOFT value became significantly lower indicating the impact of mixed mode operations. This indicates the potential need for traffic signal coordination plans that consider the different modes, and possibly other traffic control measures, to help smooth the flow of the traffic stream. The analysis and measurements were conducted using microscopic traffic simulation (VISSIM) and connected vehicle technology that will be deployable in the very near future.

7.1.2 Multi-modal system-wide evaluation of traffic signal coordination

Many optimization models tried to enhance the performance of typical vehicles on the coordinated route and do not address the impacts on minor movements, such as left turns and side streets. In addition, multi-modality is not considered in most optimization tools. A systematic analysis of traffic signal coordination in a connected vehicle environment was conducted through analysis of the time spent in the system. First, a systematic investigation into the impact of coordination on each route was conducted when the signal timing was developed based on vehicle volume. The results showed that there was a point below which system-wide performance of coordination was worse than free operation unless the signals were re-timed for the specific traffic volume. Second, a multi-modal analysis of the performance of coordination on each O-D path was conducted. It revealed how multi-modality impacted the performance of the entire system. The ratio of trucks had significant effect on the performance of both coordination and free operation, and with a high ratio of trucks (60%), the coordination plan that was optimized for unimodal condition could not outperform free operation.

7.1.3 Adaptive optimization of traffic signal coordination

Adaptive optimization of traffic signal coordination is a methodology that integrates coordination with adaptive signal control in a connected vehicle environment. Two levels of optimization were used for different objectives. At the intersection level, an adaptive control algorithm generates the optimal green time for each phase in real time using dynamic programming considering coordination constraints. At the corridor level, an offset refiner optimizes the offsets along the corridor using a mixed integer linear program. The offsets are provided to the intersection level as constraints. The model has been tested in a VISSIM simulation environment based on a model of

an arterial in San Mateo, CA. Adaptive coordination was compared with actuated-coordinated control. The results indicated that the model can reduce average delay and average number of stops for both coordinated routes and the entire network. To improve system performance under low market penetration rates, data from stop-bar detectors have been integrated.

7.1.4 Peer-to-peer priority signal control strategy

A peer-to-peer priority signal control strategy was presented as a methodology that enhances the priority signal control model in the Multi Modal Intelligent Traffic Signal System (MMITSS). To overcome the range limit of DSRC (and the MAP), peer-to-peer intersection communications were integrated with the DSRC communications. Through the integrated communication, the peer priority control strategy can create a more efficient signal plan (long term plan) for all vehicles, including prioritized vehicles. The long-term plan provides a flexible signal schedule that allows phase actuation. The peer priority strategy is effective in reducing the number of stops and delay for priority requests, while minimizing the negative impact on regular vehicles. A simulation experiment was designed to compare with different types of signal control systems using two different VISSIM simulation networks (Arizona and Utah). The result shows that the peer-to-peer long term planning strategy can improve transit service reliability, limiting adverse impact on other traffic.

7.2 Main contributions

This dissertation makes contributions to two major areas in traffic signal control systems: systematic analysis in terms of two new performance measures and two methodologies that deal

with current challenges in coordination and priority signal control. Specific contributions include the following:

1. A new concept for quantifying the smoothness of vehicle progression, which is called the Smoothness Of the Flow of Traffic (SOFT). This measure investigates how smoothly vehicles flow along a corridor based on the frequency content of vehicle speed.

2. Using the SOFT measure and DSRC messages, it is also possible to evaluate how each vehicle mode affects the smooth progression of an individual vehicle or entire group of vehicles.

3. Using queuing theory (Little's theorem), the system-wide performance of traffic signal control systems is evaluated. Through the average time that vehicles spend in the traffic system, the overall system performance of coordination for different traffic volumes and different routing scenarios, including coordinated and non-coordinated movements, is analyzed.

4. In addition, this research conducts the first attempt to investigate how multimodal traffic composition systematically affects the coordination performance.

5. An adaptive coordination algorithm that integrates coordination with adaptive signal control in a connected vehicle environment was developed. Through the optimization algorithm, the coordination parameters remain optimal despite traffic demand that fluctuate during coordination periods or even the entire day. The algorithm makes it possible to change the coordination plan offsets dynamically to accommodate demand variability and improve coordination performance.

6. An enhancement to the signal priority algorithm in MMITSS project was developed. The peer priority control strategy enables a signal controller to have a flexible long-term plan for all vehicles, including prioritized vehicles. The vehicles can benefit from the long-term plan within a secured flexible region. In addition, the peer priority strategy can prevent the near-term priority actions from having a negative impact on other traffic by providing more flexibility phase actuation.

7.3 Future research

There are several suggestions for future research.

▪ *Field implementation for systematic analysis with lower market penetration rate*

The field implementation of the two new measures presented in this dissertation is needed to validate their effectiveness in a connected vehicle environment. A 100% market penetration rate of connected vehicles was assumed for the system-wide analysis. Based on lower market penetration rates of connected vehicles, the systematic analysis needs to be enhanced to address the market penetration issue and tested in a real-world connected vehicle network.

▪ *On-line offset optimization*

In this dissertation, corridor level optimization in the adaptive coordination algorithm was conducted offline based on average flow data to determine the optimal cycle length. Future research should focus on on-line offset optimization using real-time flow data from connected vehicle trajectories. Most of the modern optimization methodologies to develop coordination

timing do not consider the mode of each vehicle. Thus, a multi-modal optimization model, which deals with different characteristics (trajectory) of each mode, needs to be developed.

▪ *Integration of coordination and peer priority signal control*

Peer priority control was implemented without consideration for coordination in the optimization. Future research should focus on an integration of peer priority-coordination signal control which creates an optimal solution that considers multiple peer requests and periodic virtual coordination requests in the same optimization framework.

In addition, previous research of priority signal control by Qing et al. (2014) and Zamanipour et al. (2016) developed a methodology that simultaneously considers signal coordination and priority, assuming coordination as virtual priority requests. They tried to achieve coordination by adding multiple virtual coordination requests within the multi-modal priority decision framework. However, the characteristic of each vehicle's mode was not considered in the optimization framework. If an approaching platoon includes multiple modes (e.g. string of vehicles), the platoon information, including length and flow rate, may be different for each platoon. Different characteristics (trajectories) of each mode, including acceleration, deceleration, reaction time to the traffic signal change, and queue dissipation time, should be considered in the optimization.

The coordination delay in the objective function assumed that the fixed split time of the coordinated phase would be occupied by platoons of vehicles. During the virtual coordination requests, only a few vehicles, and sometimes no vehicle at all, may be observed, especially at the end of the coordinated phase. Therefore, instead of using the fixed virtual coordination request from the previous model, cycle-by-cycle dynamic coordination requests from multi-modal

platoons need to be considered. Since every cycle has a different platoon size (length), coordination-priority requests should be dynamically updated.

▪ *Estimation of accurate arrival time for peer requests*

The estimation of the travel time (arrival time) for each peer request to the downstream intersection is critical. If the arrival time of the peer requests are not accurate, the performance of the prioritized vehicles and other traffic could be negatively impacted. For example, if the arrival time to the downstream intersection was forecasted to be too early, it could force off competing phases early, causing unnecessary delay or cycle failure for other traffic. On the other hand, if the arrival time was estimated to be too late, the peer priority may not take advantage of the long term planning. Thus, for future improvement, statistical methods should be investigated to estimate travel time more accurately.

▪ *Consideration of near-side bus stops*

For the peer priority signal control model, only far-side bus stops were considered. In cases where there is a near-side stop, the current method to estimate the average arrival time for peer requests at the downstream stop-bar may not be effective. Statistical approaches could be investigated to estimate the dwell time at the near-side stop.

References

Abbas, M., Bullock, D., and Head, L. (2001). "Real-time offset transitioning algorithm for coordinating traffic signals." *Transportation Research Record: Journal of the Transportation Research Board*, (1748), 26–39.

Abdelfattah, A., and Khan, A. (1998). "Models for predicting bus delays." *Transportation Research Record: Journal of the Transportation Research Board*, (1623), 8–15.

Abdy, Z. R., and Hellinga, B. R. (2010). "Analytical method for estimating the impact of transit signal priority on vehicle delay." *Journal of Transportation Engineering*, 137(8), 589–600.

Ahn, K., Rakha, H. A., Kang, K., and Vadakpat, G. (2016). "Multimodal Intelligent Traffic Signal System Simulation Model Development and Assessment." *Transportation Research Record: Journal of the Transportation Research Board*, (2558), 92–102.

Balke, K., Dudek, C., and Urbanik II, T. (2000). "Development and evaluation of intelligent bus priority concept." *Transportation Research Record: Journal of the Transportation Research Board*, (1727), 12–19.

Beak, B., Head, K. L., and Khoshmagham, S. (2017). "Systematic Analysis of Coordination using Connected Vehicle Technology." *Transportation Research Board 96th Annual Meeting*.

Bertsekas, D. P., Gallager, R. G., and Humblet, P. (1992). *Data Networks*. Prentice-Hall International New Jersey.

Byrne, N., Koonce, P., Bertini, R., Pangilinan, C., and Lasky, M. (2005). "Using hardware-in-the-loop simulation to evaluate signal control strategies for transit signal priority." *Transportation Research Record: Journal of the Transportation Research Board*, (1925), 227–234.

Chang, J., Collura, J., Dion, F., and Rakha, H. (2003). "Evaluation of service reliability impacts of traffic signal priority strategies for bus transit." *Transportation Research Record: Journal of the Transportation Research Board*, (1841), 23–31.

Cohen, D., Head, L., and Shelby, S. (2007). "Performance analysis of coordinated traffic signals during transition." *Transportation Research Record: Journal of the Transportation Research Board*, (2035), 19–31.

Coifman, B. (1998). "Vehicle Re-identification and Travel Time Measurement in Real-time on Freeways Using Existing Loop Detector Infrastructure." *Transportation Research Record: Journal of the Transportation Research Board*, (1643), 181–191.

Conrad, M., Dion, F., and Yagar, S. (1998). "Real-time traffic signal optimization with transit priority: Recent advances in the signal priority procedure for optimization in real-time model." *Transportation Research Record: Journal of the Transportation Research Board*, (1634), 100–109.

"CPLEX Optimizer Manual." (2015). *IBM*.

Day, C., Ernst, J., Brennan Jr, T., Chou, C.-S., Hainen, A., Remias, S., Nichols, A., Griggs, B., and Bullock, D. (2012). "Performance measures for adaptive signal control: Case study of system-in-the-loop simulation." *Transportation Research Record: Journal of the Transportation Research Board*, (2311), 1–15.

Day, C., Haseman, R., Premachandra, H., Brennan Jr, T., Wasson, J., Sturdevant, J., and Bullock, D. (2010). "Evaluation of Arterial Signal Coordination: Methodologies for Visualizing High-Resolution Event Data and Measuring Travel Time." *Transportation Research Record: Journal of the Transportation Research Board*, (2192), 37–49.

Denney, R. W. (2012). "The National Traffic Signal Report Card." *Institute of Transportation Engineers. ITE Journal*, 82(6), 22.

Dion, F., and Hellinga, B. (2002). "A rule-based real-time traffic responsive signal control system with transit priority: application to an isolated intersection." *Transportation Research Part B: Methodological*, 36(4), 325–343.

Dion, F., Rakha, H., and Zhang, Y. (2004). "Evaluation of potential transit signal priority benefits along a fixed-time signalized arterial." *Journal of Transportation Engineering*, 130(3), 294–303.

Duerr, P. (2000). "Dynamic right-of-way for transit vehicles: integrated modeling approach for optimizing signal control on mixed traffic arterials." *Transportation Research Record: Journal of the Transportation Research Board*, (1731), 31–39.

Ekeila, W., Sayed, T., and El Esawey, M. (2009). "Development of dynamic transit signal priority strategy." *Transportation Research Record: Journal of the Transportation Research Board*, (2111), 1–9.

Estrada, M., Trapote, C., Roca-Riu, M., and Robuste, F. (2009). "Improving bus travel times with passive traffic signal coordination." *Transportation Research Record: Journal of the Transportation Research Board*, (2111), 68–75.

Feng, Y., Head, K. L., Khoshmagham, S., and Zamanipour, M. (2015a). "A Real-Time Adaptive Signal Control in a Connected Vehicle Environment." *Transportation Research Part C: Emerging Technologies*, 55, 460–473.

Feng, Y., Khoshmagham, S., Zamanipour, M., and Head, K. L. (2015b). "A real-time adaptive signal phase allocation algorithm in a connected vehicle environment." *Transportation Research Board 94th Annual Meeting*.

Feng, Y., Zamanipour, M., Head, K. L., and Khoshmagham, S. (2016). "Connected Vehicle Based Adaptive Signal Control and Applications." *Transportation Research Board 95th Annual Meeting*.

FHWA, U. (2010). "Manual on uniform traffic control devices (2009)." *Baton Rouge: Claitor' s Law Books and Publishing*, 137–179.

Furth, P., and Muller, T. H. (2000). "Conditional bus priority at signalized intersections: better service with less traffic disruption." *Transportation Research Record: Journal of the Transportation Research Board*, (1731), 23–30.

Garrow, M., Machemehl, R. B., and others. (1997). *Development and evaluation of transit signal priority strategies*. University of Texas at Austin.

Gartner, N., and Deshpande, R. (2013). "Dynamic Programming Approach for Arterial Signal Optimization." *Transportation Research Record: Journal of the Transportation Research Board*, (2356), 84–91.

Gartner, N. H. (1983). "OPAC: A demand-responsive strategy for traffic signal control." *Transportation Research Board 62nd Annual Meeting*.

Gartner, N. H., Assmann, S. F., Lasaga, F., and Hous, D. L. (1990). "MULTIBAND–A Variable-Bandwidth Arterial Progression Scheme." *Transportation Research Record: Journal of the Transportation Research Board*, (1287).

Gartner, N. H., Little, J. D., and Gabbay, H. (1975). "Optimization of Traffic Signal Settings by Mixed-Integer Linear Programming: Part I: The Network Coordination Problem." *Transportation Science*, 9(4), 321–343.

Gartner, N. H., Pooran, F. J., and Andrews, C. M. (2001). "Implementation of the OPAC adaptive control strategy in a traffic signal network." *Intelligent Transportation Systems, 2001. Proceedings.* IEEE, 195–200.

Gazis, D. C. (1965). "Traffic Control, Time—Space Diagrams, and Networks." *Traffic Control*, Springer, 47–63.

Ghanim, M. S., and Abu-Lebdeh, G. (2015). "Real-time dynamic transit signal priority optimization for coordinated traffic networks using genetic algorithms and artificial neural networks." *Journal of Intelligent Transportation Systems*, 19(4), 327–338.

"GLPK Reference Manual." (2012). *GNU Project, Free Software Foundation (FSF)*.

Goodall, N. J., Park, B., and Smith, B. L. (2014). "Microscopic Estimation of Arterial Vehicle Positions in a Low-Penetration-Rate Connected Vehicle Environment." *Journal of Transportation Engineering*, 140(10).

Gordon, R. L., and Tighe, W. (2005). *Traffic Control Systems Handbook (2005 Edition)*.

HCM. (2010). "Highway Capacity Manual." *Transportation Research Board, National Research Council, Washington, DC*.

He, Q., Head, K., and Ding, J. (2011a). "Heuristic algorithm for priority traffic signal control." *Transportation Research Record: Journal of the Transportation Research Board*, (2259), 1–7.

He, Q., Head, K. L., and Ding, J. (2011b). "Heuristic Algorithm for Priority Traffic Signal Control." *Transportation Research Record: Journal of the Transportation Research Board*, 2259(1), 1–7.

He, Q., Head, K. L., and Ding, J. (2012). "PAMSCOD: Platoon-based Arterial Multi-modal Signal Control with Online data." *Transportation Research Part C: Emerging Technologies*, 20(1), 164–184.

He, Q., Head, K. L., and Ding, J. (2014). "Multi-modal traffic signal control with priority, signal actuation and coordination." *Transportation Research Part C: Emerging Technologies*, 46, 65–82.

Head, L. (1995). “Event—based short—term traffic flow prediction model.” *Transportation Research Record: Journal of the Transportation Research Board*, 1510, 125–143.

Head, L., Gettman, D., and Wei, Z. (2006). “Decision model for priority control of traffic signals.” *Transportation Research Record: Journal of the Transportation Research Board*, (1978), 169–177.

Hongchao, L. I. U., Zhang, J., and Cheng, D. (2008). “Analytical approach to evaluating transit signal priority.” *Journal of Transportation Systems Engineering and Information Technology*, 8(2), 48–57.

Hu, H., and Liu, H. X. (2013). “Arterial Offset Optimization Using Archived High-Resolution Traffic Signal Data.” *Transportation Research Part C: Emerging Technologies*, 37, 131–144.

Hu, J., Park, B. B., and Lee, Y.-J. (2015). “Coordinated transit signal priority supporting transit progression under connected vehicle technology.” *Transportation Research Part C: Emerging Technologies*, 55, 393–408.

Hu, J., Park, B., and Parkany, A. (2014). “Transit signal priority with connected vehicle technology.” *Transportation Research Record: Journal of the Transportation Research Board*, (2418), 20–29.

Jerri, A. J. (1977). “The Shannon sampling theorem—Its various extensions and applications: A tutorial review.” *Proceedings of the IEEE*, 65(11), 1565–1596.

Khasnabis, S., Karnati, R., and Rudraraju, R. (1996). “NETSIM-based approach to evaluation of bus preemption strategies.” *Transportation Research Record: Journal of the Transportation Research Board*, (1554), 80–89.

Kim, W., and Rilett, L. (2005). “Improved transit signal priority system for networks with nearside bus stops.” *Transportation Research Record: Journal of the Transportation Research Board*, (1925), 205–214.

Köhler, E., Möhring, R. H., and Wünsch, G. (2005). “Minimizing Total Delay in Fixed-time Controlled Traffic Networks.” *Operations Research Proceedings*, 192–199.

Koonce, P., Ringert, J., Urbanik, T., Rotich, W., and Kloos, B. (2002). “Detection range setting methodology for signal priority.” *Journal of Public Transportation*, 5(2), 6.

Koonce, P., Rodegerdts, L., Lee, K., Quayle, S., Beaird, S., Braud, C., Bonneson, J., Tarnoff, P., and Urbanik, T. (2008). *Traffic Signal Timing Manual*.

Kwong, K., Kavaler, R., Rajagopal, R., and Varaiya, P. (2009). “Arterial Travel Time Estimation Based on Vehicle Re-Identification Using Wireless Magnetic Sensors.” *Transportation Research Part C: Emerging Technologies*, 17(6), 586–606.

Lee, J., Shalaby, A., Greenough, J., Bowie, M., and Hung, S. (2005). “Advanced transit signal priority control with online microsimulation-based transit prediction model.” *Transportation Research Record: Journal of the Transportation Research Board*, (1925), 185–194.

Li, M., Yin, Y., Zhang, W.-B., Zhou, K., and Nakamura, H. (2011). "Modeling and implementation of adaptive transit signal priority on actuated control systems." *Computer-Aided Civil and Infrastructure Engineering*, 26(4), 270–284.

Liao, C.-F., and Davis, G. (2007a). "Simulation study of bus signal priority strategy: Taking advantage of global positioning system, automated vehicle location system, and wireless communications." *Transportation Research Record: Journal of the Transportation Research Board*, (2034), 82–91.

Liao, C.-F., and Davis, G. (2007b). "Simulation study of bus signal priority strategy: Taking advantage of global positioning system, automated vehicle location system, and wireless communications." *Transportation Research Record: Journal of the Transportation Research Board*, (2034), 82–91.

Ling, K., and Shalaby, A. (2004). "Automated transit headway control via adaptive signal priority." *Journal of Advanced Transportation*, 38(1), 45–67.

Little, J. D. (1966). "The Synchronization of Traffic Signals by Mixed-Integer Linear Programming." *Operations Research*, 14(4), 568–594.

Little, J. D. C. (1961). "A proof for the queuing formula: L = λW." *Operations Research*, 9(3), 383–387.

Little, J. D., M.D. Kelson, and N.H. Gartner. (1981). "MAXBAND: A Program for setting signals on arteries and triangular networks." *Transportation Research Record: Journal of the Transportation Research Board*, 795.

Liu, C. C. (1988). "Bandwidth-constrained delay optimization for signal systems." *ITE Journal*, 58(12), 21–26.

Lowrie, P. R. (1982). "The Sydney coordinated adaptive traffic system-principles, methodology, algorithms." *International Conference on Road Traffic Signalling, 1982, London, United Kingdom*.

Luk, J. Y. K. (1984). "Two traffic-responsive area traffic control methods: SCAT and SCOOT." *Traffic Engineering & Control*, 25(1), 14–22.

Ma, W., Liu, Y., and Yang, X. (2013a). "A dynamic programming approach for optimal signal priority control upon multiple high-frequency bus requests." *Journal of Intelligent Transportation Systems*, 17(4), 282–293.

Ma, W., Ni, W., Head, L., and Zhao, J. (2013b). "Effective coordinated optimization model for transit priority control under arterial progression." *Transportation Research Record: Journal of the Transportation Research Board*, (2356), 71–83.

Ma, W., and Yang, X. (2008). "Design and evaluation of an adaptive bus signal priority system base on wireless sensor network." *Intelligent Transportation Systems, 2008. ITSC 2008. 11th International IEEE Conference on*, IEEE, 1073–1077.

Ma, W., Yang, X., and Liu, Y. (2010). "Development and evaluation of a coordinated and conditional bus priority approach." *Transportation Research Record: Journal of the Transportation Research Board*, (2145), 49–58.

Manual, H. C. (1985). "Highway capacity manual." *Washington, DC*.

Messer, C. J., Whitson, R. H., Dudek, C. L., and Romano, E. J. (1973). “A Variable-sequence Multiphase Progression Optimization Program.” *Highway Research Record*, 24–33.

Mineta, N. (2006). “National strategy to reduce congestion on America’s transportation network.” *US Department of Transportation*.

Mirchandani, P. B., and Lucas, D. E. (2004). “Integrated transit priority and rail/emergency preemption in real-time traffic adaptive signal control.” *Journal of Intelligent Transportation Systems*, 8(2), 101–115.

Morgan, J. T., and Little, J. D. (1964). “Synchronizing Traffic Signals for Maximal Bandwidth.” *Operations Research*, 896–912.

Nelson, J. D., Brookes, D. W., and Bell, M. G. (1993). “Approaches to the provision of priority for public transport at traffic signals: a European perspective.” *Traffic Engineering & Control*, 34(9).

Ngan, V., Sayed, T., and Abdelfatah, A. (2004). “Impacts of various parameters on transit signal priority effectiveness.” *Journal of Public Transportation*, 7(3), 4.

“NTCIP 1202, National Transportation Communications for ITS Protocol Object Definitions for Actuated Traffic Signal Controller (ASC) Units, v02.19. November 2005.” (n.d.). .

Paniati, J. F., and Amoni, M. (2006). “Traffic signal preemption for emergency vehicles.” *RITA. US Development of Transportation Research and Innovative Technology Administration*.

Park, B., Messer, C., and Urbanik II, T. (2000). “Enhanced genetic algorithm for signal-timing optimization of oversaturated intersections.” *Transportation Research Record: Journal of the Transportation Research Board*, (1727), 32–41.

Park, B., Messer, C., and Urbanik, T. (1999). “Traffic signal optimization program for oversaturated conditions: genetic algorithm approach.” *Transportation Research Record: Journal of the Transportation Research Board*, (1683), 133–142.

PTV. (2014a). “PTV VISTRO User Manual.” *Karlsruhe, Germany*.

PTV. (2014b). “VISSIM 6.00 user manual.” *Karlsruhe, Germany*.

“PTV Vistro - the traffic engineering tool.” (n.d.). <www.vision-traffic.ptvgroup.com/en-us/products/ptv-vistro/> (Nov. 11, 2016).

Quiroga, C. A., and Bullock, D. (1998). “Travel Time Studies with Global Positioning and Geographic Information Systems: An Integrated Methodology.” *Transportation Research Part C: Emerging Technologies*, 6(1), 101–127.

Robertson, D. I. (1986). “Research on the TRANSYT and SCOOT Methods of Signal Coordination.” *ITE journal*, 56(1), 36–40.

Robertson, D. I., and Bretherton, R. D. (1991). “Optimizing networks of traffic signals in real time-the SCOOT method.” *IEEE Transactions on Vehicular Technology*, 40(1), 11–15.

Roess, R. P., Prassas, E. S., and McShane, W. R. (2011). “Traffic engineering.”

SAE International. (2016). “SAE J2735 Standard.” *Dedicated Short Range Communications (DSRC) Message Set Dictionary*.

Shalaby, A., and Farhan, A. (2004). “Prediction model of bus arrival and departure times using AVL and APC data.” *Journal of Public Transportation*, 7(1), 3.

Shmilovitz, D. (2005). “On the Definition of Total Harmonic Distortion and its Effect on Measurement Interpretation.” *IEEE Transactions on Power Delivery*, 20(1), 526–528.

Shoup, G., and Bullock, D. (1999). “Dynamic Offset Tuning Procedure Using Travel Time Data.” *Transportation Research Record: Journal of the Transportation Research Board*, (1683), 84–94.

Sims, A. G. (1979). “The Sydney coordinated adaptive traffic system.” *Engineering Foundation Conference on Research Directions in Computer Control of Urban Traffic Systems, 1979, Pacific Grove, California, USA*.

Skabardonis, A. (2000). “Control strategies for transit priority.” *Transportation Research Record: Journal of the Transportation Research Board*, (1727), 20–26.

Skabardonis, A., and Geroliminis, N. (2008). “Real-time monitoring and control on signalized arterials.” *Journal of Intelligent Transportation Systems*, 12(2), 64–74.

Stevanovic, A., Martin, P., and Stevanovic, J. (2007). “VisSim-based genetic algorithm optimization of signal timings.” *Transportation Research Record: Journal of the Transportation Research Board*, (2035), 59–68.

Stevanovic, J., Stevanovic, A., Martin, P. T., and Bauer, T. (2008). “Stochastic optimization of traffic control and transit priority settings in VISSIM.” *Transportation Research Part C: Emerging Technologies*, 16(3), 332–349.

Sunkari, S. (2004). “The benefits of retiming traffic signals.” *Institute of Transportation Engineers. ITE Journal*, 74(4), 26.

Sunkari, S. R., Beasley, P. S., Urbanik, T., and Fambro, D. B. (1995). “Model to evaluate the impacts of bus priority on signalized intersections.” *Transportation Research Record: Journal of the Transportation Research Board*, (1494), 117–123.

Sunkari, S. R., Charara, H. A., Urbanik, I. I., and others. (2000). *Reducing truck stops at high-speed isolated traffic signals*. Texas Transportation Institute, Texas Department of Transportation, Federal Highway Administration.

Tian, Z., and Urbanik, T. (2007). “System partition technique to improve signal coordination and traffic progression.” *Journal of Transportation Engineering*, 133(2), 119–128.

Trafficware. (2013). “Synchro 8.0 User’s Guide.”

TSS-Transport Simulation Systems. (2014). “Aimsun Users Manual v8.” *Aimsun Online*.

University of Arizona, University of California PATH Program, Savari Networks, Inc., Econolite. (2016). “Multi-Modal Intelligent Traffic Signal System – Phase II: System Development, Deployment and Field Test (Final report).” *Center for Transportation Studies*, <http://www.cts.virginia.edu/cvpfs_research/>.

US Department of Transportation. (2007). “Intelligent Transportation Systems for Traffic Signal Control: Deployment Benefits and Lessons Learned.” *Report No.: FHWA - JPO - 07 - 004*.

US DOT. (2015). “Multi-Modal Intelligent Traffic Signal Systems (MMITSS) Impacts Assessment.” *U.S. Department of Transportation*.

Vasudevan, M., and Chang, G.-L. (2006). "Design and Development of Integrated Arterial Signal Control Model." *Transportation Research Record: Journal of the Transportation Research Board*, (1978), 76–86.

Wahlstedt, J. (2011). "Impacts of bus priority in coordinated traffic signals." *Procedia-Social and Behavioral Sciences*, 16, 578–587.

Wallace, C. E., Courage, K. G., Reaves, D. P., Schoene, G. W., and Euler, G. W. (1984). *TRANSYT-7F user's manual*.

Welch, P. (1967). "The use of fast Fourier transform for the estimation of power spectra: a method based on time averaging over short, modified periodograms." *IEEE Transactions on Audio and Electroacoustics*, 15(2), 70–73.

Yin, Y., Li, M., and Skabardonis, A. (2007). "Offline Offset Refiner for Coordinated Actuated Signal Control Systems." *Journal of Transportation Engineering*, 133(7), 423–432.

Yu, L. (2000). "Calibration of Platoon Dispersion Parameters on the Basis of Link Travel Time Statistics." *Transportation Research Record: Journal of the Transportation Research Board*, (1727), 89–94.

Zamanipour, M., Head, K. L., Feng, Y., and Khoshmagham, S. (2016). "Efficient Priority Control Model for Multimodal Traffic Signals." *Transportation Research Record: Journal of the Transportation Research Board*, (2557), 86–99.

Zlatkovic, M., Stevanovic, A., and Martin, P. (2012a). "Development and evaluation of algorithm for resolution of conflicting transit signal priority requests." *Transportation Research Record: Journal of the Transportation Research Board*, (2311), 167–175.

Zlatkovic, M., Stevanovic, A., Martin, P., and Tasic, I. (2012b). "Evaluation of transit signal priority options for future bus rapid transit line in West Valley City, Utah." *Transportation Research Record: Journal of the Transportation Research Board*, (2311), 176–185.